


# Reelin Signaling Promotes Radial Glia Maturation and Neurogenesis

2009

Serene Keilani  
*University of Central Florida*

Find similar works at: <https://stars.library.ucf.edu/etd>

University of Central Florida Libraries <http://library.ucf.edu>

 Part of the [Microbiology Commons](#), and the [Molecular Biology Commons](#)

## STARS Citation

Keilani, Serene, "Reelin Signaling Promotes Radial Glia Maturation and Neurogenesis" (2009). *Electronic Theses and Dissertations*. 6143.  
<https://stars.library.ucf.edu/etd/6143>

This Doctoral Dissertation (Open Access) is brought to you for free and open access by STARS. It has been accepted for inclusion in Electronic Theses and Dissertations by an authorized administrator of STARS. For more information, please contact [lee.dotson@ucf.edu](mailto:lee.dotson@ucf.edu).

REELIN SIGNALING PROMOTES RADIAL GLIA MATURATION AND  
NEUROGENESIS

by

SERENE KEILANI  
B.S. University of Jordan, 2004

A dissertation submitted in partial fulfillment of the requirements  
for the degree of Doctor of Philosophy  
in the Department of Biomedical Sciences  
in the College of Medicine  
at the University of Central Florida  
Orlando, Florida

Spring Term  
2009

Major Professor: Kiminobu Sugaya

© 2009 Serene Keilani

## ABSTRACT

The end of neurogenesis in the human brain is marked by the transformation of the neural progenitors, the radial glial cells, into astrocytes. This event coincides with the reduction of Reelin expression, a glycoprotein that regulates neuronal migration in the cerebral cortex and cerebellum. A recent study showed that the dentate gyrus of the adult reeler mice, with homozygous mutation in the RELIN gene, have reduced neurogenesis relative to the wild type. Based on the above findings, our first hypothesis states that Reelin expression is important for the formation of radial glia and the generation of neurons from the neural progenitors. In order to investigate the role of Reelin in the process of cortical neurogenesis during development, we used human neural progenitor cells (hNPCs) that were isolated from a fetal cortex. These cells do not express Reelin. In this study, we show that Reelin addition to these hNPCs *in vitro* induced the formation of radial glia and increased neurogenesis significantly.

Next, we investigated the mechanism by which Reelin increases the formation of radial glia and the generation of neurons. The formation of radial glia is under the control of two pathways, these are the Reelin and the Notch-1 signaling pathways. Since the level of Notch-1 activation determines if a cell would become a radial glia or an astrocyte, and since the absence of Reelin allows the transformation of a radial glia into astrocyte, we hypothesized that Reelin induces the formation of radial glia via activating Notch-1 signaling. To test this hypothesis, we investigated the effect of Reelin addition on Notch-1 activation in hNPCs. We found that Reelin addition *in vitro* activated Notch-1 signaling by increasing the level of Notch-1 intracellular domain (NICD). On the other hand, reducing NICD release, by inhibiting  $\gamma$ -secretase activity, inhibited

the Reelin-induced radial glia, confirming that Reelin's effect on the formation of radial glia is dependent on Notch-1 activation. Furthermore, we found that the Reelin-induced tyrosine phosphorylation of Disabled-1 (Dab-1), an adaptor protein downstream of Reelin, and the subsequent activation of *Src* family kinases, are essential steps for Notch-1 activation by Reelin.

Finally, we found that Reelin addition increased the binding of Dab-1, recently identified as a nucleoshuttling protein, to NICD and enhanced NICD translocation to the nucleus. This resulted in the induction of BLBP expression and the subsequent formation of radial glia. Taken together, these data show that Reelin signaling, mediated by Dab-1 and *Src* kinase, activates Notch-1 signaling in hNPCs resulting in the induction of BLBP expression, the formation of radial glia and the generation of neurons. This work is novel because it provides that first evidence that Reelin expression is an important signal for the neuronal differentiation of the hNPCs. It also shows the crosstalk between Reelin and Notch-1 signaling, two major pathways in development and cell fate determination. The work is significant because it improves our understanding of the role of Reelin signaling in cell fate determination, differentiation and neurogenesis for the future manipulation of these processes to restore adult brain functions after brain injury or in neurodegenerative diseases.

I dedicate this work for all my family and friends who gave me endless support and love and kept their faith in me all the way. Special thanks to Dr. Kiminobu Sugaya, my mentor for five years. I thank you for all you have taught me over the years, for your patience, and continuous support.

## **ACKNOWLEDGMENTS**

I thank my committee members, Dr. Steven Ebert, Dr. Sic L. Chan and Dr. James Turkson for all their help, feedback and support.

## TABLE OF CONTENTS

LIST OF FIGURES .....	ix
LIST OF ABBREVIATIONS.....	xi
CHAPTER ONE: GENERAL INTRODUCTION .....	1
Adult Neurogenesis and Radial Glial Cells .....	1
Reelin Signaling in Radial Glial Cells .....	2
Notch-1 Signaling in Radial Glial Cells .....	6
Amyloid Precursor Protein and Neurogenesis .....	7
Rationale and Aims.....	9
CHAPTER TWO: REELIN INDUCES A RADIAL GLIAL PHENOTYPE IN HUMAN NEURAL PROGENITOR CELLS BY ACTIVATION OF NOTCH-1 .....	12
Introduction.....	12
Materials and Methods.....	15
Results.....	19
Discussion.....	37
CHAPTER THREE: REELIN ACTIVATES NOTCH-1 SIGNALING THROUGH DISABLED-1 TYROSINE PHOSPHORYLATION.....	39
Introduction.....	39
Materials and Methods.....	41



Results.....	48
Discussion.....	73
CHAPTER FOUR: DISABLED-1 PROMOTES $\gamma$ -SECRETASE-MEDIATED PROCESSING OF AMYLOID PRECURSOR PROTEIN .....	76
Introduction.....	76
Materials and Methods.....	79
Results.....	84
Discussion.....	101
CHAPTER FIVE: GENERAL CONCLUSION .....	103
REFERENCES .....	108

## LIST OF FIGURES

Figure 1: A schematic diagram that illustrates the proposed role for Reelin in neurogenesis.....	5
Figure 2: A schematic diagram that demonstrates the proposed cross-talk between Reelin and Notch-1 signaling pathways.....	11
Figure 3: The formation of radial glia in hNPCs is dependent on the growth factors FGF and EGF.....	21
Figure 4: Reelin levels in the media of HEK293 cells that are stably transfected with Reelin. ....	23
Figure 5: Reelin treatment <i>in vitro</i> induces a radial glial phenotype.....	24
Figure 6: Reelin treatment of hNPCs induces Dab-1 phosphorylation on tyrosine residue 198..	26
Figure 7: Reelin treatment induces neurogenic radial glial cells in hNPCs. ....	28
Figure 8: Reelin treatment induces a radial glial phenotype similar to Notch-1 activation. ....	30
Figure 9: The Reelin-induced radial glial phenotype is dependent on $\gamma$ -secretase activity.....	32
Figure 10: Reelin treatment activates Notch-1. ....	34
Figure 11: Reelin increases the binding of Dab-1 to Notch-1. ....	36
Figure 12: Reelin expression in the media of HEK293 cells and the media of hNPCs.....	50
Figure 13: Reelin increases neurogenesis in hNPCs <i>in vitro</i> .....	51
Figure 14: Reelin treatment increases NICD levels in hNPCs. ....	53
Figure 15: Reelin does not enhance $\gamma$ -secretase activity <i>in vitro</i> .....	55
Figure 16: Reelin-induced NICD accumulation is not due to enhanced Notch-1 endocytosis ....	58
Figure 17: Inhibition of Notch-1 signaling in the Reelin treated cells increases the ratio of the generated neurons to the produced radial glia. ....	60
Figure 18: Notch-1 is trafficked in the same vesicles as Reelin and VLDLR.....	62

Figure 19: Reelin-induced activation of Notch-1 is dependent on Dab-1 tyrosine phosphorylation.....	64
Figure 20: Reelin-induced activation of Notch-1 is dependent on <i>Src</i> activation. ....	66
Figure 21: Reelin does not bind Notch-1.....	68
Figure 22: Reelin increases NICD translocation to the nucleus and induces BLBP expression. .	70
Figure 23: Reelin enhances the binding between Dab-1 and NICD in the nuclear fraction.....	72
Figure 24: Dab-1 over-expression reduces APP-CT-GFP signals in vesicular structures.....	85
Figure 25: APP-CT-GFP signals co-localizes with the early endosomal marker (EEA1). ....	87
Figure 26: Dab-1 over-expression increases AICD generation. ....	89
Figure 27: APP-CTFs slightly accumulates in the Dab-1 overexpressing cells after $\gamma$ -secretase inhibition. ....	91
Figure 28: Dab-1 enhances $\alpha$ -secretase mediated processing of APP. ....	93
Figure 29: A schematic diagram that illustrates the effects of Dab-1 on APP processing. ....	94
Figure 30: Dab-1 over-expression promotes $\gamma$ -secretase-mediated processing of APP. ....	96
Figure 31: Accumulation of ubiquitinated proteins after MG-132 treatment.....	99
Figure 32: Dab-1 overexpression increases APP degradation via the lysosome.....	100
Figure 33: A schematic diagram that summarizes the role of Reelin signaling in the formation of neurogenic radial glia.....	107

## LIST OF ABBREVIATIONS

A $\beta$	Amyloid $\beta$ Peptide
AD	Alzheimer's disease
AICD	APP Intracellular Domain
ApoEr2	ApoE Receptor 2
APP	$\beta$ - Amyloid Precursor Protein
BACE	Beta-Site APP Cleaving Enzyme
BLBP	Brain Lipid Binding Protein
CBF1	C-promoter Binding Factor-1
CNS	Central Nervous System
CTF	C-Terminal Fragment
Dab-1	Disabled-1
EEA1	Early Endosomal Marker 1
EGF	Epidermal Growth Factor
FGF	Fibroblast Growth Factor
GFAP	Glial Fibrillary Acidic Protein
hNPCs	human Neural Progenitor Cells
hNSCs	human Neural Stem Cells
LDL	Low-Density Lipoprotein
NICD	Notch Intracellular Domain
NT2/D1	Neuron-Committed Teratocarcinoma
PI3-K	Phosphoinositide-3-Kinase

PTB	Phosphotyrosine Binding
sAPP	Secreted APP
SFK	Src Family Kinases
SGZ	Subgranular Zone
SVZ	Subventricular Zone
TGN	<i>Trans</i> -Golgi Network
VLDLR	Very Low Density Lipoprotein Receptor
VZ	Ventricular Zone

# CHAPTER ONE: GENERAL INTRODUCTION

## Adult Neurogenesis and Radial Glial Cells

Neural stem cells were found in two regions in the adult mammalian brain: the subventricular zone (SVZ) of the lateral ventricle and the dentate gyrus subgranular zone (SGZ) of the hippocampus<sup>1</sup>. Since the discovery of these cells great effort has focused on understanding the mechanism of neurogenesis to facilitate their therapeutic use in restoring brain functions after brain injury and in neurodegenerative diseases<sup>1</sup>. The two challenges are either to stimulate the endogenous resources to migrate and differentiate into the damaged areas or to expand and manipulate these cells *in-vitro* and then transplant them in the desired site. In both cases, success has been limited due to the lack of the full understanding of the adult's brain chemistry that regulates the process of functional neurogenesis<sup>1</sup>.

Radial glia cells have been recently demonstrated to be the progenitors for the majority of the central nervous system (CNS) neurons<sup>2, 3</sup>. They arise early in the development of the CNS from the neuroepithelial cells that line the ventricles<sup>4</sup>. These cells were originally studied for their role in neuronal migration. Radial glia, as their name indicates, extend a long radial process to the pial surface while having their cell bodies in the ventricular zone (VZ) thus allowing the migration of the neurons from the VZ to the post-mitotic areas<sup>5</sup>. However, the finding that these cells can also give birth to the migratory neurons, via their asymmetric division<sup>6, 7</sup>, further highlighted the significance of these cells in brain development. Interestingly, radial glial cells

disappear or transform into astrocytes in most regions of the mammalian brain after neuronal generation and migration are completed<sup>4</sup>.

Many signaling events regulate radial glia differentiation, maturation, maintenance and their transformation into astrocytes<sup>8</sup>. Thus the understanding of the mechanisms that induce and maintain the radial glial phenotype is crucial for the therapeutic manipulation of these cells to promote neurogenesis and neuronal migration in the adult brain.

### **Reelin Signaling in Radial Glial Cells**

Brain lipid binding protein (BLBP) is a hydrophobic ligand binding protein that is expressed throughout the CNS in radial glia and astrocytes during development<sup>9</sup>. BLBP is induced *in-vitro* in radial glia by neurons<sup>10</sup>. A recent elegant study using Cre/loxP fate mapping, showed that all neuronal population in the mouse brain are derived from radial glial cells expressing BLBP<sup>3</sup>. It has been suggested that the induction of BLBP marks the onset of radial glia neurogenesis where BLBP expression in radial glial cells have been shown to be up-regulated at the onset of neurogenesis and maintained as neurogenesis proceeds<sup>3</sup>. Thus, BLBP up-regulation is important to define the developmental changes that occur in the radial glial cells to drive them into their neurogenic stage. However, the mechanisms of how this protein mediates its function remain unknown.

Recently, BLBP expression in cortical radial glia as well as its role in radial process extension was found to be dependent on Reelin signaling<sup>11</sup>. Reelin is a large secreted glycoprotein that has

been shown to be an important signal for neuronal migration and proper positioning of neurons in the cerebral cortex and cerebellum<sup>12</sup>. It's been proposed that Reelin act as a detachment signal of the neuron from the radial fibers allowing the positioning of the neurons in an inside-out manner<sup>13</sup>. Reelin signal is transmitted into the cells by Disabled-1 (Dab-1), a cytoplasmic adaptor protein that bind the internalization (NPXY) motif of the lipoprotein receptors, apolipoprotein receptor2 (ApoER2) and the very low density lipoprotein receptor (VLDLR), via its phospho-tyrosine binding (PTB) domain<sup>14</sup>. Tyrosine phosphorylation of Dab-1 is initiated after Reelin binding to its receptors VLDLR and ApoER2<sup>15</sup>. Dab-1 tyrosine phosphorylation forms a binding site for Src family kinases resulting in their activation and leading to further phosphorylation of Dab-1 on its remaining tyrosine residues<sup>16, 17</sup>. This further activates Src and ultimately results in the activation of Phosphatidylinositol 3-kinase (P13-K) and Akt<sup>17</sup>. Mice deficient in VLDLR and ApoER2, Dab1 or Dab1 that cannot be tyrosine phosphorylated generates a reeler-like phenotype, which is characterized by inversion of the cortical layers and abnormalities in the laminated brain structures<sup>18</sup>.

Interestingly, Reelin effect on BLBP expression requires Dab-1 as well, as it failed to occur in Dab1<sup>-/-</sup> mice<sup>11</sup>. Supporting that, reeler and Dab1 mutant mice were shown to exhibit abnormal development of the radial glia scaffold in the dentate gyrus of the hippocampus, indicating the importance of this pathway in the formation and maintenance of the radial glial scaffold<sup>19</sup>. Components of the Reelin signaling pathway, including VLDLR, ApoER2, and Dab1 were shown to be expressed in both the hippocampal and cortical radial glia<sup>19, 20</sup>. In addition, Dab1 was tyrosine phosphorylated in ventricular zone cells upon Reelin stimulation indicating



that the radial glial cells respond directly to Reelin signal<sup>21</sup>. Furthermore, a recent study showed that adult reeler mutants have increased differentiation of the newly generated cells into astrocytes and decreased differentiation into neurons<sup>22</sup>.

Taken together, these findings suggest that Reelin signaling does not only regulate the neuronal migration but it may also regulate the neuronal differentiation via promoting the formation and maturation of the neural progenitors, the radial glial cells. In this study, we aim to identify the mechanisms through which Reelin signaling induces and maintains the radial glial phenotype to promote neurogenesis in human Neural Progenitor Cells (hNPCs).

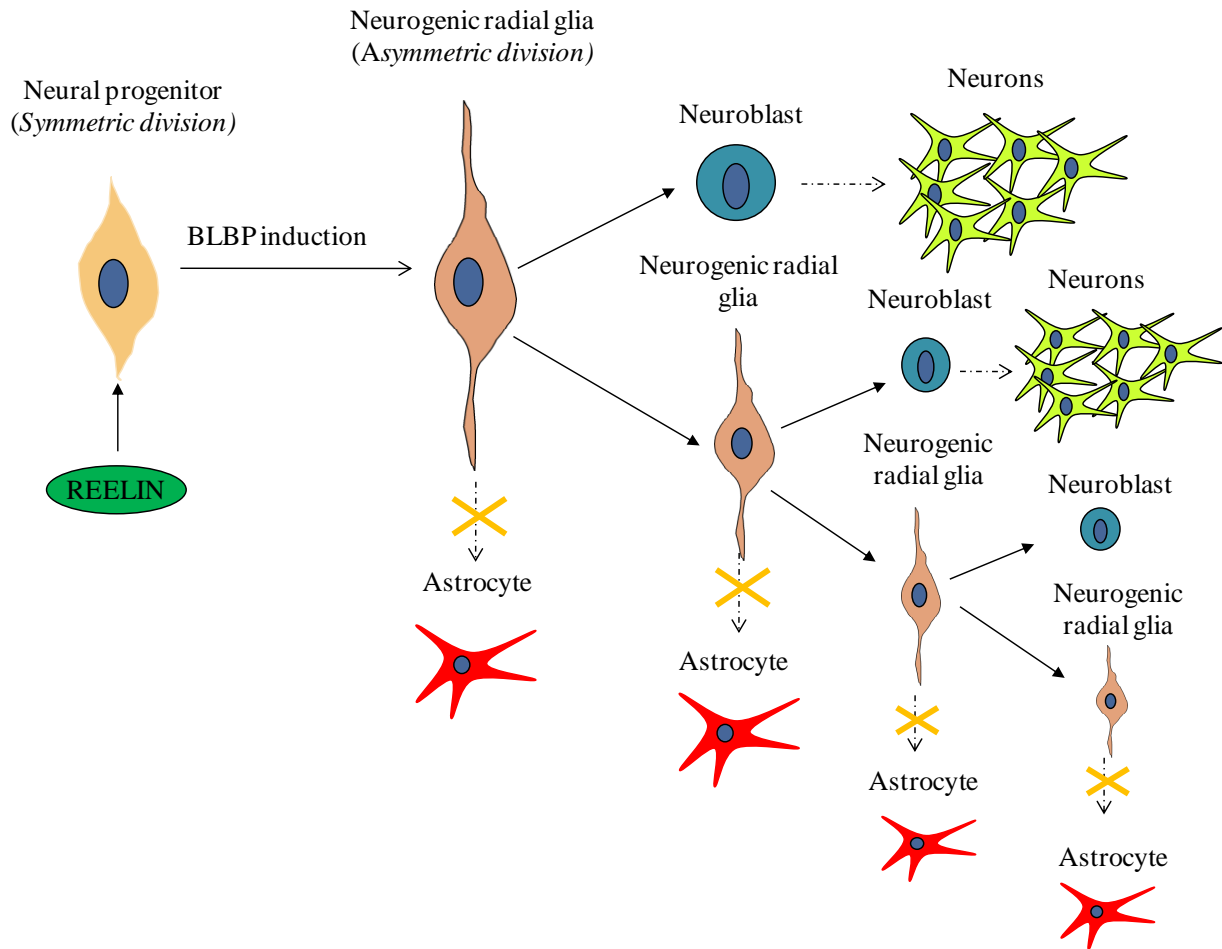


**Figure 1: A schematic diagram that illustrates the proposed role for Reelin in neurogenesis.** Reelin binding to the surface of a neural progenitor induces BLBP expression in this cell and drives its transformation into a neurogenic radial glia. The transformation includes morphological changes and a shift from a proliferative phase (symmetric division) to a neurogenic phase (asymmetric division) that will result in the generation of neurons. Reelin may also maintain the neurogenic radial glia by preventing their transformation into astrocytes.

### **Notch-1 Signaling in Radial Glial Cells**

A central pathway for the differentiation and maturation of radial glia during development of the CNS is Notch-1 signaling<sup>23-31</sup>. Recent studies showed that radial glia differentiation depends on Notch-1 receptor activation through its direct contact with the migratory neurons that express Notch-1 ligand, Jagged-1<sup>25, 26</sup>. In addition, it has been shown that Notch-1 regulates the morphological differentiation and maturation of radial glia through the transcriptional activation of BLBP<sup>25, 26</sup>. Notch-1 activation, upon binding its ligand, will initiate its cleavage by  $\gamma$ -secretase to generate Notch-1 intracellular domain (NICD). NICD translocates to the nucleus and binds C-promoter Binding Factor 1 (CBF1), converting it from transcriptional repressor to transcriptional activator<sup>27, 28</sup>. BLBP expression was recently found to be dependent on this pathway<sup>25, 26</sup>, where a binding site for the Notch effector CBF1 was found in the promoter region of BLBP<sup>29</sup>.

Interestingly, Notch-1 activation has been known for its role in promoting both phenotypes, the formation of the radial glial cells and their transformation into astrocytes. However, Notch-1 activation has been shown to induce radial glial cells differentiation prenatally and to induce astrocytic differentiation postnatally<sup>31, 32</sup>. Therefore, the presence of other signaling pathways that act to induce the radial glial phenotype prenatally but are deactivated or downregulated postnatally seems to be an attractive model to explain how Notch-1 activation leads to different cellular fates at different developmental stages.

## **Amyloid Precursor Protein and Neurogenesis**

$\beta$ - Amyloid precursor protein (APP) is the precursor of amyloid  $\beta$  peptide ( $A\beta$ ), which is associated with the pathogenesis of Alzheimer's disease (AD), a progressive neurodegenerative disease<sup>33</sup>. During its trafficking, APP is subjected to processing by proteolytic enzymes that are distributed throughout the secretory and the endocytic pathways to generate different APP fragments<sup>34, 35</sup>, which in turn regulate several neural functions including cell excitability, synaptic transmission and long-term potentiation<sup>36</sup>.

Processing of APP is initiated via the proteolytic activities of  $\alpha$ - and  $\beta$ -secretases, which cleave APP ectodomain close to its transmembrane domain to liberate soluble APP extracellular fragments ( $\alpha$ - or  $\beta$ -secreted APP respectively). APP cleavage by  $\alpha$ - or  $\beta$ -secretases is a key regulatory process in the generation of the  $A\beta$ . After the initial cleavage of APP by  $\alpha$ - and/or  $\beta$ -secretase, the remaining membrane-tethered C-terminal APP fragments (CTFs), are further cleaved within its transmembrane domain by a multimeric protein complex termed  $\gamma$ -secretase to generate p3 and  $A\beta$  respectively, and a cytosolic APP intracellular domain (AICD)<sup>33-36</sup>.

APP processing is regulated by proteins that bind its intracellular domain, particularly its YENPTY motif. This motif contains the consensus sequence for the clatherin-coated pit internalization<sup>37, 38</sup>. Dab-1, an adaptor protein that has the phosphotyrosine-binding (PTB) domain, was found to bind and regulate APP metabolism<sup>37, 38</sup>.

In our previous work, we found that the secreted APP (sAPP) can induce the glial differentiation of human Neural Stem Cells (hNSCs)<sup>39</sup>. In addition, a recent study found that sAPP binds to cells that express the epidermal growth factor (EGF) receptor in the subventricular zone resulting in increased proliferation of these neuronal progenitors<sup>40</sup>. It seems that the level of the sAPP is a determining factor in the differentiation of the stem cells<sup>39, 40</sup>. In chapter four, we will briefly explore the effects of Dab-1 overexpression on the metabolism and processing of APP to lay the grounds for further investigations of the role of APP metabolism in neurogenesis.

## **Rationale and Aims**

Radial glial cells do not only guide the migration of neurons from the ventricular zone to the post-mitotic areas, but they also give rise to these neurons *via* their asymmetric division during brain development<sup>1-9</sup>. The dual roles of the radial glia in regulating the migration and the generation of the neurons during development suggest that there is an overlap in the signaling pathways that control these two roles.

Since the end of neurogenesis in the human brain is marked by the transformation of the radial glial cells into astrocytes<sup>4</sup> and since this event coincides with the reduction of Reelin expression in the cortex<sup>41, 42</sup>, then we hypothesized that Reelin signaling prenatally enhances Notch-1 activation and induces the formation of the radial glial cells from the neural progenitors. The down-regulation of Reelin expression postnatally is therefore expected to allow the transformation of the radial glial cells into astrocytes. Supporting that, a recent study showed that adult reeler mice have increased differentiation of the newly generated cells into astrocytes and decreased differentiation into neurons<sup>22</sup>.

Our challenge is to determine if the addition of Reelin to neural progenitors that lack Reelin expression and are entering their gliogenic phase can reverse their fate to regain the neurogenic phenotype.

Our long term objective is to understand the mechanisms that regulate and enhance neurogenesis in order to manipulate them to restore brain functions in the adult brain after injury or in

neurodegenerative diseases. Our objectives are to confirm the effect of Reelin signaling on neurogenesis and to elucidate the mechanisms by which this pathway promotes the neuronal fate.

The aims of this study are:

**Aim I:** Confirm that the activation of Reelin signaling increases the neuronal differentiation of human Neural Progenitor Cells (hNPCs).

**Aim II:** Determine if Reelin signaling increases neurogenesis via Notch-1 activation.

**Aim III:** Investigate the mechanism by which Reelin signaling activates Notch-1.

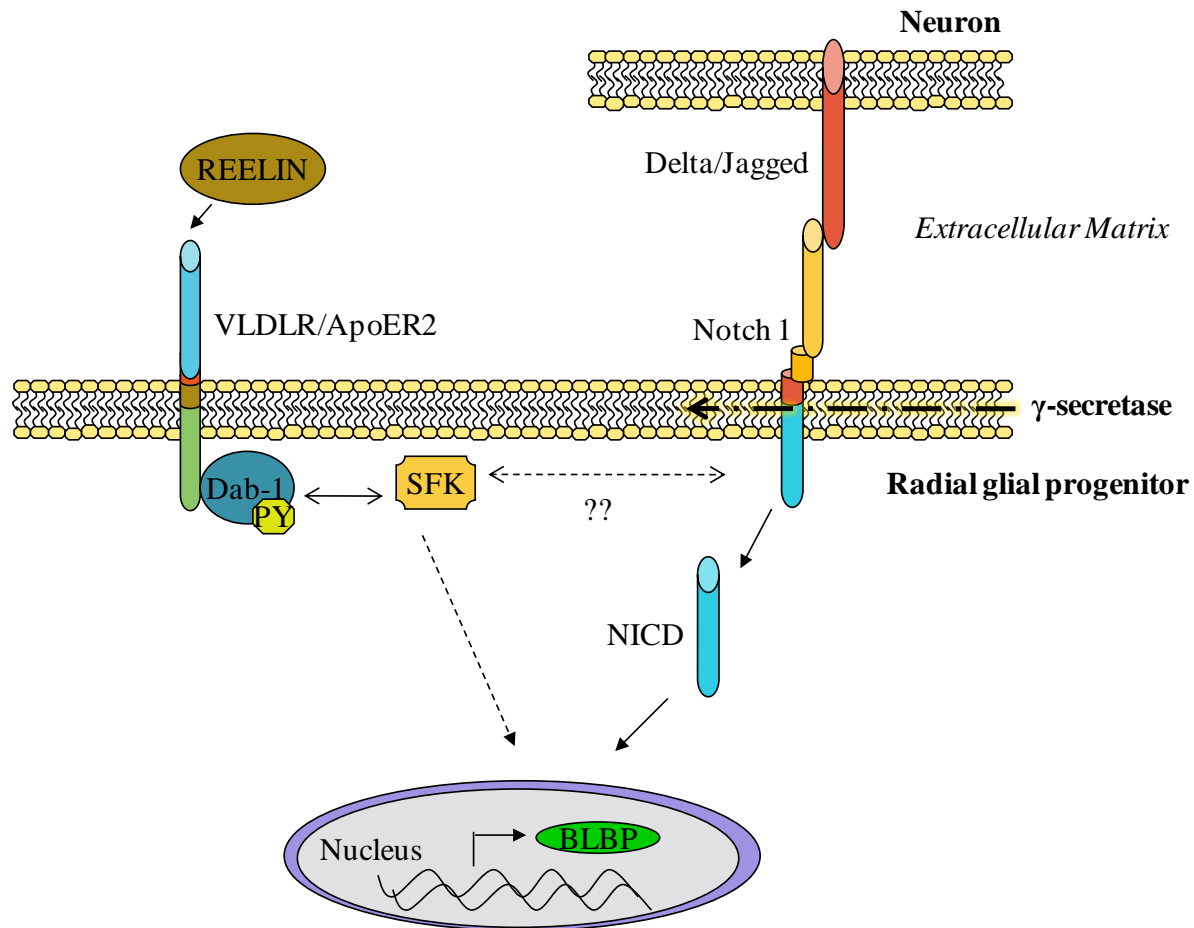


**Figure 2: A schematic diagram that demonstrates the proposed cross-talk between Reelin and Notch-1 signaling pathways.**

Upon Notch-1 activation, the released NICD translocates to the nucleus and induces BLBP expression. Reelin signaling is known to induce BLBP expression by unidentified mechanism. We propose a crosstalk between the two pathways and suggest that Reelin signaling increases NICD levels to induce BLBP expression and the subsequent formation of neurogenic radial glia. SFK; *Src* family kinases, NICD; Notch intracellular domain, BLBP; brain lipid binding protein, Dab-1; Disabled-1, VLDLR; very low density lipoprotein, ApoER2; ApoE receptor 2.



## **CHAPTER TWO: REELIN INDUCES A RADIAL GLIAL PHENOTYPE IN HUMAN NEURAL PROGENITOR CELLS BY ACTIVATION OF NOTCH-1**

### **Introduction**

Radial glial cells have been recently demonstrated to be the progenitors for the majority of the central nervous system (CNS) neurons<sup>2, 3</sup>. They arise early in the development of the CNS from the neuroepithelial cells that line the ventricles<sup>4</sup>. Radial glial cells extend a long radial process to the pial surface while having their cell bodies in the ventricular zone (VZ), allowing the migration of neurons from the VZ to the post-mitotic areas<sup>5</sup>. However, the finding that these cells can also give birth to the migratory neurons via their asymmetric division<sup>6, 7</sup> further highlighted the significance of these cells in brain development. Interestingly, radial glial cells disappear or transform into astrocytes in most regions of the mammalian brain after neuronal generation and migration are completed<sup>4</sup>.

Brain lipid binding protein (BLBP) is a hydrophobic ligand binding protein that is expressed throughout the CNS in radial glia and astrocytes during development<sup>9</sup>. A recent elegant study using Cre/loxP fate mapping, showed that all neuronal population in the mouse brain are derived from radial glial cells expressing BLBP<sup>3</sup>.

Recently, BLBP expression in cortical radial glia as well as its role in radial process extension was found to be dependent on Reelin expression<sup>11</sup>. Reelin is a large secreted glycoprotein, which has been shown to be an important signal for neuronal migration and proper positioning of

neurons in the cerebral cortex and cerebellum<sup>12</sup>. Reelin signal is transmitted into the cells by Disabled-1 (Dab-1), a cytoplasmic adaptor protein that binds the internalization (NPXY) motif of the Reelin receptors, apolipoprotein receptor2 (ApoER2) and the very low density lipoprotein receptor (VLDLR), via its phospho-tyrosine binding (PTB) domain<sup>14</sup>. The tyrosine phosphorylation of Dab-1 is initiated after Reelin binds to its receptors<sup>15</sup>. This phosphorylation creates new binding sites for *Src* kinases leading to their activation<sup>16, 17</sup>. Mice deficient in, VLDLR and ApoER2, Dab-1 or Dab-1 that cannot be tyrosine phosphorylated generates a reeler-like phenotype, which is characterized by inversion of the cortical layers and abnormalities in the laminated brain structures<sup>18</sup>.

Reelin effect on BLBP expression requires Dab-1 as well, as it failed to occur in Dab-1<sup>-/-</sup> mice<sup>11</sup>. Reeler and Dab-1 mutant mice were shown to exhibit abnormal development of the radial glia scaffold in the dentate gyrus of the hippocampus<sup>19</sup>. Furthermore, components of the Reelin signaling pathway, including VLDLR, ApoER2, and Dab1 were shown to be expressed in both the hippocampal and cortical radial glia<sup>19, 20</sup>. Interestingly, Reelin addition *in-vitro* has been shown not only to promote the process extension of the radial glial cells but also to rescue the defects in the length of these processes in the reeler mutant radial glia<sup>11</sup>.

A recent study showed that Notch-1 signaling could also regulate the molecular and the morphological differentiation of radial glia through the transcriptional activation of brain lipid binding protein (BLBP)<sup>25, 26</sup>. Notch is a single-pass transmembrane protein that was initially identified in *Drosophila* and has been shown to mediate many developmental signaling events<sup>24</sup>.

Notch-1 activation, upon binding its ligand, will initiate its cleavage by  $\gamma$ -secretase to generate Notch-1 intracellular domain (NICD). NICD translocates to the nucleus and binds C-promoter Binding Factor 1 (CBF1), converting it from transcriptional repressor to transcriptional activator<sup>27, 28</sup>. Interestingly, BLBP expression was found to be dependent on this pathway<sup>25, 26</sup>, where a binding site for the Notch-1 effector's CBF1 was found in the promoter region of BLBP<sup>29</sup>.

Since Notch-1 activation can induce the formation of radial glial cells prenatally and their transformation into astrocytes postnatally<sup>31, 32</sup>, we hypothesized that Reelin signaling may act to fine-tune Notch-1 activation to favor the induction of the radial glial phenotype prenatally. This in turn can explain how the degeneration of the cells that produces Reelin in the cortex coincides with transformation of the radial glial cells into astrocytes postnatally<sup>41, 42</sup>. In our study, *in vitro* addition of Reelin to human Neural Progenitor Cells (hNPCs), isolated from the cortex of 14 weeks old fetus, induced BLBP expression and a radial glial phenotype similar to that induced by Notch-1 activation. The inhibition of Notch-1 activation by inhibiting the activity of  $\gamma$ -secretase abolished Reelin's effect, suggesting the dependency of Reelin signaling on Notch-1 activation. Furthermore, Reelin treatment increased the level of NICD, indicating that Reelin can directly activate Notch-1. Finally, Dab-1 was observed to bind to Notch-1, thus providing an evidence of the physical interaction between these two pathways.

## **Materials and Methods**

### *Cell Culture*

We used ReNcell CX (Chemicon), an immortalized human Neural Progenitor Cell (hNPC) line. These cells were isolated from the cortex of a 14-weeks human fetal brain and immortalized by retroviral transduction with the c-myc oncogene. The cells were cultured in ReNcell NSC maintenance media (Chemicon) supplemented with 20ng/ml of the fibroblast growth factor (FGF) and 20ng/ml and of the epidermal growth factor (EGF) (Chemicon). These cells can differentiate into neurons and glial cells.

The cells were deprived of the growth factors, FGF and EGF, for 24 hours before Reelin treatment or NICD overexpression to exclude the effects of these factors on the induced radial glial phenotype.

For transfection of hNPCs, the cells were plated on laminin coated (Sigma Aldrich) 12-well culture plates (BD biosciences) for 24 hours or until they reached 90% confluency. The cells were then transiently transfected with 2- $\mu$ g of DNA/well using lipofectamine LTX and Plus reagents according to manufacturer's instructions (Invitrogen). The transfection efficiency was determined by finding the percentage of the GFP fluorescent cells 24 hours after transfecting the hNPCs with EGFP vector (Invitrogen). The transfection efficiency was optimized by transfecting the cells with different ratios of DNA/PLUS/LTX, where the best transfection efficiency was found to be 30-40%, using the ratio of 1/3/3, respectively.

For  $\gamma$ -secretase inhibition, 10  $\mu$ M of  $\gamma$ -secretase inhibitor (L-685, 458; Sigma Aldrich) or 0.1% of Dimethylsulfoxide (DMSO; Sigma Aldrich) as control, were prepared in growth media and added to the cells.

Dab-1 gene (Accession # NM\_021080) was cloned into pcDNA3.1 vector with FLAG tag on its C terminus (Invitrogen); sequencing was performed to assure that the clone is in frame. FCDN1 expressed in pBOS-EF1 (1747-2531 aa) was kindly provided by Dr. Gerry Weinmaster, UCLA.

#### *Reelin Production and Treatment*

Reelin- and control-containing media was collected from HEK293 cells stably transfected with RELIN pCRL vector (kindly provided by T. Curran, St. Jude Children's Hospital, Memphis Tennessee, USA), and a control empty pcDNA3.1 vector (Invitrogen), respectively<sup>19, 43, 44</sup>. The cells were cultured in neurobasal media (Invitrogen) for 3 days before media collection. Reelin was partially purified using columns with filters >100kDa (Chemicon) and Reelin levels were confirmed by western blotting using anti-Reelin clone G10 (Chemicon) that detected the three characteristic bands of Reelin (400 KDa, 300 KDa, and 180 KDa)<sup>15</sup>.

The control- or Reelin-conditioned media that were used to treat the hNPCs were prepared by diluting the purified control or Reelin in ReNcell CX maintenance media at a final concentration of 1:40. This concentration was determined by finding the lowest concentration of Reelin that can induce Dab-1 tyrosine phosphorylation as early as 15 minutes.

### *Protein Isolation and Western Blot Analysis*

The hNPCs were lysed in ice-cold RIPA (Radio-Immunoprecipitation Assay) lysis buffer (Sigma Aldrich) containing 150 mM NaCl, 1% IGEPAL CA-630, 0.5% sodium deoxycholate, 0.1% SDS, and 50 mM Tris, pH 8.0, supplemented with 1% Triton-X and protease inhibitor mixture (Calbiochem). The homogenates were centrifuged at 12,000 x *g* for 30 min at 4°C and the supernatants were saved for analysis. 40 µg of proteins were loaded per well. The proteins were then separated by SDS/PAGE (NuPage 4%-12% Bis-Tris, Invitrogen) for 60 min at 200 V, and then blotted onto polyvinylidene difluoride (PVDF) membranes (Bio-rad) for 120 min at 30 V. For the detection of full-length Notch-1, activated Notch-1, Reelin, BLBP, β-actin, Dab-1 and pY198Dab-1, membranes were incubated overnight with following primary antibodies, respectively: mouse anti-Notch-1 (1:1,000; Sigma Aldrich), rabbit anti-activated Notch-1 (1:500; Abcam), mouse anti-Reelin clone G10 (1:1000; Chemicon), rabbit anti-BLBP (1:500; Abcam), rabbit anti β-actin (1:1,000; Cell Signaling Technology), rabbit anti-Dab-1 (1:1000; Sigma Aldrich) and rabbit anti-Dab-1 phospho tyrosine 198 (1:1000; Chemicon). After washing the membranes they were incubated with horseradish peroxidase-conjugated secondary antibodies at concentration of 1:5000 (anti-mouse IgG and anti-rabbit IgG; Jackson ImmunoResearch, West Grove, PA) for 1–2 h. Signals were detected by chemiluminescence using the enhanced chemiluminescence (ECL) system (Amersham Biosciences Corp) on a Kodak Imaging Station IS2000MM. The optical density of each specific band relative to β-actin was analyzed by the public domain National Institutes of Health Image J software.

### *Immunoprecipitation*

700µg of proteins were incubated for 3 hours at 4°C with the primary antibody anti-Notch-1 (1:100; Sigma Aldrich), or anti-Flag (1:200; Sigma Aldrich), or anti-NICD (1:500; Abcam), Protein G- or A-Sepharose beads were added for 1 hr at 4°C, and then immunoprecipitates were washed 5X with lysis buffer. Immunoprecipitated proteins were solubilized in 1% SDS solution and resolved on a 4-12% Bis-Tris gel (Invitrogen).

### *Fluorescent Immunocytochemistry*

The hNPCs were fixed with 4% Paraformaldehyde (Sigma Aldrich) overnight at 4°C. The next day, the cells were washed three times with phosphate buffered saline (PBS-Sigma Aldrich) at room temperature and blocked with 3% donkey serum (Jackson ImmunoResearch Labs) in phosphate buffered saline with 0.1% Triton-X (PBST- Sigma Aldrich) for 1 hour at room temperature. For analyzing the radial glial phenotypes, hNPCs were incubated with rabbit anti-BLBP (1:50; Abcam) and mouse anti- GFAP (1:500; Sigma Aldrich) for 24 hrs at 4° C. After washing the cells with PBS for three times the cells were incubated with Tetramethyl Rhodamine Iso-Thiocyanate (TRITC)-conjugated anti-rabbit and Fluorescein isothiocyanate (FITC)-conjugated anti-mouse (1: 500; Jackson ImmunoResearch Labs) for 2 hrs at room temperature in the dark. The cells were washed again and mounted with vectasheild with DAPI (vector laboratories) and cover slipped for microscopic observations.

### *Microscopy and Analysis*

The induced radial glial phenotype was calculated by finding the percentage of the GFAP positive cells that had an induced BLBP expression<sup>45</sup> and a bipolar morphology, with at least one thin process longer than 50  $\mu\text{m}$ . This criterion was based on previous studies<sup>11, 46</sup>. Adobe Photoshop CS3 software was used to count the number of cells. Microscopic images were taken with the QImaging MicroPublisher 5.0 color digital imaging system and processed using the QCapture software (Leeds, Irving, TX).

### *Statistical Analysis*

Each data point represents triplicated experiments and displayed as the mean  $\pm$  standard error. A one-way Analysis of Variance was performed to test the hypothesis that the average mean values across categories of GROUP were equal. In the presence of significance for the omnibus ANOVA test, Tukey multiple comparison test is used to perform pairwise comparisons. Statistics were performed using WINKS SDA Software (Texasoft, Cedar Hill, TX.).

## **Results**

### *Reelin Treatment of hNPCs Induces a Radial Glial Phenotype*

Radial glial cells transform into astrocytes postnatally<sup>4</sup>, an event that coincides with the degeneration of the layer that produces Reelin in the cortex<sup>41, 42</sup>. In addition, a recent study



showed that adult reeler mice have increased differentiation of the newly generated cells into astrocytes and decreased differentiation into neurons<sup>22</sup>.

In order to investigate the role of Reelin on the formation of radial glia, we used human Neural Progenitor Cells (hNPCs) that were isolated from the cortex of a 14 weeks old fetus and immortalized *in-vitro*. In culture, these cells appear as a pure culture of glial fibrillary acidic protein (GFAP) positive cells with long radial processes (Figure 3, a).

FGF and EGF pathways are known to promote the formation of radial glia<sup>48, 49</sup>. To exclude the effects of FGF and EGF on the formation of radial glia, we deprived the hNPCs of these growth factors for 24 hours before treating the cells with Reelin. As expected, the deprivation of these growth factors reduced the radial glial phenotype, which was characterized by the retraction of the radial processes in the GFAP positive cells (Figure 3, b).

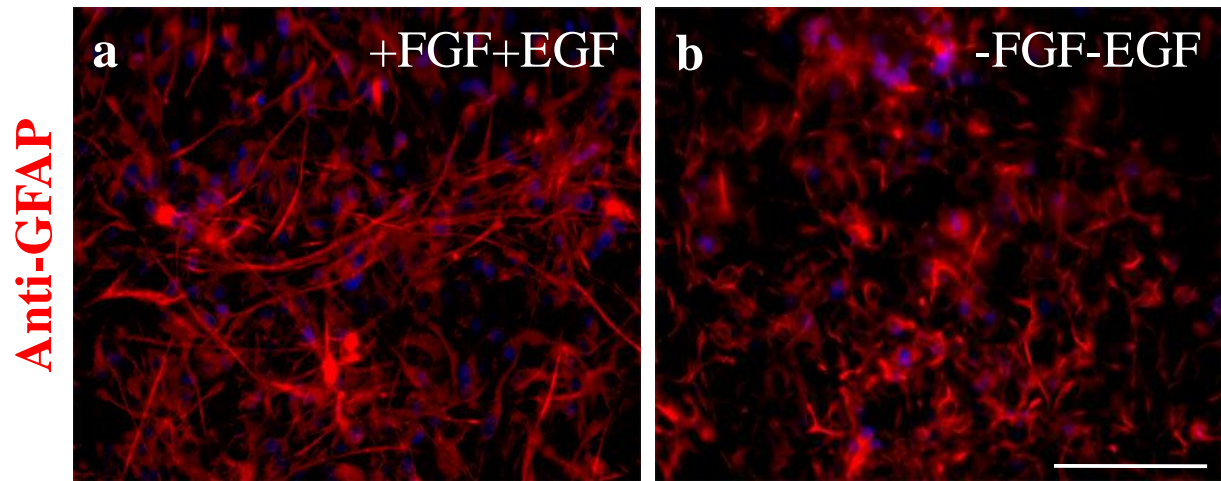


**Figure 3: The formation of radial glia in hNPCs is dependent on the growth factors FGF and EGF.**

The deprivation of the growth factors FGF and EGF for 24 hours results in the retraction of the radial processes in the GFAP positive cells (red). Scale bar is 100  $\mu\text{m}$ .

In order to characterize the effects of Reelin on the hNPCs, we treated the hNPCs with Reelin for 24 hours. Control- and Reelin-containing media were collected from HEK293 cells transfected with either control empty vector or Reelin, respectively. Reelin was partially purified (P.P) from the medium by column centrifugation and its expression was verified by western blotting using anti-Reelin clone G10 (Figure 4). The cells were treated with control or Reelin-conditioned media that was prepared by diluting the purified control or Reelin in the maintenance media at a final concentration of 1:40.

As a result, Reelin treatment was observed to re-induce the formation radial glia from the hNPCs that has been deprived of FGF and EGF. The newly formed radial glia was characterized by increased radial process extension in the GFAP positive cells (Figure 5).

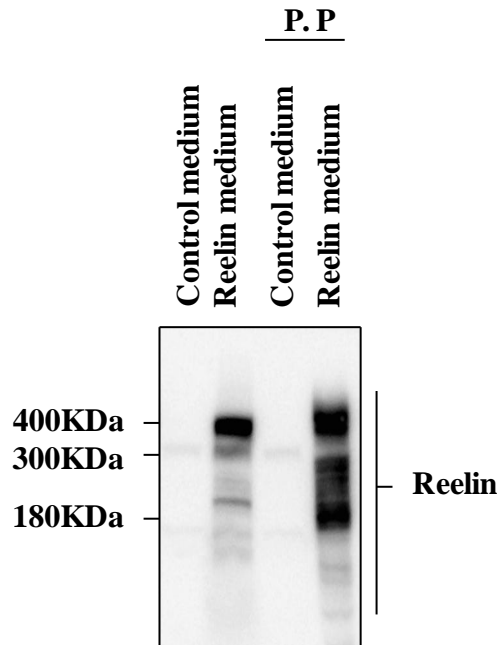


**Figure 4: Reelin levels in the media of HEK293 cells that are stably transfected with Reelin.** Control and Reelin-containing media were collected from HEK293 cells transfected with either an empty vector or Reelin, respectively. Reelin was partially purified (P.P) from the medium by column centrifugation and its expression was verified by western blotting using anti-Reelin clone G10.

(-) FGF and EGF

---

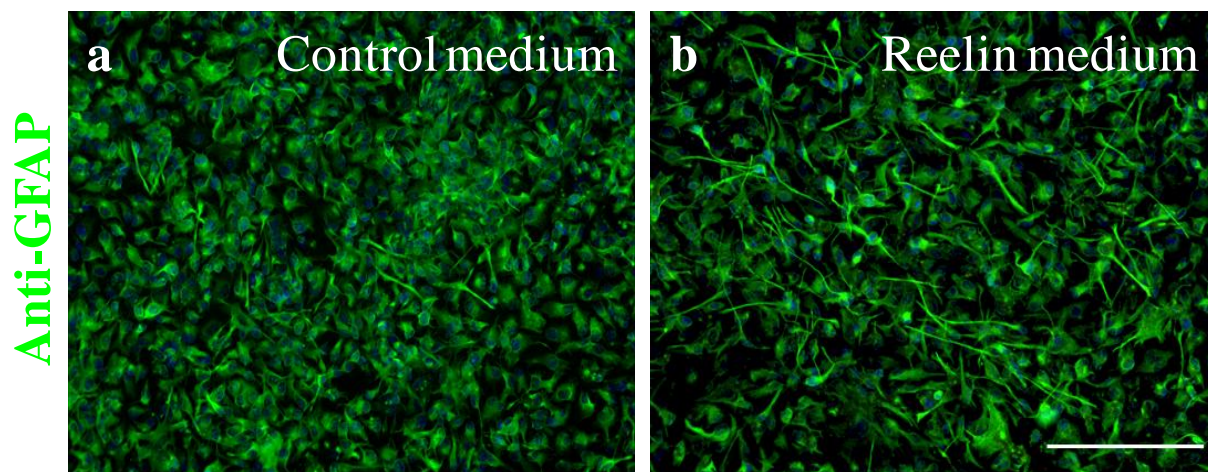


**Figure 5: Reelin treatment *in vitro* induces a radial glial phenotype.**

The hNPCs were deprived of FGF and EGF for 24 hours and treated with control or Reelin-conditioned media for another 24 hours before fixation. The cells were later stained against GFAP. Scale bar is 200  $\mu\text{m}$ .

To confirm that Reelin signaling is induced after Reelin treatment, the hNPCs were treated with control- or Reelin-conditioned media for 0, 15, 30 or 60 minutes. The conditioned media was prepared by diluting the purified control or Reelin in ReNcell CX maintenance media at a final concentration of 1:40. The induction of Reelin signaling was determined by measuring the level of Dab-1 phosphorylation on the tyrosine residue 198. As a result, we found that Dab-1 tyrosine phosphorylation increased with time after Reelin treatment, whereas it remained constant with the control treatment (Figure 6).

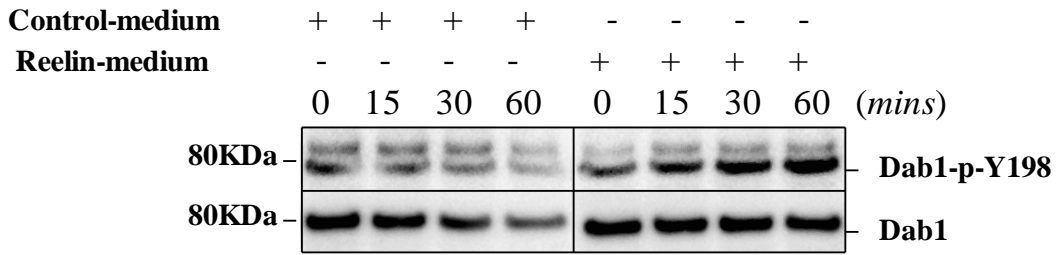


**Figure 6: Reelin treatment of hNPCs induces Dab-1 phosphorylation on tyrosine residue 198.**

The hNPCs were treated with control- or Reelin-conditioned media for 0, 15, 30 or 60 minutes before cell isolation. Dab-1 phosphorylation was measured by detecting the phosphorylation level on the tyrosine residue 198.

### *Reelin Treatment of hNPCs Induces the Formation of Neurogenic Radial Glia*

A recent elegant study using Cre/loxP fate mapping, showed that all neuronal population in the mouse brain are derived from radial glial cells expressing BLBP<sup>3</sup>. It's been suggested that the induction of BLBP marks the onset of radial glia neurogenesis where BLBP expression in radial glial cells have been shown to be up-regulated at the onset of neurogenesis and maintained as neurogenesis proceeds<sup>3</sup>. BLBP expression in cortical radial glia as well as its role in radial process extension was recently found to be dependent on Reelin signaling<sup>11</sup>.

To investigate if the Reelin-induced radial glial cells we observed in (Figure 5) are neurogenic, we measured the expression of BLBP in the formed radial glia. The hNPCs were deprived of FGF and EGF for 24 hours and then treated with control- or Reelin- conditioned media for another 24 hours before fixation. The induced neurogenic radial glia were determined by finding the percentage of the GFAP positive cells that had induced BLBP expression and a bipolar morphology with at least one thin process longer than 50  $\mu\text{m}$ <sup>11,46</sup>.

As shown in (Figure 7), Reelin treatment up-regulated BLBP expression and induced a bipolar radial morphology. The percentage of the neurogenic radial glia increased from (3.40 $\pm$ 0.04) % in the control treated cells to (9.48 $\pm$ 0.68) % in the Reelin treated cells, \*p-value < 0.05.



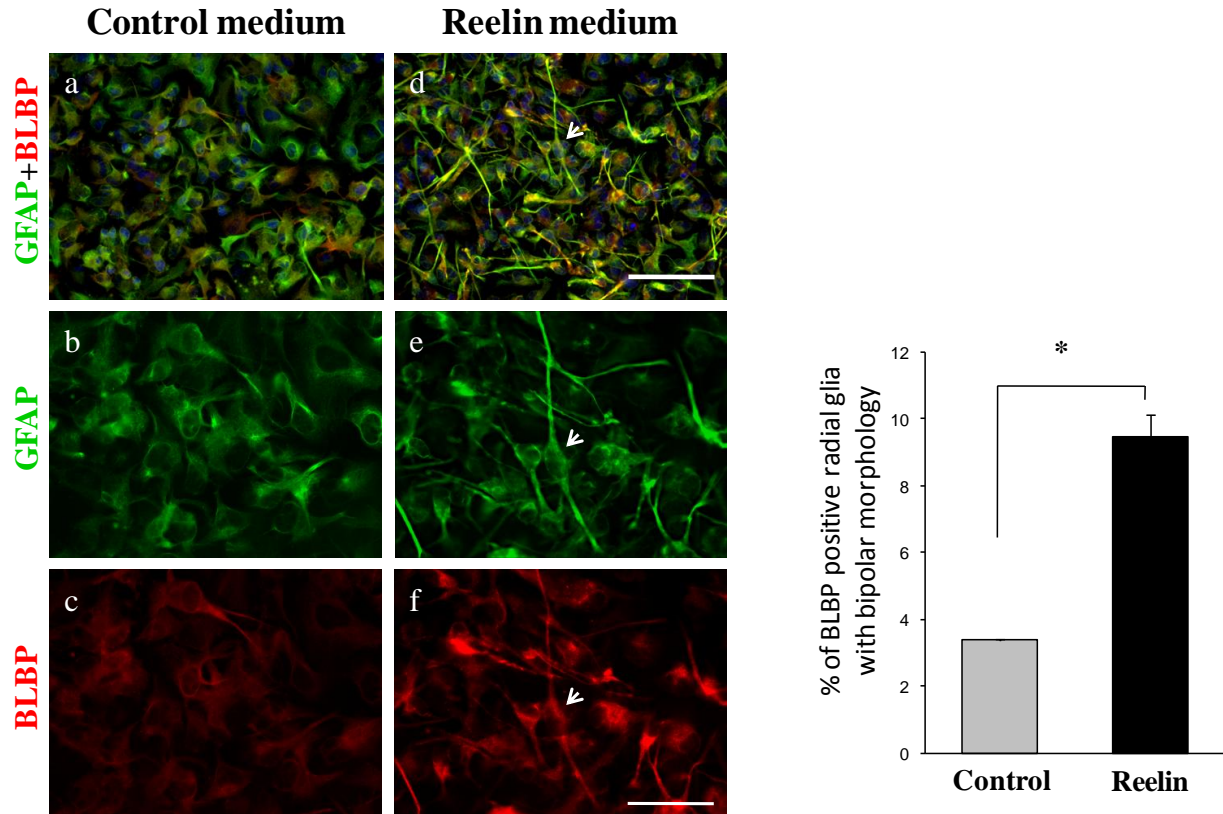


**Figure 7: Reelin treatment induces neurogenic radial glial cells in hNPCs.**

The hNPCs were deprived of FGF and EGF for 24 hours and then treated with either control- or Reelin-conditioned media for another 24 hours before fixation. The cells were then stained against GFAP (green) and BLBP (red). The percentage of the BLBP-positive radial glia increased from (3.40±0.04) % in the control treated cells (a-c) to (9.48±0.68) % in the Reelin treated cells (d-f), \*p-value< 0.05. Arrows point to a GFAP positive cell with induced BLBP expression and a bipolar morphology. The data points represent the mean ± standard error of at least three independent experiments. One-way ANOVA followed by Tukey's post-hoc test was used for the statistical analysis. Values that are significantly different from each other according to Tukey's test are indicated by asterisks. Scale bars for a and d is 100 μm and for b, e, c and f is 50 μm.

*The Reelin-induced Radial Glial Phenotype is Dependent on Notch-1 Activation*

It has been shown that Notch-1 signaling regulates the molecular and the morphological differentiation and maturation of radial glia through the transcriptional activation of BLBP<sup>25, 26</sup>.

To test if Reelin acts on Notch-1 activation to promote the formation of the neurogenic radial glia, we first compared the induced radial glial phenotype obtained after Reelin treatment and Notch-1 activation.

NICD overexpression was used to mimic Notch-1 activation. The hNPCs were deprived from FGF and EGF for 24 hours and were then treated with Reelin or transfected with NICD for another 24 hours before fixation. The cells were later stained against BLBP and GFAP and the induced neurogenic radial glia was determined by finding the percentage of the GFAP positive cells that had induced BLBP expression and a bipolar morphology with at least one thin process longer than 50  $\mu\text{m}$ <sup>11, 46</sup>.

As shown in (Figure 8), Reelin treatment and NICD transfection resulted in similar neurogenic radial glial phenotype. NICD transfection increased the percentage of the BLBP-positive radial glia from (2.31±0.23) % in the empty vector transfected cells to (6.19±0.28) % in the NICD transfected cells, \*p-value< 0.05. In contrast, Reelin treatment increased their percentage from (3.40±0.04) % in the control treated cells to (9.48±0.68) % in the Reelin treated cells, \*\*p-value< 0.05.

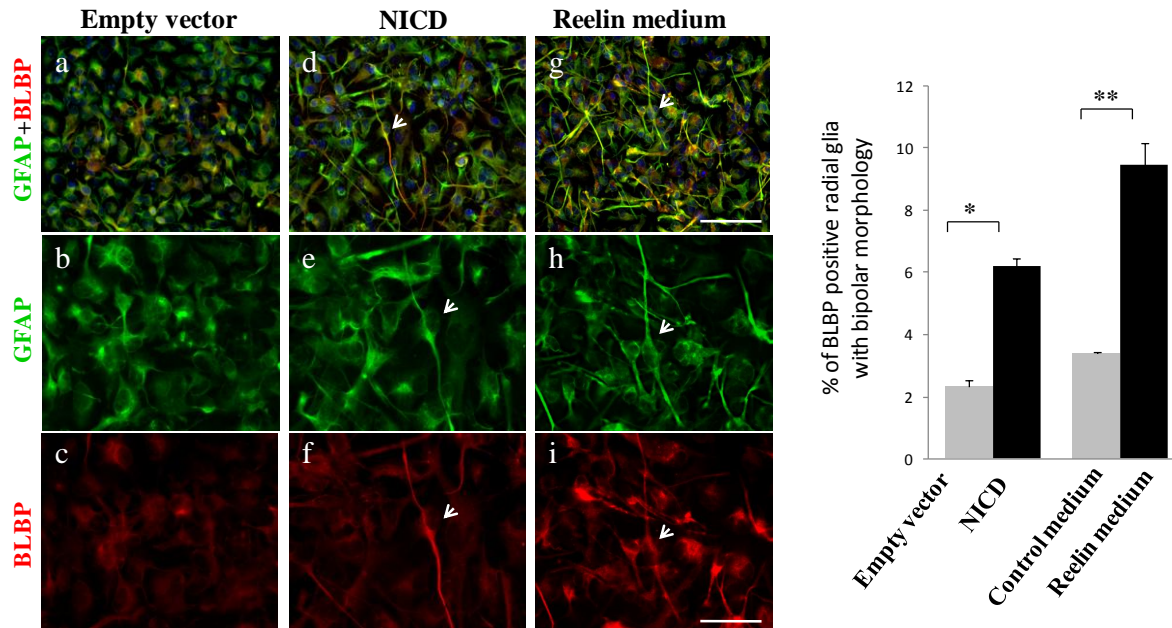


**Figure 8: Reelin treatment induces a radial glial phenotype similar to Notch-1 activation.**

The hNPCs were deprived of FGF and EGF for 24 hours prior to their transfection or treatment. The cells were later transfected with either the empty vector or NICD for 24 hours before fixation. The percentage of the BLBP-positive radial glia increased from (2.31±0.23) % in the empty vector transfected cells (a-c) to (6.19±0.28) % in the NICD transfected cells (d-f), \*p-value < 0.05. In comparison, the percentage of the BLBP-positive radial glia increased from (3.40±0.04) % in the control treated cells to (9.48±0.68) % in the Reelin treated cells (g-i), \*\*p-value < 0.05. Arrows point to a GFAP positive cell with induced BLBP expression and a bipolar morphology. The data points represent the mean ± standard error of at least three independent experiments. One-way ANOVA followed by Tukey's post-hoc test was used for the statistical analysis. Values that are significantly different from each other according to Tukey's test are indicated by asterisks. Scale bar for a, d and g is 100 µm and for b, e, c, f, h and i is 50 µm.

To test the dependency of Reelin signaling on Notch-1 activation to induce the radial glial phenotype, we blocked NICD release by inhibiting the activity  $\gamma$ -secretase. The cells were deprived of FGF and EGF for 24 hours and then treated with either control- or Reelin-conditioned media supplemented with 10  $\mu$ M of the  $\gamma$ -secretase inhibitor (L- 685, 458) for another 24 hours.

As shown in (Figure 9), the inhibition of  $\gamma$ -secretase activity in the Reelin treated cells reduced the percentage of the radial glial cells from (9.48 $\pm$ 0.68) % to (1.58 $\pm$ 0.03) %, \*\*\*p-value < 0.05. These data suggest that Reelin's role in inducing the radial glial phenotype is dependent on the activity of  $\gamma$ -secretase.

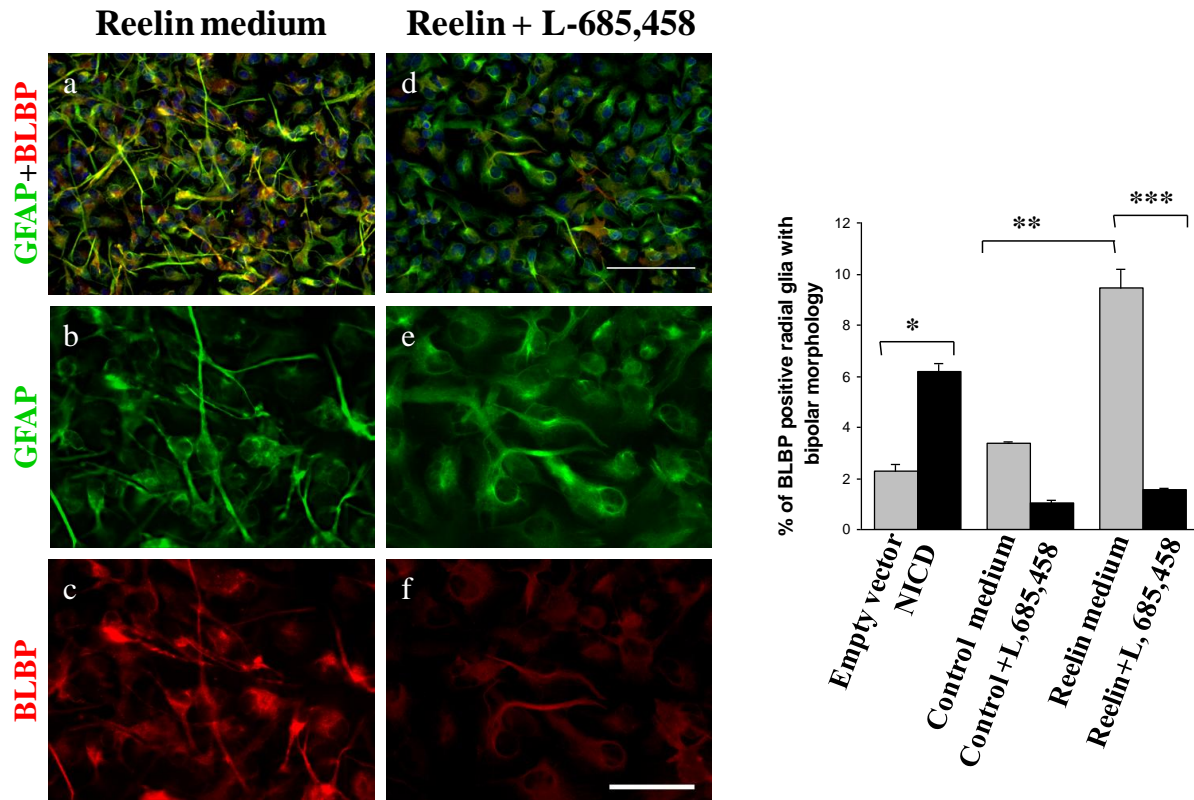


**Figure 9: The Reelin-induced radial glial phenotype is dependent on  $\gamma$ -secretase activity.**

The hNPCs were deprived of FGF and EGF for 24 hours and then treated with control- or Reelin-conditioned media supplemented with either 0.1% DMSO as a control or 10  $\mu$ M of the  $\gamma$ -secretase inhibitor L-685,458 for another 24 hours. The inhibition of  $\gamma$ -secretase activity in the Reelin treated cells abolished Reelin's effect by reducing the percentage of the BLBP-positive radial glia from (9.48 $\pm$ 0.68) % to (1.58 $\pm$ 0.03) %, \*\*\*p-value<0.05. The data points represent the mean  $\pm$  standard error of at least three independent experiments. One-way ANOVA followed by Tukey's post-hoc test was used for the statistical analysis. Values that are significantly different from each other according to Tukey's test are indicated by asterisks. Scale bar for a and d is 100  $\mu$ m and for b, e, c and f is 50  $\mu$ m.

### *Reelin Treatment Activates Notch-1*

To determine if Reelin regulates Notch-1 signaling, we measured the protein levels of NICD after Reelin treatment using an antibody that can recognize only the activated form of Notch-1 (NICD). The hNPCs were treated with control- or Reelin-conditioned media supplemented with either 0.1% DMSO or 10  $\mu$ M of the  $\gamma$ -secretase inhibitor (L, 685, 458) for 24 hours. As shown in (Figure 10), Reelin treatment increased NICD levels by (1.68 $\pm$ 0.07) fold when compared to the control treated cells (1.00 $\pm$ 0.10) fold, \*p-value<0.05. In contrast, the inhibition of  $\gamma$ -secretase activity in the Reelin-treated cells reduced NICD levels back to (1.13 $\pm$ 0.02) fold, \*\*p-value<0.05.

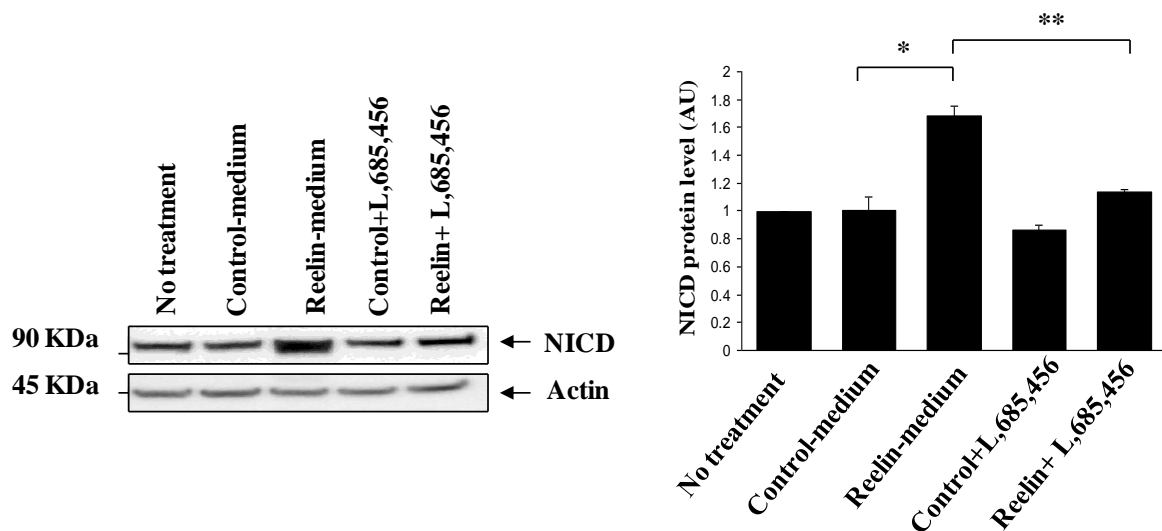


**Figure 10: Reelin treatment activates Notch-1.**

The hNPCs were treated with control- or Reelin-conditioned media supplemented with either 0.1% DMSO or 10 $\mu$ M of the  $\gamma$ -secretase inhibitor (L, 685, 458) for 24 hours. Reelin addition *in vitro* increased the accumulation of NICD by (1.68 $\pm$ 0.07) fold when compared to the control treated hNPCs (1.00 $\pm$ 0.10) fold, \* p-value<0.05. The inhibition of  $\gamma$ -secretase activity abolished this increase and reduced NICD levels back to (1.13 $\pm$ 0.02) fold, \*\* p-value<0.05. The data points represent the mean  $\pm$  standard error of at least three independent experiments. One-way ANOVA followed by Tukey’s post-hoc test was used for the statistical analysis. Values that are significantly different from each other according to Tukey’s test are indicated by asterisks.

### *Reelin Increases Dab-1 Binding to Notch-1*

Next we tested if Dab-1 binds to Notch-1 and if Reelin can increase the binding of Dab-1 to Notch-1. The hNPCs were treated with control- or Reelin-conditioned media for 15 minutes at 4°C to allow Reelin binding the cell surface. The unbound Reelin was then washed away with PBS and the cells were incubated for 15 minutes at 37 °C before isolation.

An immunoprecipitation using an antibody recognizing Notch-1 co-immunoprecipitated Dab-1 in both the control and the Reelin treated cells (Figure 11-a). Similarly, an immunoprecipitation using an antibody against Dab-1 was able to co-immunoprecipitate full-length Notch-1 in both the control and the Reelin treated cells (Figure 11-b). In both cases, Reelin treatment increased the binding of Dab-1 to Notch-1.



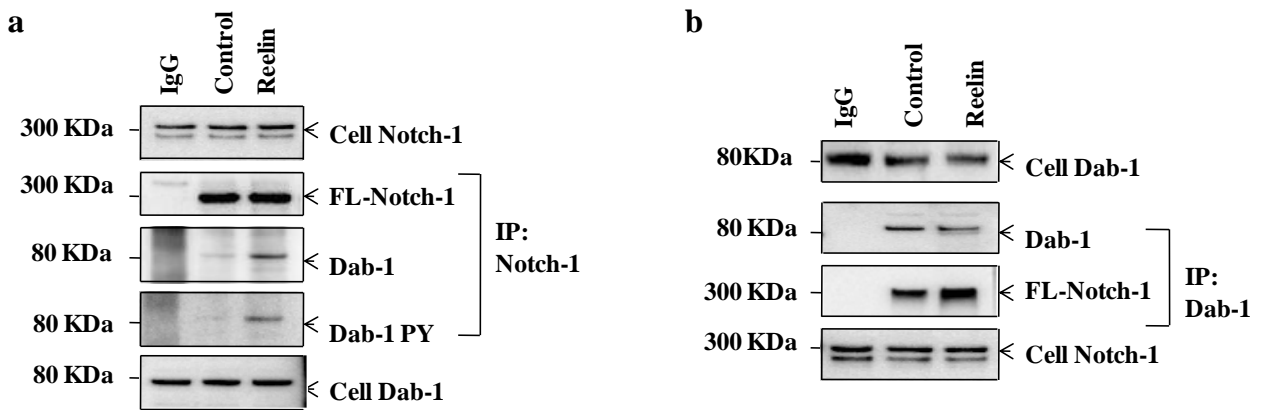


**Figure 11: Reelin increases the binding of Dab-1 to Notch-1.**

The hNPCs were treated with control- or Reelin-conditioned media for 15 minutes at 4°C to allow Reelin binding the cell surface. The unbound Reelin was then washed away with PBS and the cells were incubated for 15 minutes at 37 °C before isolation. Western blots showing reciprocal co-immunoprecipitation (IP). (a) Co-immunoprecipitation of Dab-1 by Notch-1 (b) Co-immunoprecipitation of Notch-1 by Dab-1.

## Discussion

Reelin and Notch-1 signaling pathways have been recently found to be necessary to induce the expression of BLBP and to promote the process extension and the maturation of the neuronal progenitors, the radial glial cells<sup>11, 25, 26, 29</sup>.

The end of neurogenesis in the cortex is marked by the transformation of the radial glial cells into astrocytes<sup>4</sup>. Notch-1 activation has been known for its role in promoting both phenotypes, the formation of the radial glial cells and their transformation into astrocytes. Interestingly, Notch-1 activation has been shown to induce radial glial cells differentiation prenatally and to induce astrocytic differentiation postnatally<sup>31, 32</sup>. Therefore, the presence of other signaling pathways that act to induce the radial glial phenotype prenatally but are deactivated or downregulated postnatally seems to be an attractive model to explain how Notch-1 activation leads to different cellular fates at different developmental stages.

Reelin signaling has been recently shown to induce the radial glial phenotype *in vitro* and to rescue the defects in the reeler mutant radial glia<sup>11</sup>. Interestingly, Cajal-Retzius cells, the cells that produce Reelin in the cortical marginal zone, are thought to either degenerate postnatally<sup>41</sup> or undergo developmental dilution<sup>42</sup>.

Here, we propose that Reelin signaling promotes Notch-1 activation to favor the radial glial phenotype prenatally. To test our hypothesis, we used human neural progenitor cells that were

isolated from the cortex of 14 weeks fetus. We show that these cells responded to Reelin treatment by inducing a bipolar morphology in the GFAP positive cell indicating the formation of radial glia (Figure 7). Since this Reelin-induced phenotype was dependent on  $\gamma$ -secretase activity (Figure 9), and since Reelin treatment increased the protein levels of NICD (Figure 10), then we concluded that Reelin signaling promotes the radial glial phenotype by activating Notch1.

Reelin signaling might regulate Notch-1 activation via increasing Dab-1 binding to Notch-1 (Figure 11). It's possible that Reelin signaling mediated by Dab-1 increases the NICD protein levels by either increasing Notch-1 processing by  $\gamma$ -secretase or by stabilizing the released NICD. Since Dab-1 has been recently shown to act as a nucleocytoplasmic shuttling protein<sup>50</sup>, Dab-1 may in turn mediate the translocation of NICD into the nucleus to activate downstream genes such as BLBP. However, the exact mechanism needs further elucidation.

Taken together, this study offers a new insight of how Reelin and Notch-1 signaling are determining that fate of the neural progenitor cells and maintaining the radial glial phenotype in the developing brain.

## **CHAPTER THREE: REELIN ACTIVATES NOTCH-1 SIGNALING THROUGH DISABLED-1 TYROSINE PHOSPHORYLATION**

### **Introduction**

Reelin is a large secreted glycoprotein that has been shown to be an important signal for neuronal migration and proper positioning of neurons in the cerebral cortex and cerebellum<sup>12</sup>. Reelin signal is transmitted into the cells after Reelin binds its receptors, apolipoprotein receptor2 (ApoER2) and the very low density lipoprotein receptor (VLDLR). Reelin binding initiates Disabled-1 (Dab-1) binding to the internalization (NPXY) motif of ApoER2 and VLDLR, leading to the induction of Dab1 tyrosine phosphorylation<sup>14</sup>. Tyrosine phosphorylation of Dab-1 creates new binding sites for Src kinases and results in the activation of phosphoinositide-3-Kinase (P13-K)-dependent kinase and Akt<sup>15-17</sup>. Mice deficient in VLDLR and ApoER2, Dab1 or Dab1 that cannot be tyrosine phosphorylated generates a reeler-like phenotype, which is characterized by inversion of the cortical layers and abnormalities in the laminated brain structures<sup>18</sup>.

Recently, reeler mice were shown to exhibit abnormal development of the radial glial scaffold in the dentate gyrus of the hippocampus<sup>19</sup>. Radial glia, as their name indicates, extend a long radial process to the pial surface while having their cell bodies in the ventricular zone (VZ) thus allowing the migration of neurons from the VZ to the post-mitotic areas<sup>5</sup>. However, the finding that these cells can also give birth to the migratory neurons, via their asymmetric division<sup>6, 7</sup>, further highlighted the significance of these cells in brain development. Interestingly, radial glial

cells disappear or transform into astrocytes in most regions of the mammalian brain after neuronal generation and migration are completed<sup>4</sup>.

A recent study showed that Notch-1 signaling regulates the molecular and the morphological differentiation of radial glia through the transcriptional activation of brain lipid binding protein (BLBP)<sup>25, 26</sup>. Notch activation, upon binding its ligand, will initiate its cleavage by  $\gamma$ -secretase to generate Notch intracellular domain (NICD). NICD translocates to the nucleus and binds C-promoter Binding Factor 1 (CBF1), converting it from transcriptional repressor to transcriptional activator<sup>27, 28</sup>. Interestingly, BLBP expression was found to be dependent on this pathway<sup>25, 26</sup>, where a binding site for the Notch effector CBF1 was found in the promoter region of BLBP<sup>29</sup>. BLBP expression in cortical radial glia as well as its role in radial process extension was also found to be dependent on Reelin signaling<sup>11</sup>.

In our previous work (Chapter two), we found that Reelin addition to the hNPCs induced BLBP expression and increased the formation of radial glia. The Reelin-induced radial glial cells were shown to be dependent on Notch-1 activation. We found that Reelin activates Notch-1 signaling by increasing the level of Notch-1 intracellular domain (NICD). Reducing NICD levels, by inhibiting  $\gamma$ -secretase activity, inhibited the Reelin-induced radial glia. These data indicated that Reelin induces BLBP expression and the formation of radial glia via activating Notch-1<sup>51</sup>.

Here, we investigated the molecular mechanisms by which Reelin activates Notch-1. We found that the Reelin-induced tyrosine phosphorylation of Dab-1 and the subsequent activation of Src

family kinases are essential steps for Notch-1 activation by Reelin. In addition, Reelin treatment increased Dab-1 binding to NICD and enhanced NICD translocation to the nucleus to induce the expression of BLBP. Reelin treatment did not enhance  $\gamma$ -secretase processing of Notch-1, suggesting that Reelin increases NICD levels by an alternative mechanism. Finally, Reelin treatment significantly enhanced neurogenesis in hNPCs *in vitro*.

## **Materials and Methods**

### *Cell Culture*

We used ReNcell CX (Chemicon), an immortalized human neural progenitor cell line (hNPCs). The cells were cultured in ReNcell NSC maintenance media (Chemicon) supplemented with 20ng/ml of the fibroblast growth factor (FGF) and 20ng/ml and of the epidermal growth factor (EGF) (Chemicon).

For transfection of hNPCs, the cells were plated on laminin coated (Sigma Aldrich) 12-well culture plates (BD biosciences) for 24 hours or until they reached 90% confluency. The cells were then transiently transfected with 2  $\mu$ g of DNA/well using lipofectamine LTX and PLUS reagents according to manufacturer's protocol (Invitrogen). The transfection efficiency was determined by finding the percentage of the Green Fluorescent Protein (GFP) positive cells 24 hours after transfecting the hNPCs with EGFP vector (Invitrogen). The transfection efficiency was optimized by transfecting the cells with different ratios of DNA/PLUS/lipofectamine, where the best transfection efficiency was found to be 30-40%, using the ratio of 1/3/3, respectively.

For  $\gamma$ -secretase inhibition, 10  $\mu$ M of the  $\gamma$ -secretase inhibitor (L-685, 458; Sigma Aldrich) was dissolved in the maintenance media. For the control cells, we added the maintenance media containing 0.1% DMSO.

To inhibit cell endocytosis, we treated hNPCs with a hypertonic sucrose solution (0.5M)<sup>52</sup>. The cells were first treated with control- or Reelin-conditioned media for 15 minutes at 4°C. The unbound Reelin was washed away with PBS and the cells were incubated with 0.5M sucrose prepared in cell media for 30 minutes at 37°C.

To inhibit Src activity, hNPCs were pre-treated with 10  $\mu$ M of the Src inhibitor PP2 for 1 hour at 37°C<sup>52</sup>. As a control, hNPCs were pre-treated with 10  $\mu$ M of PP3 (inactive analog of PP2). The cells were later treated with either control- or Reelin-conditioned media for 1 hour in the presence of PP2 or PP3.

pDsDab1RFP (wild-type mouse Dab1-RFP fusion protein) and pDsDab1RFP-5F (a Dab1 mutant with five tyrosines mutated to phenylalanines) clones<sup>53</sup> were kindly provided by Dr. Brian W. Howell, Neurogenetics Branch, National Institute of Neurological Diseases and Stroke, National Institutes of Health, Bethesda, Maryland.

### *Reelin Production and Treatment*

Reelin- and control-containing media were collected from HEK293 cells stably transfected with RELIN pCRL vector (kindly provided by T. Curran, St. Jude Children's Hospital, Memphis Tennessee, USA), and a control empty pcDNA3.1 vector (Invitrogen), respectively<sup>19, 43, 44</sup>. The cells were cultured in neurobasal media (Invitrogen) for 3 days before media collection. Reelin was partially purified using columns with filters >100kDa (Chemicon) and Reelin level was estimated by Western blotting using anti-Reelin clone G10 (Chemicon) that detected the three characteristic bands of Reelin (400 KDa, 300 KDa, and 180 KDa)<sup>15</sup>.

The conditioned media that was used to treat hNPCs was prepared by diluting the purified Reelin in ReNcell CX maintenance media at a final concentration of 1:40. This concentration was determined by finding the lowest concentration of Reelin that can induce Dab-1 phosphorylation as early as 15 minutes.

The hNPCs were also co-cultured with HEK293 cells that stably express Reelin using millicell culture inserts (Millipore). The hNPCs were plated at the bottom of the 6-well plates while the HEK293 cells were plated in the insert. The cells were deprived of FGF and EGF and the media for both cell lines was partially changed (50%) every day. Reelin expression in Hek293 cells and in its passage through the insert's membrane was confirmed by detecting the levels of Reelin in the media of the co-cultured HEK293 cells and hNPCs using western blotting.



### *Protein Isolation and Western Blot Analysis*

The hNPCs were lysed in ice-cold RIPA (Radio-Immunoprecipitation Assay) lysis buffer (Sigma Aldrich) containing 150 mM NaCl, 1% IGEPAL CA-630, 0.5% sodium deoxycholate, 0.1% SDS, and 50 mM Tris, pH 8.0, supplemented with 1% Triton-X and protease inhibitor mixture (Calbiochem). The cell lysates were centrifuged at 12,000 xg for 30 min at 4°C and the supernatants were saved for analysis. Proteins (40µg/well) were separated by SDS-Polyacrylamide gel electrophoresis (NuPage 4%-12% Bis-Tris gel, Invitrogen) for 60 min at 200 V, and then blotted onto polyvinylidene difluoride (PVDF) membranes (Bio-rad) for 120 min at 30 V. For the detection of full-length Notch-1, NICD, Reelin,  $\beta$ -actin, Dab-1 and pY198Dab-1, the PVDF membranes were incubated overnight with following primary antibodies, respectively: mouse anti-Notch-1 (1:1,000; Sigma Aldrich), rabbit anti-activated Notch-1 (1:500; Abcam), mouse anti-Reelin clone 142 (1:1000; Chemicon), rabbit anti- $\beta$ -actin (1:1,000; Cell Signaling Technology, Danvers, MA), rabbit anti-Dab1 (1:1000; Abcam) and rabbit anti-Dab1 phosphotyrosine 198 (1:1000; Abcam). After washing the membranes with phosphate buffered saline with Tween 20 (PBST- Sigma Aldrich), the membranes were incubated with the appropriate horseradish peroxidase-conjugated secondary antibodies at concentration of 1:5000 (anti-mouse IgG or anti-rabbit IgG; Jackson ImmunoResearch, West Grove, PA) for 2 hrs. Immunoreactivities were detected by chemiluminescence using the enhanced chemiluminescence (ECL) system (Amersham Biosciences Corp) on a Kodak Imaging Station IS2000MM. The optical density of each specific band relative to  $\beta$ -actin was analyzed by Image J software (National Institutes of Health).

For nuclear extraction, the plated hNPCs were lysed using a subcellular fractionation buffer (250 mM Sucrose, 20 mM HEPES (pH 7.4), 10 mM KCl, 1.5 mM MgCl<sub>2</sub>, 1 mM EDTA, 1 mM EGTA, 1 mM DTT, supplemented with protease inhibitor mixture (Calbiochem)). The nuclear pellet (P1) was centrifuged out at 3000 rpm for 5 minutes and then washed once by adding 500µl of the fractionation buffer. The nuclear pellet was centrifuged again at 3000 rpm for 10 minutes and the pellet was resuspended in the nuclear buffer (RIPA with 10% glycerol and 0.1% SDS). The pellet was then sonicated briefly for 3 seconds at a power setting of 2-continuous. Finally, the nuclear pellet was centrifuged at 16,000 xg for 30 minutes and the final supernatant was used for analysis.

### *Immunoprecipitation*

The hNPCs were lysed in ice-cold RIPA (Radio-Immunoprecipitation Assay) lysis buffer (Sigma Aldrich) containing 150 mM NaCl, 1% IGEPAL CA-630, 0.5% sodium deoxycholate, 0.1% SDS, and 50 mM Tris, pH 8.0, supplemented with 1% Triton-X and protease inhibitor mixture (Calbiochem). 700µg proteins were incubated for 3 hours at 4°C with the primary antibody anti-Dab1 (1:100; Abcam) or anti-NICD (1:500; Abcam). Protein A-Sepharose beads were added for 1 hr at 4°C, and then immunoprecipitates were washed 5 times with RIPA lysis buffer. Immunoprecipitated proteins were solubilized in sample buffer containing 1% SDS and resolved on a 4-12% Bis-Tris gel (Invitrogen).

### *Fluorescent Immunocytochemistry*

The hNPCs were plated on laminin coated (Sigma Aldrich) 8-wells-chambers slides (BD biosciences) for 24 hours. After treatment, hNPCs were fixed with 4% Paraformylaldehyde (Sigma Aldrich) overnight at 4°C. Then, the cells were washed three times with phosphate buffered saline (PBS- Sigma Aldrich) at room temperature and blocked with 3% donkey serum (Jackson ImmunoResearch Labs) in phosphate buffered saline with Tween 20 (PBST- Sigma Aldrich) for 1 hour at room temperature. The hNPCs were incubated for 24 hrs at 4° C, with the following primary antibodies: rabbit anti-Nestin (1:200; Millipore) with Goat anti-Doublecortin (C-18) (1:50; Santa Cruz biotech); rabbit anti-BLBP (1:50; Abcam) with mouse anti-Notch-1 (1:500; Sigma Aldrich), rabbit anti- Notch-1 (1:500; cell signaling) or rabbit anti-VLDLR (H-95) (1:500; Santa Cruz Biotech) with mouse anti-Reelin clone 142 (1:1000; Chemicon). After washing the cells with PBS for three times the cells were incubated with Tetramethyl Rhodamine Iso-Thiocyanate (TRITC)-conjugated or Fluorescein isothiocyanate (FITC)-conjugated anti-mouse or anti-rabbit or anti-goat (1: 500; Jackson ImmunoResearch Labs) for 2 hrs at room temperature in the dark. The cells were washed again and mounted with vectasheild with DAPI (vector laboratories) and cover slipped for microscopic observations.

### *Microscopy and Analysis*

The percentage of radial glial phenotype in a culture was calculated by counting the number of the Nestin positive cells that had a bipolar morphology with at least one thin process longer than 50 µm against the total number of cells. This criterion was based on previous studies<sup>11, 46</sup>. Adobe

Photoshop CS3 software was used to count the number of cells. Microscopic images were taken with the QImaging MicroPublisher 5.0 color digital imaging system and processed using the QCapture software (Leeds, Irving, TX).

#### *In-vitro $\gamma$ -secretase Assay*

To measure  $\gamma$ -secretase activity after Reelin treatment, hNPCs were treated with either control- or Reelin-conditioned medium for 12 hours. As a positive control, hNPCs were treated with either 10  $\mu$ M of the  $\gamma$ -secretase inhibitor L-685,458 or 0.1% DMSO for 12 hours. The  $\gamma$ -secretase activity was measured using a  $\gamma$ -secretase activity kit according to manufacturer's protocol (R & D systems). The treated hNPCs were extracted using the extraction buffer provided with the kit. The assay was set-up in triplicates. In short, 50  $\mu$ L of cell lysate (i.e. derived from approximately 2 - 5 x 10<sup>6</sup> cells or 25 - 200  $\mu$ g of total protein), 50  $\mu$ L of 2X Reaction Buffer and 5  $\mu$ L of Substrate were added to each well of a microplate. The plate was incubated in the dark at 37°C for 2 hours. The plate was read on a fluorescent microplate reader using light filters that allow for the excitation of the reporter molecule EDANS at 355 nm wavelengths. Emission was measured at 510 nm. As a negative control, the reactions were prepared without the cell lysate. The results were expressed as the percent of increase of fluorescence over that of the negative control.

### *Statistical Analysis*

Each data point represents triplicated experiments and displayed as the mean  $\pm$  standard error. A one-way Analysis of Variance was performed to test the hypothesis that the average mean values across categories of GROUP were equal. In the presence of significance for the omnibus ANOVA test, Tukey multiple comparison test is used to perform pairwise comparisons. Statistics were performed using WINKS SDA Software (Texasoft, Cedar Hill, TX.)

## **Results**

### *Reelin Increases Neurogenesis in hNPCs*

We have previously shown that Reelin treatment of hNPCs *in vitro* induces a neurogenic radial glial phenotype that was characterized by the induction of BLBP expression in the bipolar GFAP positive cells (Figure 7). Since radial glial cells were reported to serve as neural progenitors for the majority of neurons in the CNS<sup>2, 3</sup> and since all the neuronal population in the mouse brain were found to be derived from radial glial cells expressing BLBP<sup>3</sup>, then we hypothesized that Reelin may increase neurogenesis by increasing the generation of BLBP positive radial glial cells.

To investigate this hypothesis, we co-cultured hNPCs with HEK293 cells that stably express Reelin in a culture insert (Figure 12), as described in materials and methods section. HEK293 cells that were stably transfected with an empty vector and thus lack the expression of Reelin were used as the control. Three days after the co-culture, hNPCs were fixed and stained with

Nestin as a marker for proliferating radial glial cells and Doublecortin (DCX) as a marker for newly born neurons (Figure 13).

To confirm that Reelin was able to pass through the membrane and diffuse into the hNPCs media, we checked the level of Reelin in the media from inside (HEK293 media) and outside (hNPCs media) of the culture insert 3 days after the co-culture. To detect both exogenous mouse and endogenous human Reelin, we used Reelin antibody clone 142. As shown in (Figure 12), Reelin is present in the media of the hNPCs only after the co-culture with the HEK293 cells that express Reelin; this confirms that these hNPCs do not produce Reelin by themselves and that Reelin can pass through the insert's membrane.

As supporting our previous results, Reelin treatment significantly increased the percentage of the bipolar radial glial cells *in vitro* (Figure 13). Radial glial cells were characterized as bipolar Nestin positive cells that extended a process longer than  $50\mu\text{m}$ <sup>11, 46</sup>. The percentage of the radial glial cells increased from  $(10.17\pm 0.67)$  % in the control treated cells to  $(18.51\pm 0.80)$  % in the Reelin treated cells,  $*p<0.05$ . Most importantly, Reelin treatment increased the percentage of the DCX immuno-positive cells from  $(7.13\pm 0.52)$  % in the control treated cells to  $(22.44\pm 0.46)$  % in the Reelin treated cells,  $(**p<0.05)$  (Figure 13). This suggests that in addition to Reelin's role in inducing the formation of neurogenic radial glia, it can also enhance neurogenesis in hNPCs *in vitro*.

Millicell cell culture insert-Side view

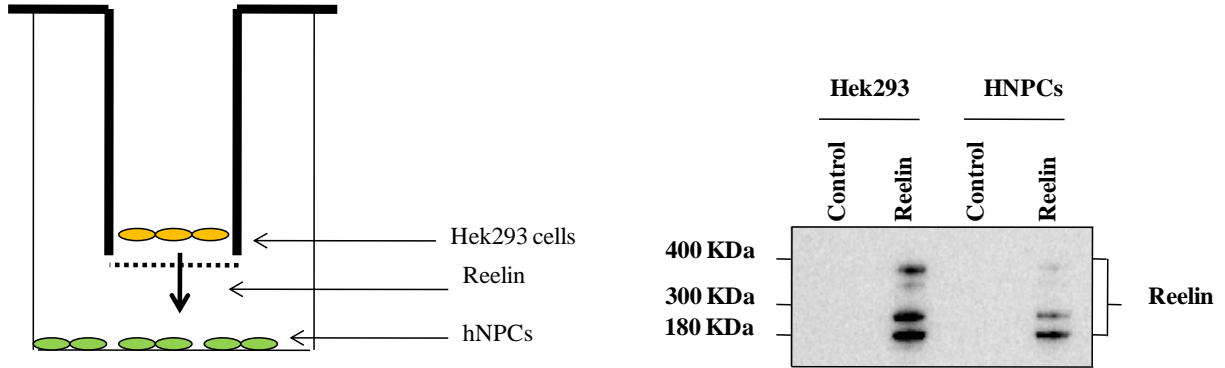


**Figure 12: Reelin expression in the media of HEK293 cells and the media of hNPCs.**

Reelin expression was confirmed in the media of HEK293 cells that were stably transfected with Reelin and plated in the insert and in the media of the underlying hNPCs after 3 days of the co-culture using western blotting. Reelin antibody clone 142 was used to detect the expression of both endogenous human and exogenous mouse Reelin. Reelin is shown to be present in the media of the hNPCs only after the co-culture with HEK293 cells that express Reelin.

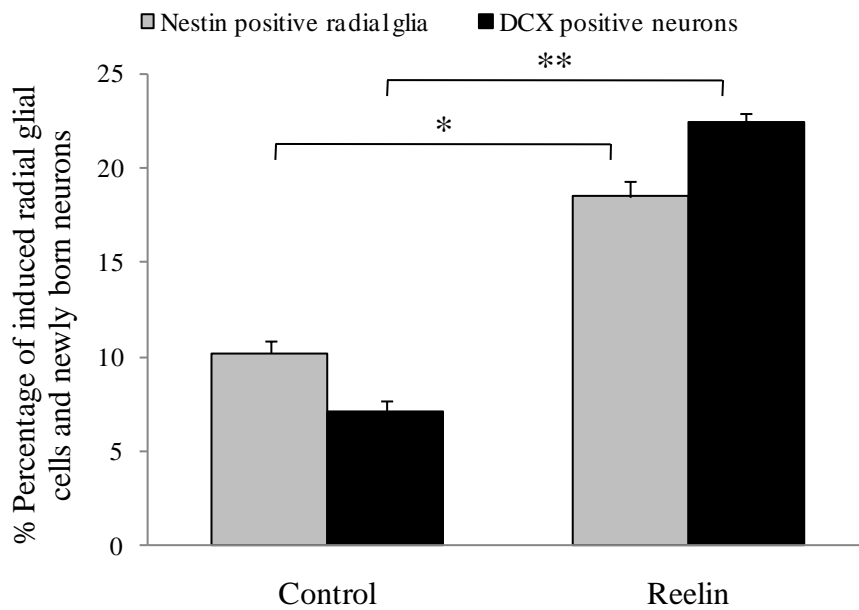
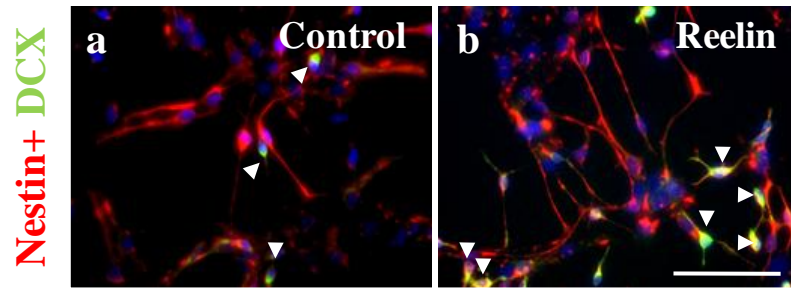


**Figure 13: Reelin increases neurogenesis in hNPCs *in vitro*.**

The hNPCs were co-cultured for 3 days with HEK293 cells that express Reelin. The cells were then fixed and stained with anti-Nestin (red) and anti-Doublecortin (green). Reelin treatment of the hNPCs increased the percentage of the bipolar radial glial cells from (10.17±0.67) % to (18.51±0.80) %, \*p<0.05, and increased the percentage of the Doublecortin immunopositive neurons from (7.13±0.52) % to (22.44±0.46) %, \*\*p<0.05. Blue is a DAPI for nuclei counterstaining. The data points represent the mean ± standard error of at least three independent experiments. One-way ANOVA followed by Tukey's post-hoc test was used for the statistical analysis. Values that are significantly different from each other according to Tukey's test are indicated by asterisks. Scale bars in the figure represent 100 μm.



*Reelin-induced NICD Levels is not via Increased Notch-1 Processing by  $\gamma$ -secretase*

In our previous study (Figure 10), we reported that treating hNPCs with Reelin increases the levels of NICD. To confirm our results we treated the hNPCs with control- or Reelin-conditioned media for 0, 3, 6, and 12 hours. As shown in (Figure 14), Reelin treatment increases NICD accumulation as early as 3 hours. After 6 hours of treatment, NICD levels reaches a peak (\*\* $p < 0.05$ ), and the level of the full length Notch-1 is significantly reduced (\* $p < 0.05$ ).

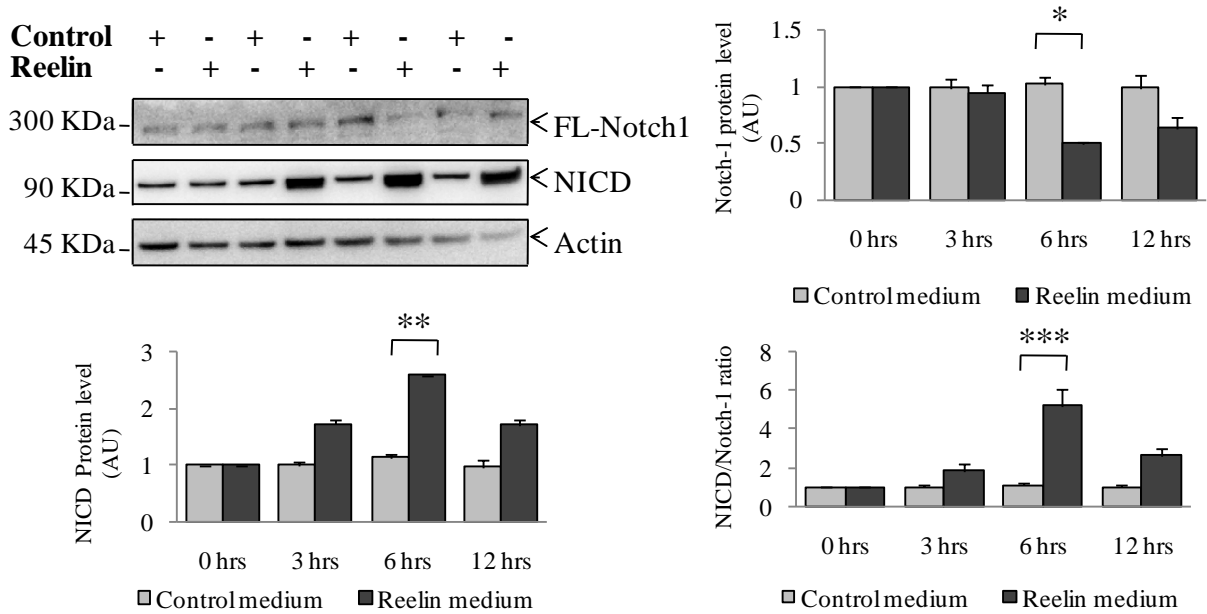


**Figure 14: Reelin treatment increases NICD levels in hNPCs.**

The hNPCs were treated with control- or Reelin-conditioned media for 0, 3, 6 and 12 hours before isolation. The levels of full length Notch-1 and NICD were normalized to  $\beta$ -actin levels. Reelin treatment increased NICD accumulation as early as 3 hours. After 6 hours of treatment, NICD level reaches a peak (\*\* $p < 0.05$ ), and the level of the full length Notch-1 is significantly reduced (\* $p < 0.05$ ). The data points represent the mean  $\pm$  standard error of at least three independent experiments. One-way ANOVA followed by Tukey's post-hoc test was used for the statistical analysis. Values that are significantly different from each other according to Tukey's test are indicated by asterisks.

NICD accumulation can be either due to increased processing of Notch-1, reduced degradation of NICD<sup>54</sup> or both. To examine if Reelin activates  $\gamma$ -secretase to enhance the processing of Notch-1 and to increase the release of NICD from the membrane, we performed an *in vitro* assay to measure the changes in the activity of  $\gamma$ -secretase after Reelin treatment. The hNPCs were treated with control- or Reelin- conditioned media for 12 hours. As a control, the hNPCs were treated with either 0.1% DMSO or 10  $\mu$ M of the  $\gamma$ -secretase inhibitor (GSI) L-685,458 for 12 hours. As shown in (Figure 15), inhibiting the activity of  $\gamma$ -secretase using the inhibitor L-685,458, reduced the enzymatic activity of  $\gamma$ -secretase from (4.25 $\pm$ 0.28) % to (1.32 $\pm$ 0.13) %, \*p<0.05. However, we didn't observe any significant changes in the activity of  $\gamma$ -secretase after Reelin treatment.

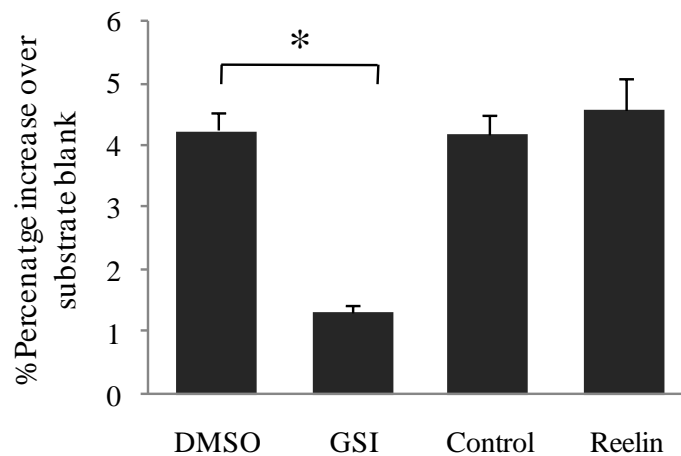


**Figure 15: Reelin does not enhance  $\gamma$ -secretase activity *in vitro*.**

To determine if Reelin activates  $\gamma$ -secretase, we measured the changes in the activity of  $\gamma$ -secretase using an *in vitro* assay after Reelin treatment. Treating hNPCs with 10  $\mu$ M of the  $\gamma$ -secretase inhibitor L-685,458 for 12 hours, reduced the enzymatic activity of  $\gamma$ -secretase from (4.25 $\pm$ 0.28) % to (1.32 $\pm$ 0.13) %, \* $p$ <0.05. However, we didn't observe any significant changes in the activity of  $\gamma$ -secretase after Reelin treatment. The data points represent the mean  $\pm$  standard error of at least three independent experiments. One-way ANOVA followed by Tukey's post-hoc test was used for the statistical analysis. Values that are significantly different from each other according to Tukey's test are indicated by asterisks. GSI stands for  $\gamma$ -secretase inhibitor.

Nevertheless, we thought that Reelin might be enhancing  $\gamma$ -secretase-mediated processing of Notch-1 by enhancing Notch-1 trafficking into sites of high  $\gamma$ -secretase activity. It has been documented that endocytosis of Notch-1 into early endosomes is important for Notch-1 activation<sup>55</sup>. Early endosomes have been identified to have high  $\gamma$ -secretase activity due to its low pH value<sup>56,57</sup>.

In order to determine if Reelin enhances Notch-1 trafficking to the early endosomes, we treated hNPCs with 0.5 M sucrose solution to inhibit cell endocytosis, as described in materials and methods. The hNPCs were treated with either control- or Reelin-conditioned media for 15 minutes at 4°C to allow Reelin binding to the cells. The cells were then washed and treated with 0.5M sucrose solution for 30 minutes at 37°C. In addition, we inhibited the activity of  $\gamma$ -secretase in the hNPCs as a reference point to compare it to the inhibition of NICD release by the sucrose treatment. Similarly, the cells were treated with control- or Reelin-conditioned media for 15 minutes at 4°C to allow Reelin binding to the cells. The cells were then washed and treated with 10  $\mu$ M of the  $\gamma$ -secretase inhibitor (GSI) L-685,458 for 30 minutes at 37°C.

As shown in (Figure 16, c),  $\gamma$ -secretase inhibition in the Reelin treated cells shifted NICD signals from diffused cytosolic signals as in (Figure 16, b) to membrane-bound signals. On the other hand, the inhibition of endocytosis using a hypertonic sucrose solution caused accumulation of Notch-1 on the cell surface and reduced its entry into the early endosomes (Figure 16, d).

Inhibiting  $\gamma$ -secretase activity in the Reelin treated cells reduced NICD levels from  $(1.97\pm 0.05)$  fold to  $(1.01\pm 0.12)$  fold,  $*p < 0.05$ . On the other hand, treating the cells with the hypertonic sucrose solution reduced the NICD levels in the Reelin treated cells to only  $(1.60\pm 0.08)$  fold,  $**p < 0.05$ . These data suggest that although the inhibition of endocytosis in the Reelin treated cells reduced the Reelin-induced NICD levels, it did not completely abolish Reelin's effect on NICD accumulation, indicating that Reelin increases NICD levels by a mechanism that does not involve enhanced  $\gamma$ -secretase processing of Notch-1.

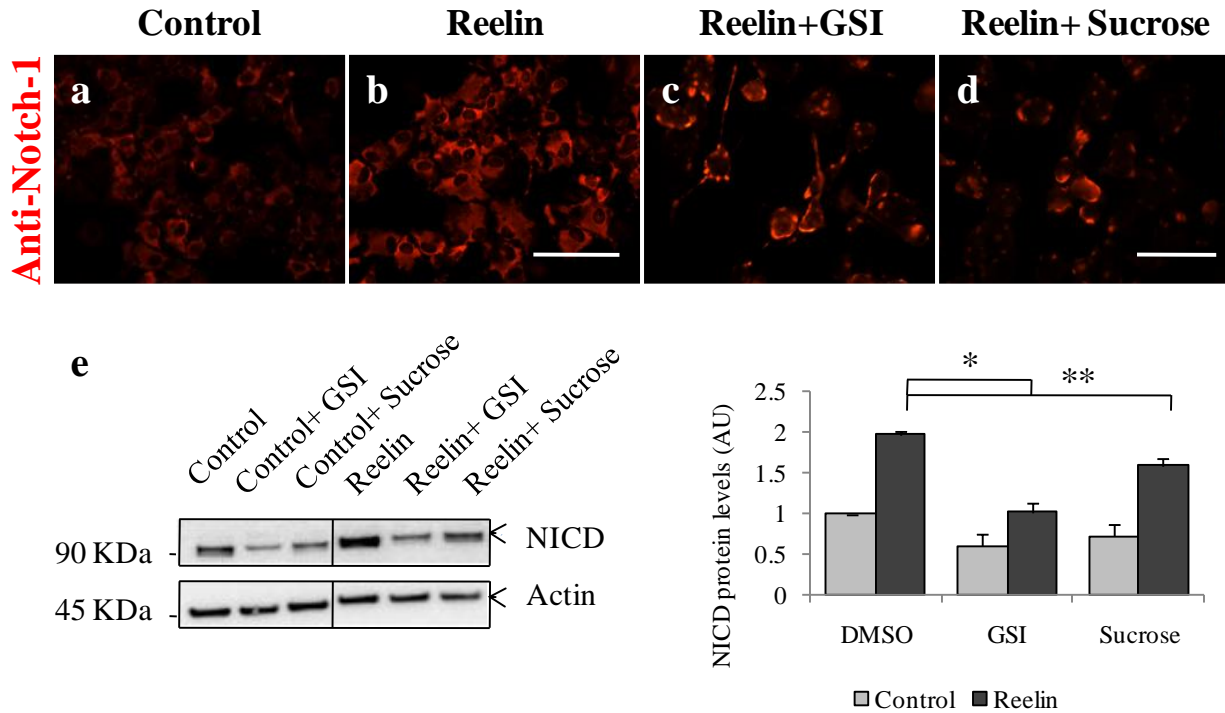


**Figure 16: Reelin-induced NICD accumulation is not due to enhanced Notch-1 endocytosis**

To investigate if Reelin increases NICD levels by enhancing Notch-1 endocytosis, we re-measured NICD levels after inhibiting endocytosis using 0.5M sucrose solution. The hNPCs were treated with control- or Reelin-conditioned media for 15 minutes at 4°C. The unbound Reelin was washed away using PBS and the cells were further incubated with 0.5M sucrose in for 30 minutes at 37°C. We inhibited the activity of  $\gamma$ -secretase in the hNPCs as a reference point to compare it to the inhibition of NICD release by the sucrose treatment. (a-b) Reelin treatment increased the levels of cytosolic NICD (red) when compared to the control treated cells. (c) Inhibiting  $\gamma$ -secretase activity in the Reelin treated cells shifts the cytoplasmic signal of NICD (red) into membrane-bound and reduced the fold change in the NICD levels from (1.97±0.05) fold to (1.01±0.12) fold, \*p<0.05. (d) The inhibition of endocytosis using 0.5 M sucrose retained Notch-1 on the membrane and reduced NICD levels in the Reelin treated cells to only (1.60±0.08), \*\*p<0.05. The data points represent the mean ± standard error of at least three independent experiments. One-way ANOVA followed by Tukey’s post-hoc test was used for the statistical analysis. Values that are significantly different from each other according to Tukey’s test are indicated by asterisks. Scale bars for a and b are 100  $\mu$ m and for c and d are 50  $\mu$ m. GSI stands for  $\gamma$ -secretase inhibitor.

We have previously shown that the Reelin-induced BLBP expression and the subsequent formation of the neurogenic radial glial cells were dependent on NICD generation (Figure 9). To determine if the Reelin-induced neurogenesis is dependent on NICD generation as well, we inhibited the activity of  $\gamma$ -secretase in the Reelin treated cells using the  $\gamma$ -secretase inhibitor (L-685,458). The hNPCs were co-cultured with HEK293 cells that stably express Reelin for 3 days and the maintenance media was supplemented with 10  $\mu$ M of  $\gamma$ -secretase inhibitor (L-685,458).

As shown in (Figure 17), the inhibition of  $\gamma$ -secretase activity in the Reelin treated cells reduced the percentage of the radial glial cells from (18.51 $\pm$ 0.80) % to (3.9 $\pm$ 0.29) % (\* $p$ <0.05), and reduced the percentage of Reelin-generated neurons from (22.44 $\pm$ 0.46) % to (14.8 $\pm$ 0.33) % (\*\* $p$ <0.05).



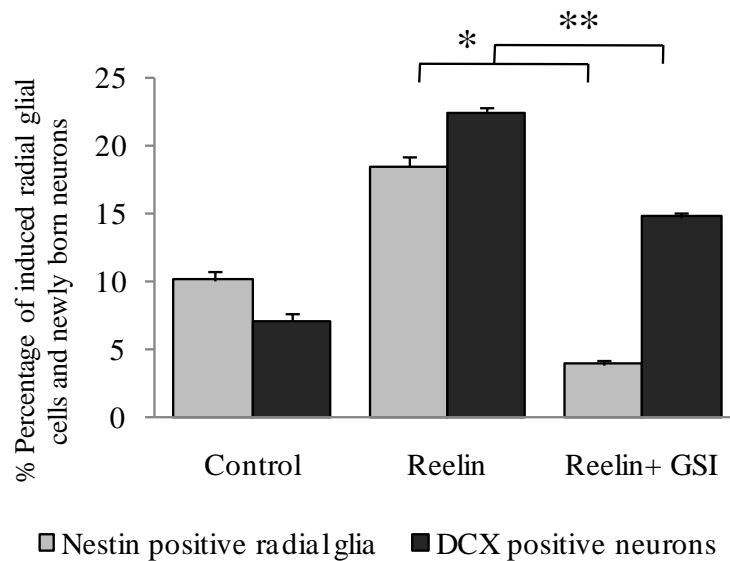


**Figure 17: Inhibition of Notch-1 signaling in the Reelin treated cells increases the ratio of the generated neurons to the produced radial glia.**

The inhibition of  $\gamma$ -secretase activity in the Reelin treated cells significantly reduced the percentage of the radial glial cells to  $(3.9 \pm 0.29)$  %,  $*p < 0.05$ , and reduced the Reelin-generated neurons to only  $(14.8 \pm 0.33)$  %,  $**p < 0.05$ . The data points represent the mean  $\pm$  standard error of at least three independent experiments. One-way ANOVA followed by Tukey's post-hoc test was used for the statistical analysis. Values that are significantly different from each other according to Tukey's test are indicated by asterisks. GSI is the  $\gamma$ -secretase inhibitor L-685,458.

*Notch-1 is Trafficked in the Same Vesicles as Reelin and VLDLR*

To gain insight into the possible mechanism by which Reelin acts on Notch-1, we investigated the localization of Reelin and its receptors relative to Notch-1 before and after Reelin treatment. The hNPCs were treated with either control- or Reelin- conditioned media for 15 minutes at 4°C to allow Reelin binding to the cells. The cells were then washed and incubated for 30 minutes at 37°C to allow Reelin internalization. The treated hNPCs were then fixed and stained with Reelin antibody clone 142 to detect both human and mouse Reelin. As expected, we didn't observe any Reelin staining in the control treated cells (data not shown), indicating that the positive stain we observed in the Reelin treated cells corresponds to the mouse Reelin that we used for treating the cells. As shown in (Figure 18), Reelin co-localized with Notch-1 in intracellular vesicles that are similar to the vesicles that contained Reelin and its receptor VLDLR.

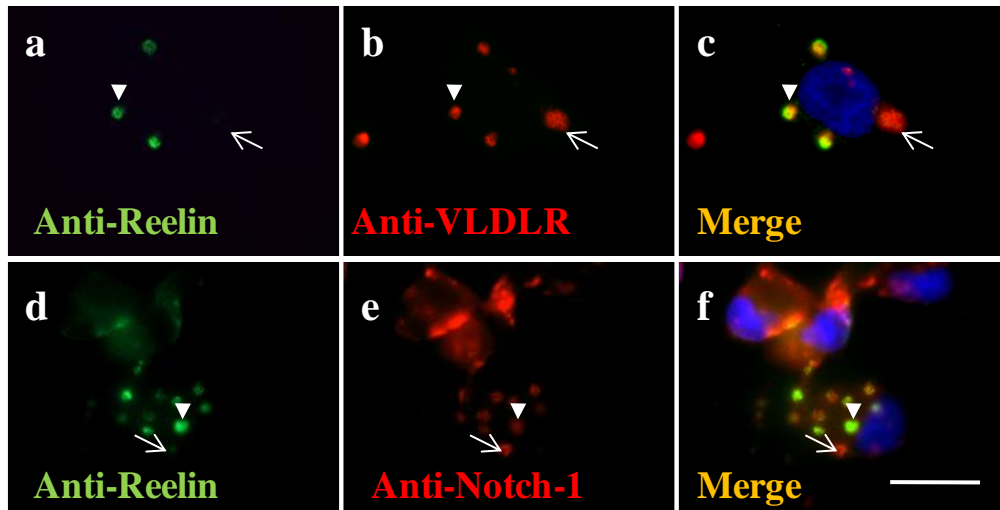


**Figure 18: Notch-1 is trafficked in the same vesicles as Reelin and VLDLR.**

The co-localization of Reelin and Notch-1 was examined before and after Reelin treatment. The hNPCs were treated with either control- or Reelin-conditioned media for 15 minutes at 4°C to allow Reelin binding to the cells. The cells were then washed and incubated for 30 minutes at 37°C to allow Reelin internalization. The treated hNPCs were fixed and stained with Reelin antibody clone 142 to detect both human and mouse Reelin. (a-c) Reelin (green) co-localizes with VLDLR (red). (d-f) Reelin (green) co-localizes with Notch-1 (red). Short arrows point to intracellular vesicles that showed co-localization while long arrows point to vesicles without co-localization. Blue is a DAPI for nuclei counterstaining. Scale bars are 20 μm.

*Dab-1 Tyrosine Phosphorylation is Essential to Mediate Reelin-induced Notch-1 Activation*

Once Reelin binds its receptors VLDLR and ApoER2, Reelin signal gets propagated into the cells via the induction of Dab-1 tyrosine phosphorylation and the activation of downstream Src family kinases<sup>15-17</sup>.

To examine if Dab-1 tyrosine phosphorylation is important to mediate Reelin's effect on NICD accumulation, we used a Dab-1 mutant that cannot be tyrosine phosphorylated because its 5 tyrosine residues have been mutated into phenylalanines (Dab-1 5F)<sup>53</sup>. We transfected hNPCs with wild type Dab-1 (Dab-1 WT) and the mutant Dab-1 5F for 24 hrs and then treated the cells with control or Reelin-conditioned media for 1 hour. Dab-1 tyrosine phosphorylation was confirmed by immunoprecipitating Dab-1 from all the collected samples using an antibody against Dab-1 C-terminus, running the immunoprecipitated proteins on SDS-PAGE and then blotting the membranes with an antibody that recognizes the tyrosine phosphorylated Dab-1 on tyrosine residue 198.

As shown in (Figure 19), Dab-1 WT transfection had no significant effect on the levels of NICD. However, Dab-1 WT transfection with Reelin treatment had synergistic effect and increased the levels of NICD to a level higher than that obtained with Reelin treatment only, (\* $p < 0.05$ ). Most importantly, Dab-1 5F mutant transfection resulted in complete loss of Reelin's effect on NICD accumulation and brought NICD levels close to basal levels, (\*\* $p < 0.05$ ). These data indicate that the induction of Dab-1 tyrosine phosphorylation by Reelin is important to mediate Reelin's effect on NICD accumulation.

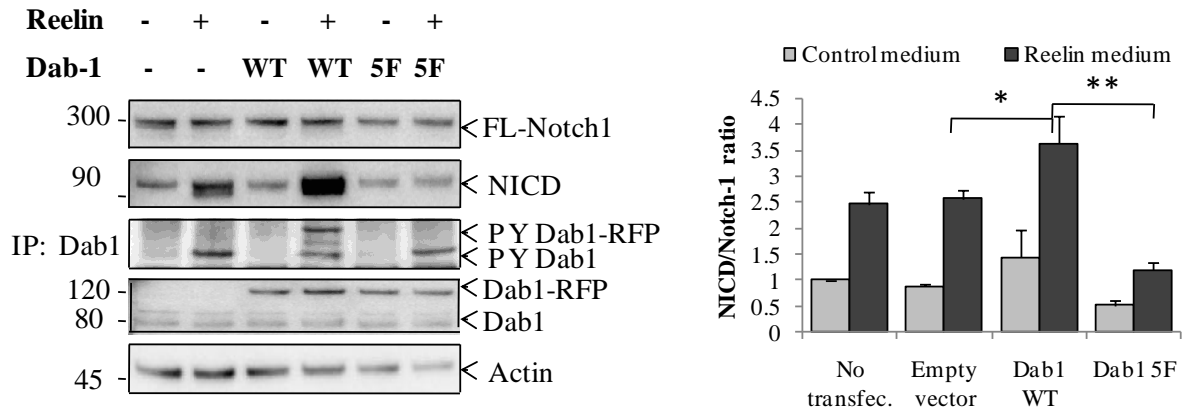


**Figure 19: Reelin-induced activation of Notch-1 is dependent on Dab-1 tyrosine phosphorylation.**

The involvement of Dab-1 tyrosine phosphorylation in NICD accumulation was tested by the over-expression of Dab1 5F mutant. As a control, the cells were transfected with wild type Dab-1 (Dab-1 WT). Dab-1 tyrosine phosphorylation was assessed by Western blotting of immunoprecipitated Dab-1 with Dab-1(phospho Y198) antibody. Reelin treatment induced Dab-1 tyrosine phosphorylation and NICD accumulation (\* $p < 0.05$ ) in all the samples but the ones transfected with Dab-1 5F mutant (\*\* $p < 0.05$ ). The data points represent the mean  $\pm$  standard error of at least three independent experiments. One-way ANOVA followed by Tukey's post-hoc test was used for the statistical analysis. Values that are significantly different from each other according to Tukey's test are indicated by asterisks. Dab1-RFP stands for Dab-1 with a red fluorescent protein (RFP) tag.

### *Inhibition of Src Family Kinases Blocks Reelin-induced NICD Accumulation*

Since Dab-1 is tyrosine phosphorylated by Src family kinases and since Dab-1 tyrosine phosphorylation acts to further activate these kinases<sup>16</sup>, we examined if the activity of Src family kinases is also important to mediate Reelin's effect on NICD accumulation.

Therefore, we pre-treated hNPCs for 1 hour with 10  $\mu$ M of either the Src inhibitor PP2 or PP2's inactive analog PP3 as a control. The cells were then treated with either control or Reelin-conditioned media for 1 hour in the presence of these inhibitors. As shown in (Figure 20), inhibiting Src kinases using PP2 inhibited Dab-1 tyrosine phosphorylation and the accumulation of NICD in the Reelin treated cells, (\* $p < 0.05$ ).

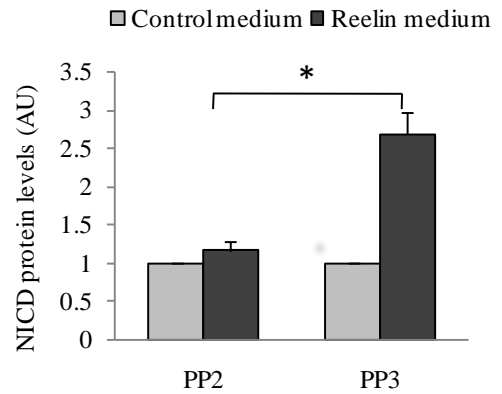
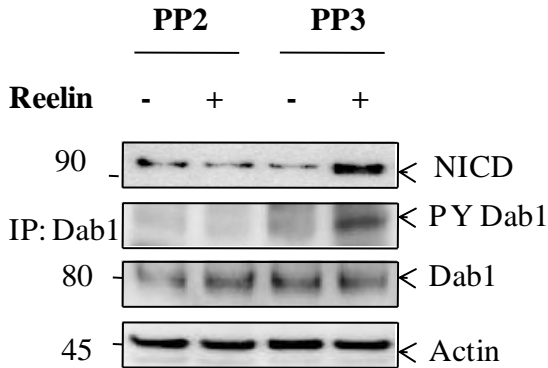


**Figure 20: Reelin-induced activation of Notch-1 is dependent on *Src* activation.**

The hNPCs were pre-treated for 1 hour with 10 $\mu$ M of the *Src* inhibitor PP2 or its inactive analog PP3 to investigate the importance of the activation of *Src* family kinases on NICD accumulation in response to Reelin. The cells were then treated with control or Reelin-conditioned medium for 1 hour in the presence of the inhibitors. The inhibition of *Src* activity inhibited Dab-1 tyrosine phosphorylation and NICD accumulation in the Reelin treated cells (\* $p$ <0.05). The data points represent the mean  $\pm$  standard error of at least three independent experiments. One-way ANOVA followed by Tukey's post-hoc test was used for the statistical analysis. Values that are significantly different from each other according to Tukey's test are indicated by asterisks.

### *Reelin Does not Bind to Notch-1*

In addition, we tested the possibility of a direct interaction between Reelin and Notch-1 using co-immunoprecipitation. The hNPCs were treated with control or Reelin-conditioned media for 15 minutes to allow Reelin binding to the cell surface. The unbound Reelin was then washed away with PBS and the cells were isolated. However, although we found an interaction between Reelin and VLDLR after Reelin treatment, we couldn't detect any interaction between Notch-1 and Reelin (Figure 21). These data confirm that Reelin effect on Notch-1 is mediated by intracellular signals rather than by Reelin and Notch-1 direct interaction.



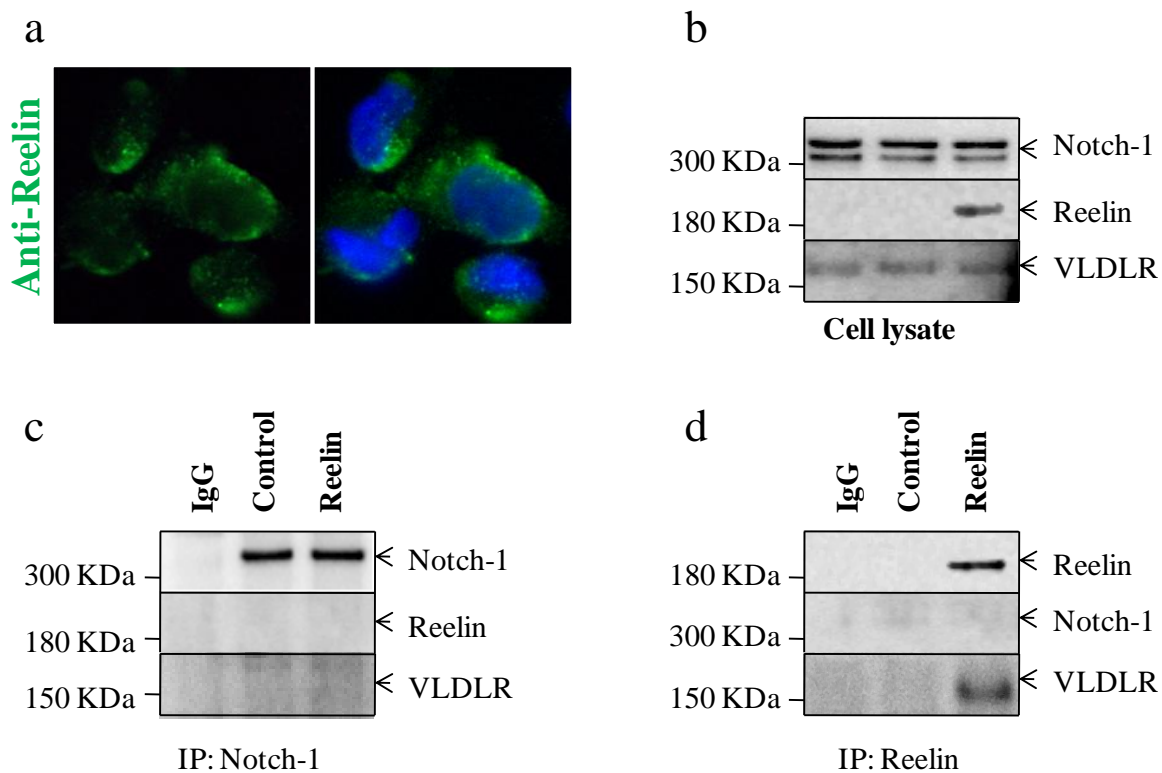


**Figure 21: Reelin does not bind Notch-1.**

(a) The hNPCs were treated with Reelin for 15 minutes at 4°C to allow Reelin to bind the cell surface. The unbound Reelin was then washed away with PBS. The cells were then fixed and stained with anti-Reelin. Reelin stain (green) confirms that Reelin was bound to the cell surface without being internalized. Blue is a DAPI for nuclei counterstaining (b) Western blot that shows the levels of Notch-1, Reelin and VLDLR in the cell lysate. (c) Co-immunoprecipitation against Notch-1 didn't yield Reelin or VLDLR. (d) Co-immunoprecipitation against Reelin yielded VLDLR after Reelin treatment but didn't yield Notch-1.

### *Reelin Increases NICD Translocation to the Nucleus*

Next, we examined NICD localization in the cells after Reelin treatment. The cells were treated with control or Reelin-conditioned media for 12 hours before fixation. The cells were then stained with a Notch-1 antibody that has a high affinity to Notch-1 intracellular domain and with BLBP antibody, a gene downstream of NICD. As shown in (Figure 22), Notch-1 localizes on the membrane or in vesicular structures before Reelin treatment with only basal levels of BLBP expression in these cells. Reelin treatment resulted in the translocation of NICD to the nucleus and the induction of BLBP in these cells.

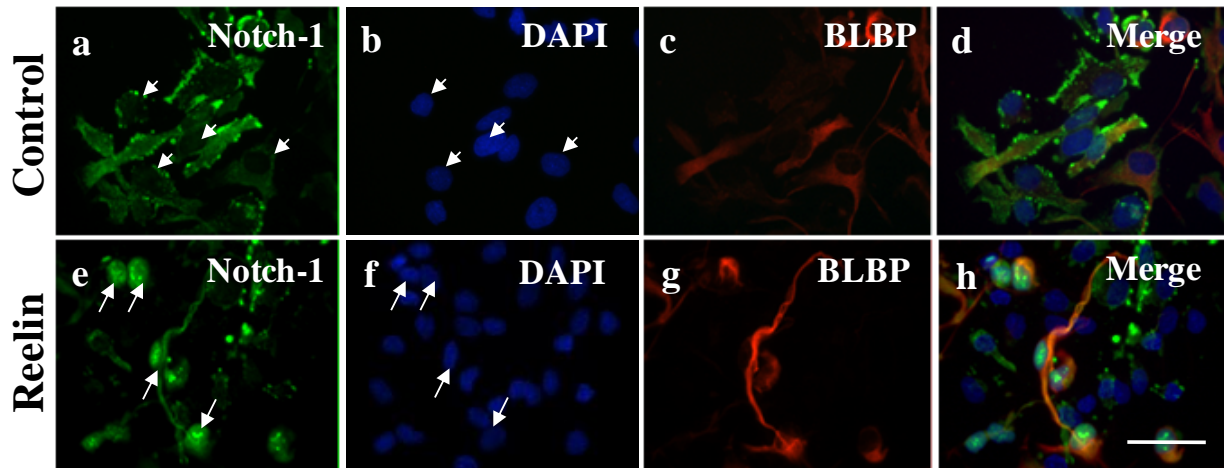


**Figure 22: Reelin increases NICD translocation to the nucleus and induces BLBP expression.**

To examine NICD localization after Reelin treatment, hNPCs were treated with control or Reelin-conditioned media for 12 hours. The cells were then fixed and stained with anti-Notch1 (green). The cells were also stained with anti-BLBP (red) to confirm the expression of BLBP in the Reelin treated cells that contain nuclear NICD. In the control treated cells, Notch-1 signal is mainly membrane-bound without any nuclear staining, short arrows point to the nuclei with negative Notch-1 immunoreactivity. Reelin treatment shifted Notch-1 signal from the membrane to the nucleus and induced BLBP expression, long arrows point to the nuclei with positive Notch-1 immunoreactivity. Blue is a DAPI for nuclei counterstaining. Scale bar is 50  $\mu$ m.

*Reelin Increases Dab-1 Binding to NICD in the Nucleus*

Next, we investigated if Reelin can increase the interaction between Dab-1 and NICD in the nucleus. Dab-1 was recently identified as a nucleoshuttling protein<sup>50</sup>. The hNPCs were treated with control or Reelin-conditioned media for 12 hours before isolation. The cell lysates were then fractionated and the nuclear fractions were used to co-immunoprecipitate Dab-1 and NICD. As shown in (Figure 23), Reelin treatment increased the level of NICD that co-immunoprecipitated with Dab-1 (Figure 23, b) and increased the level of Dab-1 that co-immunoprecipitated with NICD (Figure 23, a) in the nuclear fraction. These data indicate that Reelin treatment can increase the interaction between NICD and Dab-1 in the nucleus.

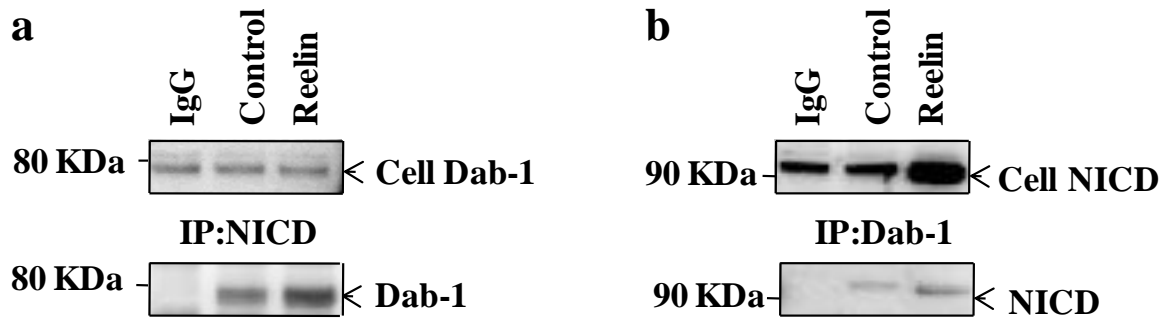


**Figure 23: Reelin enhances the binding between Dab-1 and NICD in the nuclear fraction.**

The hNPCs were treated with control or Reelin-conditioned medium for 12 hours before cell extraction. NICD and Dab-1 were co-immunoprecipitated from the nuclear fraction using anti-NICD (a) and anti-Dab-1 (b) antibodies, respectively. Reelin treatment increased Dab-1 and NICD interaction in the nucleus.

## Discussion

We have previously shown that Reelin treatment of fetal cortical hNPCs *in vitro* induces neurogenic radial glial cells<sup>51</sup>. Since it has been found that radial glial cells serve as neural progenitors for the majority of neurons in the CNS<sup>2, 3</sup>, and since all the neuronal population in the mouse brain were found to be derived from radial glial cells that express BLBP<sup>3</sup>, we questioned if our Reelin-induced BLBP positive radial glia can produce neurons. As shown in (Figure 13), we found that Reelin addition to the hNPCs for 3 days enhances their neurogenic potential and increases the percentage of the DCX immuno-positive cells from (7.13±0.52) % in the control treated cells to (22.44±0.46) % in the Reelin treated cells, (\*\*p<0.05).

To determine if Reelin's effect on neurogenesis is dependent on Notch-1 activation, we re-analyzed the hNPCs' neurogenic potential after inhibiting the activity of  $\gamma$ -secretase. Surprisingly, inhibiting Notch-1 activation in the Reelin treated cells did not reduce the generation of neurons dramatically and therefore increased the ratio of the generated neurons to the produced radial glia (Figure 17). This can be explained by considering the role of Notch-1 signaling in cell fate determination during the asymmetric division of the radial glial cells<sup>4</sup>. As the radial glial cell is asymmetrically dividing, one of the daughter cells inherits the protein Numb. This protein will inhibit the activity of Notch-1 in that cell driving it to acquire the neuronal fate. On the other hand, Notch-1 will remain activated in the other daughter cell driving it to become a radial glia<sup>4</sup>. Accordingly, performing the co-culture in the presence of the Notch-1 inhibitor will result in the transformation of both daughter cells into neurons and increasing the

ratio of the generated neurons to the produced radial glia cells. On the long term this will result in the depletion of the neuronal progenitors and reduction in the overall rate of neurogenesis.

The first step in the activation of Reelin signaling is the induction of Dab-1 tyrosine phosphorylation<sup>15</sup>. The tyrosine phosphorylated Dab-1 acts as link between Reelin and its downstream kinases. Dab-1 tyrosine phosphorylation forms a binding site for *Src* family kinases resulting in their activation and leading to further phosphorylation of Dab-1 on its remaining tyrosine residues<sup>16, 17</sup>. This will further activate *Src* and will ultimately result in the activation of the kinases PI3-K and Akt<sup>17</sup>. To determine if Dab-1 tyrosine phosphorylation is crucial to mediate the effect of Reelin on Notch-1 activation, we used a Dab-1 mutant that cannot be tyrosine phosphorylated in response to Reelin<sup>53</sup>. The use of this mutant completely abolished Reelin's effect on Notch-1 activation and brought NICD levels back to basal levels (Figure 19). Similarly, inhibiting the activity of *Src* inhibited the effect of Reelin on NICD accumulation (Figure 20). Interestingly, Reelin treatment was also found to enhance the interaction between Dab-1 and NICD (Figure 23) and increased NICD translocation to the nucleus (Figure 22).

Notch-1 activation and the release of NICD from the membrane depend on two sequential proteolytic events of Notch-1. The first step is initiated after Notch-1 binding to its ligand on the cell membrane. Notch-1 extracellular domain gets endocytosed into the signal-sending cell and the rest of the receptor undergoes cleavage by a protease of the ADAM family. This yields an extracellular fragment and a membrane bound fragment that serve as the precursor for the second

cleavage. The second cleavage is mediated by  $\gamma$ -secretase, which usually takes place in the early endosomes. This yields the final fragment of Notch-1, NICD<sup>58</sup>.

In our study, Reelin treatment did not increase Notch-1 processing by  $\gamma$ -secretase (Figure 15 & 16). Since Notch-1 full length levels were reduced after Reelin treatment (Figure 14), Reelin might increase the levels of the NICD precursor by enhancing the processing of the full length Notch-1 on the cell surface leading to increased NICD levels. In addition, a recent study has showed that the activation of Reelin signaling can directly act on inhibiting NICD degradation via the proteasome<sup>54</sup>, this indicates the Reelin is also acting downstream of  $\gamma$ -secretase to increase the levels of NICD.

In conclusion, Reelin and Notch-1 pathways are two important pathways in development. We recently reported their crosstalk and showed that Reelin signaling pathway can act to fine tune Notch-1 activation to favor the induction of neurogenic radial glial cells in hNPCs. Here, we investigated the molecular mechanisms by which Reelin activates Notch-1. This study furthers our knowledge about the molecular regulation of Notch-1 activity in cell fate determination and provides us with new targets to manipulate the process of neurogenesis.



## **CHAPTER FOUR: DISABLED-1 PROMOTES $\gamma$ -SECRETASE-MEDIATED PROCESSING OF AMYLOID PRECURSOR PROTEIN**

### **Introduction**

$\beta$ - Amyloid precursor protein (APP) is the precursor of amyloid  $\beta$  peptide ( $A\beta$ ), which is associated with the pathogenesis of Alzheimer's disease (AD), a progressive neurodegenerative disease<sup>33</sup>. The APP gene is alternatively spliced to produce three different isoforms of 695, 751 and 770 amino acids in length, where APP695 is the major isoform in neurons. The product of this isoform is an integral type I transmembrane glycoprotein that has a large amino terminal extracellular/ luminal domain and a short cytoplasmic tail<sup>34</sup>.

APP is trafficked through the constitutive secretory pathway where it matures into the O-glycosylated form in the Golgi apparatus<sup>35</sup>. During trafficking, APP is subjected to processing by proteolytic enzymes that are distributed throughout the secretory and the endocytic pathways to generate different APP fragments, which in turn regulate several neural functions including cell excitability, synaptic transmission and long-term potentiation<sup>36</sup>.

Processing of APP is initiated via the proteolytic activities of  $\alpha$ - and  $\beta$ -secretases, which cleave APP ectodomain close to its transmembrane domain to liberate soluble APP extracellular fragments ( $\alpha$ - or  $\beta$ -sAPP respectively). APP cleavage by  $\alpha$ - or  $\beta$ -secretases is a key regulatory process in the generation of the  $A\beta$ .

$\beta$ -secretase has been identified as the aspartyl protease BACE1 and has been localized in the *trans*-Golgi network (TGN) and endosomes, where it cleaves APP at the N-terminus of the A $\beta$  peptide domain catalyzing the first step in A $\beta$  peptide generation. In contrast,  $\alpha$ -secretase is found at the cell surface and cleaves APP within the A $\beta$  sequence thereby precluding its generation.

After the initial cleavage of APP by  $\alpha$ - and/or  $\beta$ -secretase, the remaining membrane-tethered C-terminal APP fragments (CTFs), are further cleaved within its transmembrane domain by a multimeric protein complex termed  $\gamma$ -secretase to generate p3 and A $\beta$  respectively, and a cytosolic APP intracellular domain (AICD)<sup>33-36</sup>. The specific localization of  $\gamma$ -secretase activity remains controversial, however recent studies have localized it to the *trans*-Golgi network (TGN) and the endosomal/lysosomal compartments, the major sites of A $\beta$  generation<sup>56, 57, 59, 60</sup>.

Recent evidence shows that APP processing is regulated by proteins that bind its intracellular domain, particularly its YENPTY motif, which contains the consensus sequence for the clathrin-coated pit internalization<sup>37, 38</sup>. Deletion of this motif impairs APP internalization and decreases A $\beta$  secretion by precluding endosomal/lysosomal APP processing<sup>61, 62</sup>.

Most of the proteins found to bind this motif are adaptor proteins possessing the phosphotyrosine-binding (PTB) domain, such as Fe65, X11, JIP and Dab protein families. These proteins bridge APP to different complexes that can assemble around its intracellular domain to regulate its trafficking and metabolism<sup>37, 38</sup>. The X11 family of adaptor proteins (X11  $\alpha$ ,  $\beta$ ,  $\gamma$ ), for

example, has been shown to bind and to stabilize cellular APP, increase its half-life and reduce the production and secretion of sAPP $\alpha$ , A $\beta$ 40 and A $\beta$ 42<sup>63-66</sup>.

On the other hand, Disabled-1 (Dab-1) effect on APP processing has only recently been investigated<sup>67, 68</sup>. Dab-1 is a cytoplasmic adaptor protein that has been extensively studied as a key element in the Reelin-signaling pathway controlling neuronal migration, laminar positioning and organization. It transmits Reelin signal by binding the NPXY motif of the Reelin receptors, very low density lipoprotein receptor (VLDLR) and apolipoprotein E receptor 2 (ApoEr2), via its PTB domain, serving as a link between Reelin and downstream kinases<sup>15-17</sup>. Mutation in Dab-1 generates a reeler-like phenotype, which is characterized by inversion of the cortical layers and abnormalities in the laminated brain structures<sup>18</sup>. Interestingly, disrupting APP and its two homologues amyloid precursor-like protein (APLPs) 1 and 2, results in cortical dysplasia and neuronal migration defects<sup>69</sup> that are a similar but not identical to disruption of Reelin, Dab-1 or its receptors ApoER2 or VLDLR<sup>18</sup>.

Recently, Dab-1 over-expression was reported to increase the cell surface expression level of APP, increase APP  $\alpha$ -cleavage<sup>67, 68</sup> and reduce its  $\beta$ -cleavage in transfected cells and in primary neurons<sup>68</sup>. In this study, we investigated the effects of Dab-1 over-expression on APP cleavage by  $\gamma$ -secretase, the final step in APP processing. We report that Dab-1 over-expression increases the  $\gamma$ -secretase-mediated processing of APP, resulting in increased release of APP intracellular domain (AICD) from the membrane.

## **Materials and Methods**

### *Cell Culture*

NT2/ D1 cells, human neuron-committed teratocarcinoma cell line, were maintained in Dulbecco's Modified Eagle's Medium (DMEM/F12) supplemented with 10% fetal bovine serum (FBS) (Invitrogen), 1% antibiotic-antimycotic (Invitrogen) and 1% glutamate (Invitrogen), in a 5% CO<sub>2</sub> incubator at 37°C. NT2 cells were cultured in six-well plates (BD biosciences) and transiently transfected with 4µg of plasmid using Lipofectamine 2000 reagent according to the manufacturer's instructions (Invitrogen). The cells were cultured for 24 hours post transfection in DMEM/F12 medium supplemented with 10% FBS and 1% glutamate.

For  $\gamma$ -secretase inhibition, 6 hours post transfection, the media was totally removed and 10 µM of  $\gamma$ -secretase inhibitor (L-685, 458 - Sigma Aldrich) or 0.1% Dimethylsulfoxide (DMSO- Sigma Aldrich) as control, were prepared in growth media and added to the cells for 12 hours before lysis. For proteasomal inhibition, 6 hours post transfection, the media was totally removed and the cells were incubated with 50 µM MG-132 (CalBioChem) or 0.1% DMSO as a control in growth media for 6 hours at 37 °C before lysis. For lysosomal inhibition, the cells were treated with 100 µM of the lysosome inhibitor chloroquine (Sigma Aldrich) for 6 hours at 37 °C.

cDNA constructs. Dab-1 gene (Accession # NM\_021080) was isolated from Human Neural Stem cells and cloned into pcDNA3.1 vector with FLAG tag on its C terminus (Invitrogen);

sequencing was performed to assure that the clone is in frame. pCEP-APP-GFP and pCEP-APP695 were kindly provided by Dr. Beth Ostaszewski, Harvard Medical School. Dab1- $\Delta$ PTB in pEF-BOS expression vector was kindly provided by Dr Shiro Suetsugu, The University of Tokyo.

### *Immunocytochemistry and Microscopy*

Cells were fixed with 4% Paraformylaldehyde (Sigma Aldrich) for 24 hrs at 4°C. The next day, the cells were washed three times with phosphate buffered saline (PBS- Sigma Aldrich ) at room temperature and blocked with 3% donkey serum (Jackson ImmunoResearch Labs) in phosphate buffered saline with 0.1% Triton X ( PBST- Sigma Aldrich) for 1 hour at room temperature. The cells were then incubated with the appropriate antibody for 24 hrs at 4°C. After washing the cells with PBS for three times the cell were incubated with anti-rabbit or anti-mouse Tetramethyl Rhodamine Iso-Thiocyanate (TRITC)-conjugated antibodies (1: 500 Jackson ImmunoResearch Labs) for 2 hrs at room temperature in the dark. The cells were washed again and mounted with vectashield with DAPI (vector laboratories) to stain nuclei and for microscopic observations. Microscopic images were taken with the QImaging MicroPublisher 5.0 color digital imaging system and processed using the QCapture software (Leeds, Irving, TX)

Primary antibodies that have been used: mouse anti- EEA1 (1:200; Abcam), rabbit Dab-1 antibody (1:1000; Abcam), mouse anti-Cathepsin D (1:200; Abcam), rabbit anti-Mannosidase II (1:200; Abcam) and rabbit anti-Calreticulin (1:200; Abcam).

### *Western Blot Analysis and Immunoprecipitations*

NT2 Cells were lysed 24 hr post-transfection in ice-cold lysis buffer containing 1% Nonidet P-40, 150 mM NaCl, 50 mM Tris (pH 8.0), and protease inhibitor mixture (Roche, Indianapolis, IN). The homogenates were centrifuged at 12,000 x g for 30 min at 4°C and the supernatants were saved for analysis. 30 µg of protein was loaded per well, and proteins were separated by SDS/PAGE (NuPage 4%-12% Bis-Tris, Invitrogen) and then blotted onto polyvinylidene difluoride (PVDF) membranes (Bio-rad) for 120 min at 30 V. The membranes were then immunoblotted with the following antibodies overnight at 4°C: Anti-Amyloid Precursor Protein C-terminal (1:1000; Sigma Aldrich), anti-Dab-1 (1:1000; Abcam), anti-β actin (1:1000; Cell Signaling), anti-ubiquitin (1:1000; Cell Signaling), and mouse anti- beta amyloid (6E10) (1:250; Abcam). After washing, membranes were incubated with horseradish peroxidase-conjugated secondary antibodies (anti-mouse IgG and anti-rabbit IgG; Jackson Immunoresearch, West Grove, PA) for 1–2 h. Signals were detected by chemiluminescence using the enhanced chemiluminescence (ECL) system (Amersham Biosciences Corp) on a Kodak Imaging Station IS2000MM. The optical density of each specific band relative to β-actin was analyzed by the public domain National Institutes of Health Image J software. For immunoprecipitations, 600µg of protein was incubated for 3 hours at 4°C with the primary antibody Anti-Amyloid Precursor Protein C-terminal (1:1000; Sigma Aldrich). Protein A-Sepharose beads were added for 1 hr at 4°C, and then immunoprecipitates were washed 5X with lysis buffer. Immunoprecipitated proteins were solubilized in 1% SDS solution and resolved on a 4-12% Bis-Tris gel (Invitrogen).

### *RNA Isolation and Real Time RT-PCR*

The RNA of each sample was isolated at a specific time point using TRIZOL reagent according to the manufacturer's instructions. The quantification of each of the gene transcripts was done by real-time RT-PCR using I script one-step RT-PCR kit with SYBR green (Bio-Rad Laboratories Inc) according to manufacturer's instructions. Reactions were done in duplicates using I-Cycler from Bio-Rad and the threshold values (Ct) were averaged after dropping reactions with PCR inhibitors or a varying slope. The PCR efficiency for each gene transcript using a specific set of primers was measured from a standard curve done for each transcript using two-fold serial dilutions, the correlation coefficient was found to be higher than .98 for each curve and the PCR efficiencies values was found to be, for  $\beta$ -actin 94%, Dab-1 98%, and APP 95%. These values were then incorporated in PFAFFL equation<sup>70</sup> along with the averaged threshold values to calculate the fold change in the gene expression relative to the fold change in the reference gene;  $\beta$ -actin was used as the reference gene that was also run in duplicates for each sample we had. 10  $\mu$ l of the reaction were separated on 2% E-gel (Invitrogen).

The following primers were used:

APP (+) 5'-CTTGAGTAAACTTTGGGACATGGCGCTGC-3'

(-) 5'-GAACCCTACGAAGAAGCC-3'

$\beta$ -actin (+) 5'-GACAGGATGCAGAAGGAGAT-3'

(-) 5'-TTGCTGATCCACATCTGCTG-3'

### *In-vitro AICD Generation Assay*

AICD was generated from membranous fractions using previously described methods<sup>71, 72</sup>. In short, the cells were lysed with buffer A (50 mM HEPES, 150 mM NaCl, 5 mM EDTA, PH 7.4) supplemented with protease inhibitor cocktail set I (Calbiochem). The homogenates were sequentially fractionated at 2500 xg for 15 minutes to collect unbroken cells and nuclei and the supernatant was saved as the cytosolic fraction. The post-nuclear fraction was then centrifuged at 16,000 xg for 30 minutes and the pellet was washed once with buffer A and resuspended in buffer B (50 mM HEPES, 150 mM NaCl, 5 mM EDTA, PH 7.0) supplemented with protease inhibitor cocktail set I (Calbiochem). The pellet was allowed to dissolve for 4 hours at either 37°C or 4°C as a negative control with vigorous shaking. After the incubation was complete, the samples were chilled on ice to stop the reactions and the membranes were collected by centrifugation at 16,000 xg for 30 minutes (P0). The final supernatant was used for analysis to detect AICD levels (P1).

### *Statistical Analysis*

Each data point represents triplicated experiments and displayed as the mean  $\pm$  standard error. A one-way Analysis of Variance was performed to test the hypothesis that the average mean values across categories of GROUP were equal. In the presence of significance for the omnibus ANOVA test, Tukey multiple comparison test is used to perform pairwise comparisons. Statistics were performed using WINKS SDA Software (Texasoft, Cedar Hill, TX.).



## Results

### *Dab-1 Overexpression Reduces APP-CT-GFP Signals in the Early Endosomes*

In order to study the effects of Dab-1 on APP metabolism, we examined the effects of Dab-1 over-expression on the distribution of the GFP signals in NT2/D1 cells transfected with APP tagged with GFP. Co-transfection of Dab-1 and APP tagged with GFP on its C-terminus (APP-CT-GFP) reduced the APP-CT-GFP signals that accumulated in intracellular vesicles (Figure 24, a-e). As shown in (Figure 24, d and e) Dab-1 co-localized with APP on the plasma membrane (*short arrow*) and on the membrane of intracellular vesicles (*long arrow*).

Dab-1 was previously found to bind to APP via its PTB domain<sup>68</sup>. The PTB domain of Dab-1 binds the internalization motif (NPXY) located on the intracellular domain of APP<sup>37, 38</sup>. To determine if Dab-1 mediates its effect on APP via binding it, we used a Dab-1 mutant that has its PTB domain deleted (Dab-1  $\Delta$  PTB). As shown in (Figure 24, i) Dab-1  $\Delta$  PTB and APP were not observed to localize, confirming that Dab-1  $\Delta$  PTB could not bind to APP. The co-transfection of APP-CT-GFP and Dab-1  $\Delta$  PTB resulted in an enhanced accumulation of APP in large vesicles that surrounded the nucleus (Figure 24, g-i).

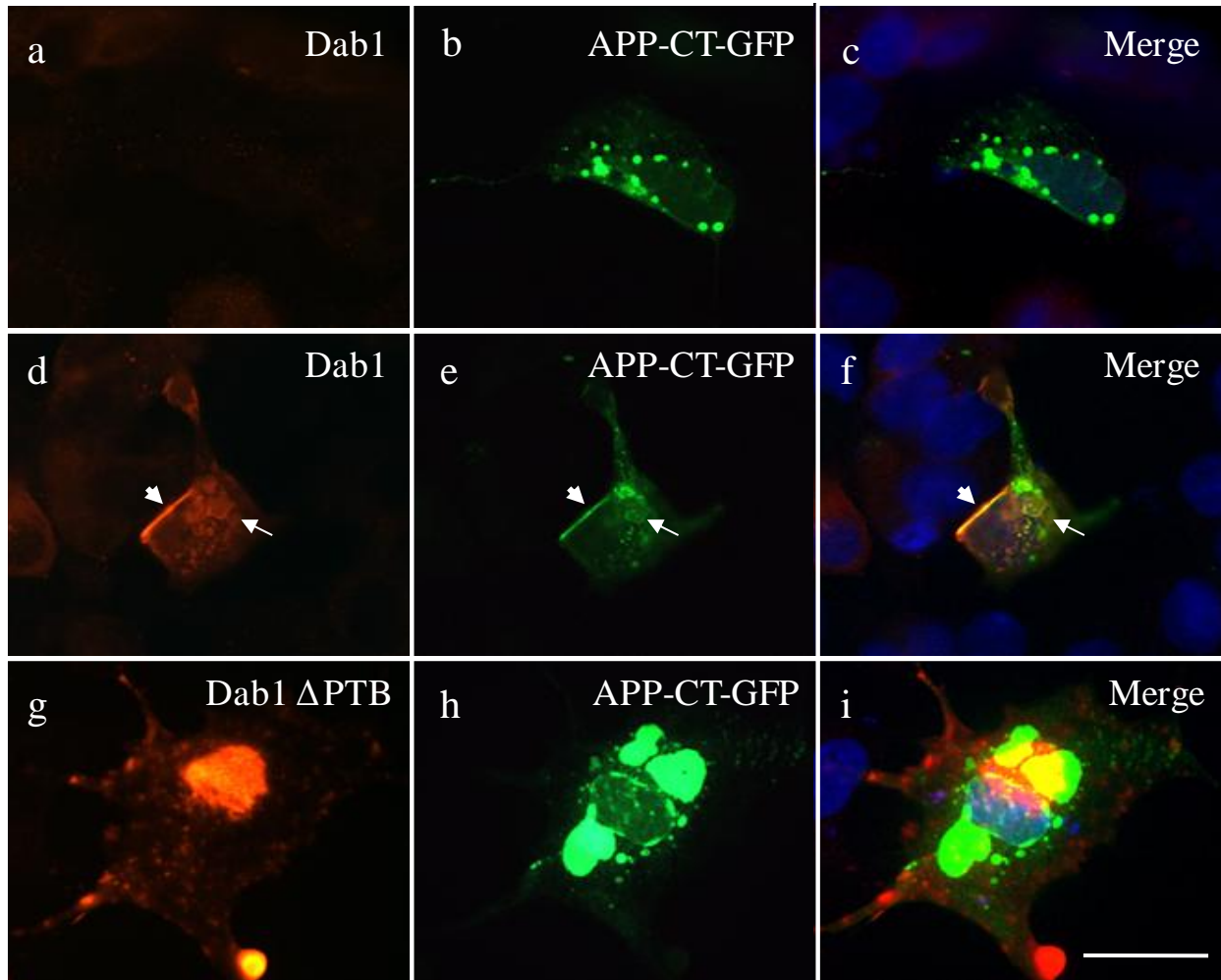


**Figure 24: Dab-1 over-expression reduces APP-CT-GFP signals in vesicular structures.**

NT2/D1 cells were co-transfected with APP-CT-GFP and an empty vector as a control (a-c), APP-CT-GFP and Dab-1 (d-e) or APP-CT-GFP and Dab-1  $\Delta$  PTB (g-i) for 24 hours. The cells were then fixed and immunostained against Dab-1 (red) using an antibody that binds Dab-1 C-terminus and can thus recognize the wild type and the mutant Dab-1. Dab-1 over-expression reduced the APP-CT-GFP signals in the vesicles (a-f). The co-transfection of Dab-1  $\Delta$  PTB with APP-CT-GFP resulted in enhanced accumulation of APP-CT-GFP signals in large vesicles (g-i). Blue is a DAPI for nuclei counterstaining. Scale bar is 50  $\mu$ m.

To identify the intracellular vesicles that APP-CT-GFP signals accumulated in, we co-localized these signals with markers for the early endosomes (EEA1), trans-Golgi network (Mannisodase II), the endoplasmic reticulum (Calreticulin) and the lysosome (Cathepsin D). Although faint co-localization was observed between APP-CT-GFP signals, the ER, the *trans*-Golgi network and the lysosomal markers (data not shown), most of the APP-CT-GFP signals co-localized with the early endosomal marker (Figure 25). These data suggest that the transfected APP accumulated in the early endosomes after being endocytosed from the membrane.

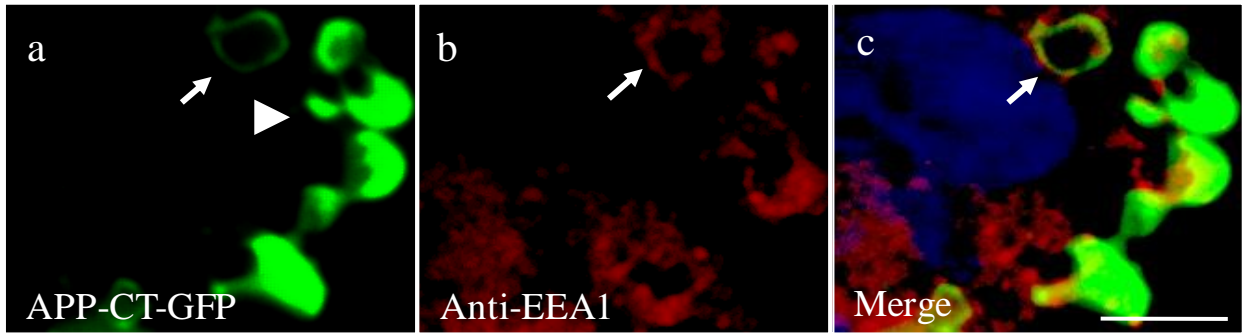


**Figure 25: APP-CT-GFP signals co-localizes with the early endosomal marker (EEA1).** After transfecting NT2/D1 cells with APP-CT-GFP for 24 hours, the cells were fixed and stained with the early endosomal marker (EEA1). Long arrow points to co-localized APP-CT-GFP signals while short arrow points to un-localized signals. Scale bar is 20  $\mu\text{m}$ .

### *Dab-1 Overexpression Increases the Release of APP Intracellular Domain*

Based on our observation that Dab-1 overexpression resulted in diffusion of APP-CT-GFP signals into the cytosol, we hypothesized that Dab-1 might be increasing APP processing by  $\gamma$ -secretase in the early endosomes to release AICD-GFP into the cytosol.

The processing of APP by  $\gamma$ -secretase is the final step in APP processing that results in releasing APP intracellular domain (AICD) from the membrane<sup>33-36</sup>. To determine if Dab-1 overexpression increases AICD level, we transfected NT2/D1 cells with either an empty vector as control or Dab-1 for 6 hours and then treated the cells with either 10  $\mu$ M of the  $\gamma$ -secretase inhibitor (L-685, 458) or with 0.1% DMSO as a control for 12 hours. AICD was generated *in vitro* by incubating the samples at 37°C for 4 hours. The supernatant (P1) fractions that were obtained from solublizing the post-nuclear fraction were used for analysis.

As we expected, Dab-1 transfection increased AICD level relative to the empty vector transfected cells (Figure 26-lane 2). In contrast, AICD release was completely inhibited in the Dab-1 over-expressing cells that were treated with the  $\gamma$ -secretase inhibitor (L-685, 458) (Figure 26-lane 4). These data confirm that Dab-1 increases AICD release from the membrane and that this effect is  $\gamma$ -secretase dependent.

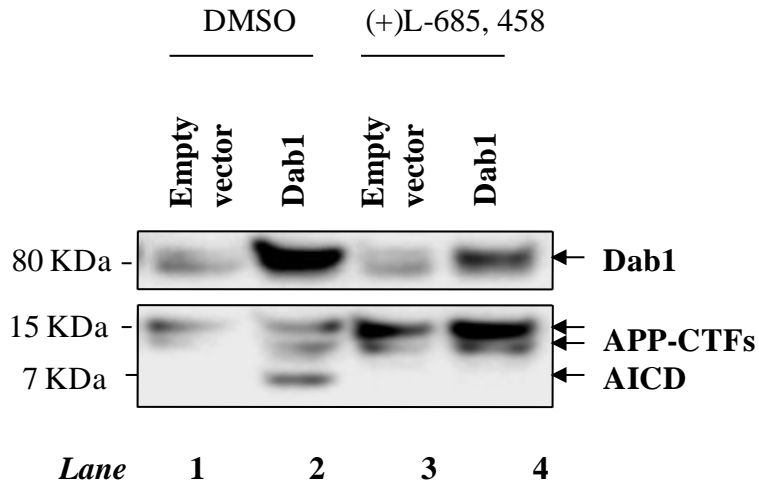


**Figure 26: Dab-1 over-expression increases AICD generation.**

NT2/D1 cells were transfected with Dab-1 or empty vector as a control for 6 hours. AICD release was measured before and after Dab-1 transfection, with and without  $\gamma$ -secretase inhibition. AICD was detected using an antibody that binds to APP C-terminal. Dab-1 over-expression increased AICD production (*lane 2*), where AICD production was totally demised by L-685, 458 treatment (*lane 4*).

APP-CTFs in the supernatant fraction (P1) seemed to accumulate after  $\gamma$ -secretase inhibition due to their decreased processing (Figure 27-lanes 3 and 4). However, to further analyze Dab-1 effect on APP processing, we analyzed the change in the total level of APP-CTFs after Dab-1 transfection. The cells were again transfected with either an empty vector as a control or Dab-1 for 6 hours and the total level of APP-CTFs was analyzed in the total cell lysate and after immunoprecipitation using an antibody against APP-C terminal (Figure 27).

Although the level of total APP-CTFs did not significantly change after Dab-1 transfection (Figure 27-lanes 1 and 2), we saw a slight accumulation of APP-CTFs in the Dab-1 overexpressing cells only after  $\gamma$ -secretase inhibition (Figure 27-lanes 3 and 4).

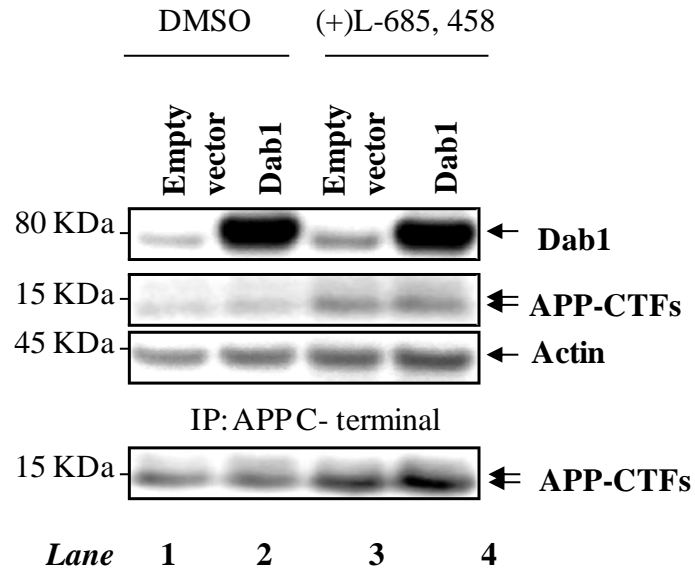


**Figure 27: APP-CTFs slightly accumulates in the Dab-1 overexpressing cells after  $\gamma$ -secretase inhibition.**

The total level of APP-CTFs was analyzed after Dab-1 transfection with and without  $\gamma$ -secretase inhibition. Samples were either directly ran on SDS-PAGE gel (second row) or immunoprecipitated with APP C-terminal antibody (fourth row). The membrane was then blotted with the same antibody.



Recently Dab-1 was shown to enhance  $\alpha$ -secretase mediated processing of APP<sup>67, 68</sup>. If that applies to our system as well, then it's possible that Dab-1 is increasing  $\alpha$ - and  $\gamma$ - cleavage of APP equivalently resulting in no net change in the total level of APP-CTFs. Thus, only upon the inhibition of  $\gamma$ -secretase activity, APP-CTFs that have been generated by  $\alpha$ -secretase are expected to accumulate. To confirm that in our system, we measured the amount of  $\alpha$ -sAPP released into the media after Dab-1 transfection using anti-6E10. The level of total sAPP was measured using anti-22C11. The cells were transfected with Dab-1 for 24 hours before media collection. The effects of Dab-1 over-expression on exogenous APP were also tested by co-transfecting Dab-1 and APP using APP transfection as the control. As we expected, Dab-1 over-expression significantly increased the level of both exogenous (\*\*p<0.05) and endogenous  $\alpha$ -sAPP (\*p<0.05) in the media (Figure 28).

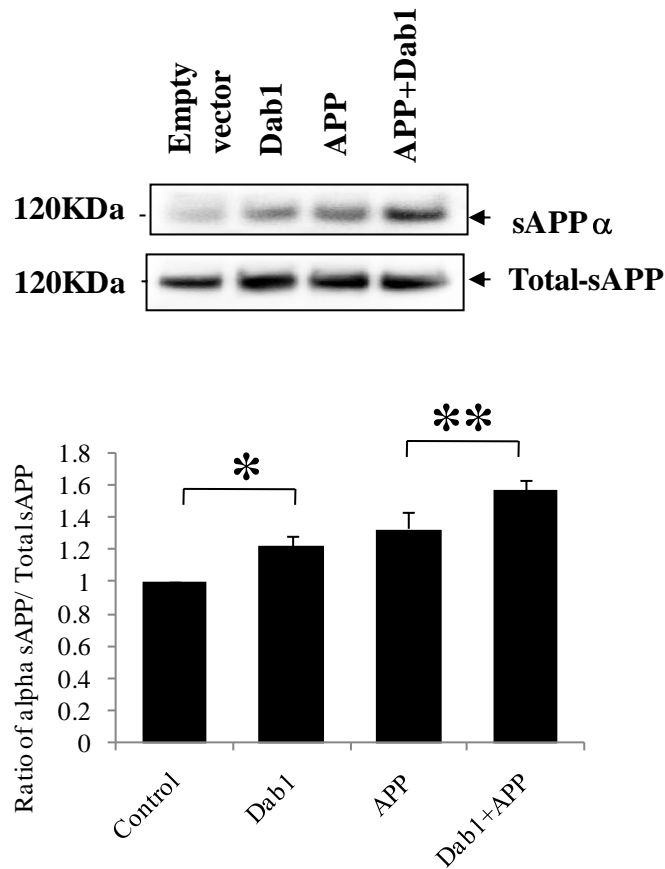


**Figure 28: Dab-1 enhances  $\alpha$ -secretase mediated processing of APP.**

Secreted APP levels were measured in the media collected from Dab-1 over-expressing cells. NT2/D1 Cells were transfected with empty vector (control), Dab-1 (Dab-1), APP and empty vector (APP) and APP and Dab-1 (APP+Dab-1) for 24 hours before media collection. Dab-1 over-expression significantly increased the level of both exogenous (\*\* $p < 0.05$ ) and endogenous  $\alpha$ -sAPP (\* $p < 0.05$ ) in the media. The data points represent the mean  $\pm$  standard error of at least three independent experiments. One-way ANOVA followed by Tukey's post-hoc test was used for the statistical analysis. Values that are significantly different from each other according to Tukey's test are indicated by asterisks.

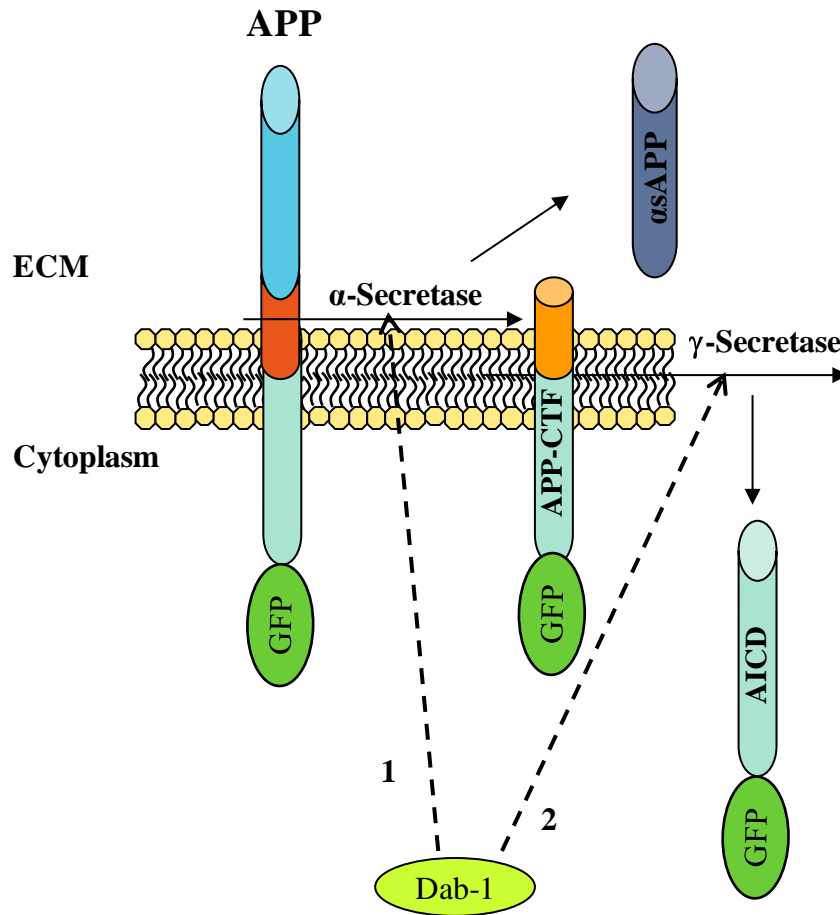


**Figure 29: A schematic diagram that illustrates the effects of Dab-1 on APP processing.**

Dab-1 increases AICD release from the membrane by (1) Enhancing APP processing on the membrane by  $\alpha$ -secretase yielding APP-CTF. (2) Enhancing APP-CTF processing by  $\gamma$ -secretase.

*Dab-1 Overexpression Promotes APP Processing by  $\gamma$ -secretase*

To confirm that Dab-1 over-expression reduces APP-CT-GFP signals in endosomal compartments by promoting  $\gamma$ -secretase activity, we inhibited the activity of  $\gamma$ -secretase in cells co-transfected with Dab-1 and APP-CT-GFP. APP-CT-GFP and empty vector co-transfection was used as the control. As we expected,  $\gamma$ -secretase inhibition abolished Dab-1 over-expression effects on APP-CT-GFP signals, retaining them as membrane-bound and preventing their cytosolic dispersion (Figure 30).

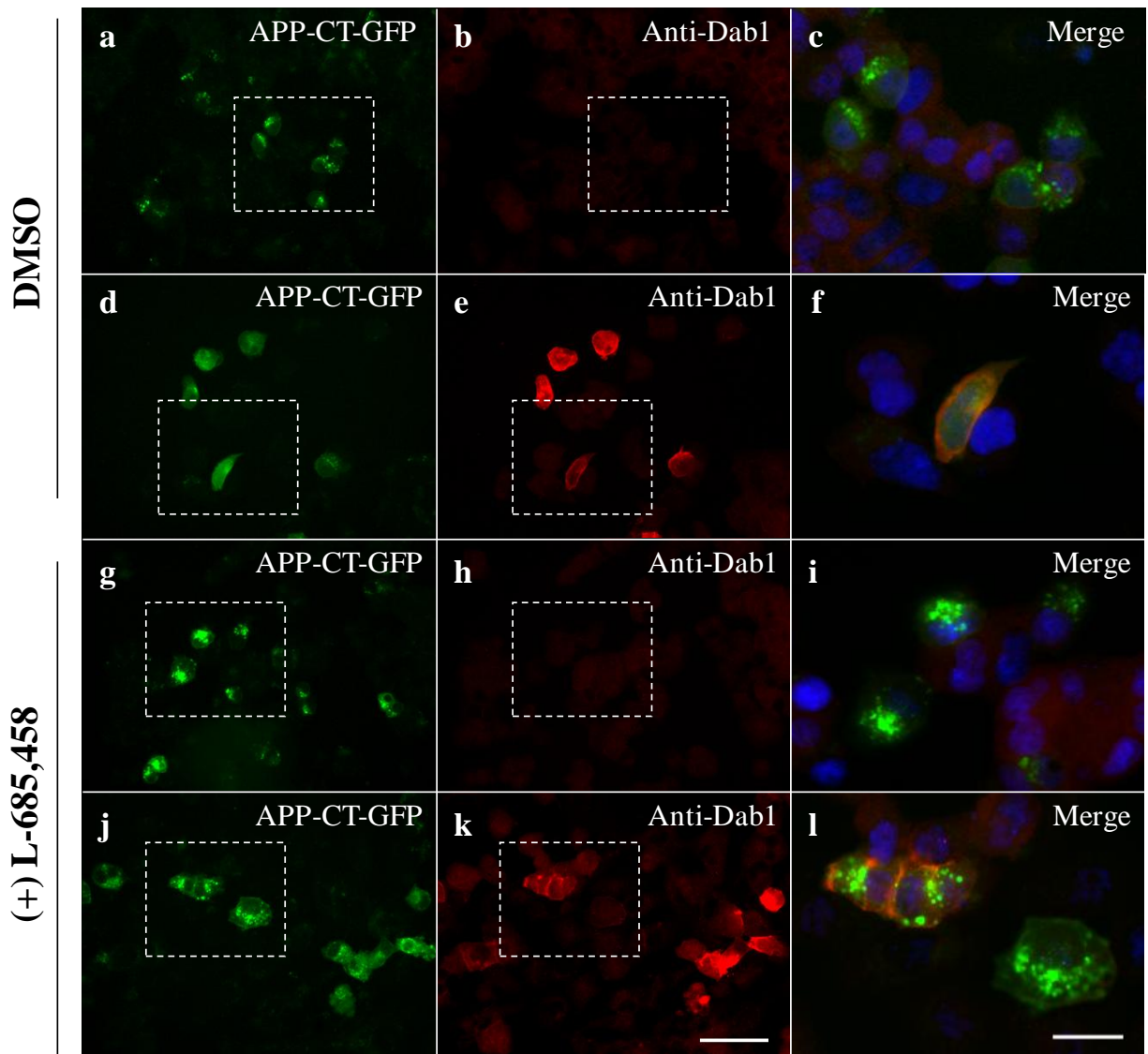


**Figure 30: Dab-1 over-expression promotes  $\gamma$ -secretase-mediated processing of APP.**

To test if Dab-1 effect is  $\gamma$ -secretase-dependent, NT2/D1 cells were co-transfected with APP-CT-GFP and empty vector (a-c and g-i) or APP-CT-GFP and Dab-1 (d-f and j-l) for 6 hours and treated with either 0.1% DMSO as a control or 10  $\mu$ M of the  $\gamma$ -secretase inhibitor (L-685, 458) for 12 hours. The cells were then fixed and immunostained against Dab-1 (red).  $\gamma$ -secretase inhibition abolished Dab-1 over-expression effects on APP-CT-GFP signals retaining them as membrane-bound (j-l). Blue is a DAPI for nuclei counterstaining. Scale bar for (a, b, d, e, g, h, j, k) is 72 $\mu$ m and for (c, f, l) is 27  $\mu$ m.

### *Dab-1 Overexpression Mediates APP Lysosomal Degradation*

In addition to Dab-1 effect on APP processing, we observed a reduction in the level of APP-CT-GFP signals as they seemed to be fainter after Dab-1 transfection (Figure 24). As a result, we hypothesized that Dab-1 might be also increasing the degradation of APP.

A recent study found that Numb, a related adaptor protein, promotes the ubiquitination of the membrane-tethered Notch1 and the degradation of the cleaved Notch intracellular domain (NICD) following the receptor activation<sup>73</sup>. In addition, a direct interaction between Dab-1 and the E3 ligase Siah 1 has been previously reported<sup>74</sup>.

To further delineate Dab-1 effect on APP metabolism, we tested if Dab-1 over-expression can mediate the degradation of APP. NT2/D1 cells were transfected with either Dab-1, Dab-1  $\Delta$  PTB or an empty vector as a control. The cells were then treated with either 50 $\mu$ M of the proteasome inhibitor MG-132 or with 0.1% DMSO as a control for 6 hours at 37°C before lysis. The accumulation of the ubiquitinated proteins in the cells treated with MG-132 was confirmed by analyzing the levels of the ubiquitinated proteins in the treated samples using antibody against ubiquitin (Figure 31).

As shown in (Figure 32) Dab-1 transfection resulted in reducing APP levels relative to the empty vector transfection (*lane 2*). On the other hand, the transfection of Dab-1  $\Delta$  PTB prevented the degradation of APP (*lane 3*). Interestingly, inhibiting the proteasome using MG-132 did not recover APP levels in the Dab-1 transfected cells (*lane 5*).

In (Figure 24) we observed that transfecting the Dab-1 mutant (Dab-1  $\Delta$  PTB) prevented the clearance of APP from the early endosomes, resulting in marked accumulation of APP in enlarged endosomal structures that surrounded the nucleus. It's possible that Dab-1 overexpression enhances the trafficking of APP from the early endosomes to the lysosomes leading to clearance of APP from the early endosomes and increased APP degradation in the lysosome.

To determine if Dab-1 increases APP degradation via the lysosome instead, we inhibited the lysosomal degradation in the Dab-1 transfected cells. NT2/D1 cells were transfected with either an empty vector, Dab-1 or Dab-1  $\Delta$  PTB. The next day, the cells were treated with either 0.1% DMSO as a control or with 100  $\mu$ M of the lysosomal inhibitor Chloroquine for 6 hours.

As expected, inhibiting the lysosome recovered APP levels in the Dab-1 transfected cells (*lane 8*), indicating that Dab-1 binding to APP mediates the trafficking of APP from the endosomes to the lysosome for degradation.

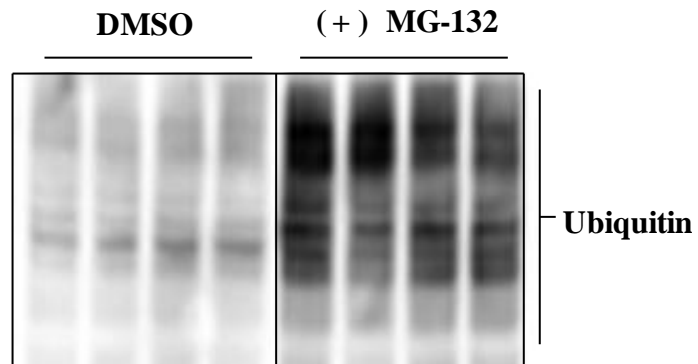


**Figure 31: Accumulation of ubiquitinated proteins after MG-132 treatment.**

NT2/D1 cells were transfected with either empty vector (control), Dab-1 or Dab-1  $\Delta$  PTB for 24 hours and then treated with either 0.1% DMSO (first four lanes) or with 50 $\mu$ M MG-132 (last four lanes) for 6 hours before lysis. Accumulated ubiquitinated proteins were detected using antibody against ubiquitin.



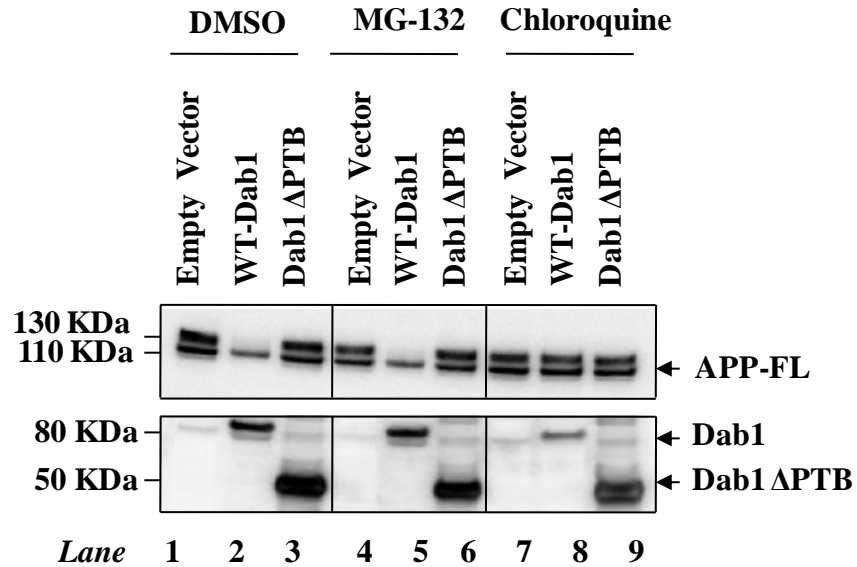


**Figure 32: Dab-1 overexpression increases APP degradation via the lysosome.**

NT2/D1 cells were transfected with either an empty vector, Dab-1 or Dab-1 $\Delta$  PTB for 24 hours. The cells were then treated with either 0.1% DMSO as a control (lanes 1-3), or with 50  $\mu$ M of the proteasomal inhibitor MG-132 for 6 hours (lanes 4-6), or with 100  $\mu$ M of the lysosomal inhibitor Chloroquine for 6 hours (lanes 7-9). Inhibiting the lysosome recovered APP levels in the Dab-1 transfected cells (lane 8).

## **Discussion**

Recent studies have pointed to the possibility that Dab-1 may interfere with APP trafficking to increase its cell surface expression, subjecting it to more  $\alpha$ -secretase- and less  $\beta$ -secretase-mediated processing, thereby, increasing  $\alpha$ -sAPP and  $\alpha$ -CTF levels<sup>67, 68</sup>, while reducing  $\beta$ -sAPP,  $\beta$ -CTF and  $A\beta$  levels<sup>68</sup>. In our study, Dab-1 overexpression increased AICD release from the membrane via increasing  $\gamma$ -secretase-mediated processing of APP (Figure 26).

Dab-1 is an adaptor protein that can bind the NPXY internalization motif of some transmembrane proteins including APP via its PTB domain<sup>37, 38</sup>. It has been shown that the binding of Dab-1 to these proteins can regulate their trafficking<sup>76-78</sup>. In this study, we found that the overexpression of a Dab-1 mutant that lack its PTB domain (Dab-1  $\Delta$ PTB) prevented the lysosomal degradation of APP, indicating the importance of Dab-1 binding to APP in the regulation of APP metabolism.

The proteasomal inhibition didn't cause an accumulation in the level of the full length APP nor did it rescue the reduction in its levels upon Dab-1 overexpression (Figure 32). This indicated that APP degradation is via the lysosome rather than the proteasome (Figure 32). Thus, in addition to Dab-1 overexpression effect on  $\gamma$ -secretase activity, Dab-1 seems to also enhance the clearance of APP from the early endosomes by targeting APP to the lysosome for degradation. This in turn can explain the observed reduction in APP-CT-GFP signals and the reduction in the full-length levels of APP after Dab-1 overexpression.

In conclusion, Dab-1 modulates APP metabolism and promotes  $\alpha$ - and  $\gamma$ -secretase-mediated processing of APP to release AICD without an increase in A $\beta$ . However, the effects of Reelin and its downstream kinases on APP degradation via the lysosome have to be investigated to confirm the significance of the Dab-1 overexpression effects on APP. Interestingly, disrupting APP and its two homologues APLP1 and APLP2 results in cortical dysplasia and neuronal migration defects<sup>69</sup> that are similar but not identical to disruption of Reelin, Dab-1 or its receptors ApoER or VLDLR<sup>18</sup>. Dab-1 may be a crucial link between some of the critical cellular pathways in the brain; elucidating how Dab-1 mediates and links these molecules maybe a valuable tool to understand proper brain development and AD pathology.

## CHAPTER FIVE: GENERAL CONCLUSION

The adult mammalian brain has limited neurogenerative potential meaning that if was subjected to an insult such a stroke, brain injury or a neurodegenerative disease, it lacks the ability to fully regenerate the lost tissue. This will lead to the loss of the cognitive function associated with that lost tissue. However, hope emerged with the discovery of the neural stem cells in the adult mammalian brain as they were found to retain their abilities to divide, differentiate and migrate<sup>1</sup>. Since the discovery of these cells, efforts have focused on increasing the potential of these cells either via increasing their proliferative rate, stimulating their differentiation into certain type of cells or regulating their migration into a desired site<sup>1</sup>. The therapeutic approaches can be classified in two categories: First, expand and manipulate an exogenous source of stem cells *in vitro* and then transplant these cells into the desired site. Second, stimulate the endogenous sources of stem cells to divide, differentiate and migrate into the damaged areas<sup>1</sup>. Nevertheless, success has been limited so far by the lack of the full understanding of the adult's brain environment that controls the process of functional neurogenesis.

In the adult mammalian brain neural stem cells were found to reside in two restricted regions of the brain, these are: the subventricular zone of the lateral ventricle and the dentate gyrus of the hippocampus<sup>1</sup>. Radial glial cells have been recently identified to be the neuronal progenitors for most of the neurons in the CNS<sup>2, 3</sup>. The end of neurogenesis in the cortex is marked by the transformation of the radial glial cells into astrocytes<sup>4</sup>. Reelin signaling has been recently shown to induce the radial glial phenotype *in vitro* and to rescue the defects in the reeler mutant radial

glia<sup>11</sup>. In addition, a recent study showed that the adult reeler mutants have increased differentiation of the newly generated cells into astrocytes and decreased differentiation into neurons<sup>22</sup>. Interestingly, Cajal-Retzius cells, cells that produce Reelin in the cortical marginal zone, are thought to either degenerate postnatally<sup>41</sup> or undergo developmental dilution<sup>42</sup>.

On the other hand, Notch-1 activation has been known for its role in promoting both phenotypes, the formation of the radial glial cells and their transformation into astrocytes. Interestingly, Notch-1 activation has been shown to induce radial glial cells differentiation prenatally and to induce astrocytic differentiation postnatally<sup>31, 32</sup>. Therefore, the presence of other signaling pathways that act to induce the radial glial phenotype prenatally but are deactivated or downregulated postnatally seems to be an attractive model to explain how Notch-1 activation leads to different cellular fates at different developmental stages.

Accordingly, we proposed that Reelin signaling promotes Notch-1 activation to favor the radial glial phenotype prenatally. Thus, the down-regulation of Reelin in the cortex after birth is expected to allow the transformation of the radial glial cells into astrocytes and thereby end cortical neurogenesis.

To test our hypothesis, we used hNPCs that were isolated from the cortex of 14 weeks old fetus. These cells do not produce Reelin and are the end of their neurogenic phase. Our challenge was to confirm that adding Reelin to these cells will prevent them from transforming into astrocytes and maintain them in a neurogenic radial glial phenotype. We found that these cells respond to

Reelin treatment by inducing BLBP expression and the subsequent formation of bipolar morphology in the GFAP positive cells indicating the formation of neurogenic radial glia *in vitro* (Figure 7). Most importantly, we found that Reelin treatment increased the neurogenic potential of these hNPCs and significantly increased neurogenesis (Figure 13).

Next, we investigated the mechanism by which Reelin increases the formation of radial glia and the generation of neurons. We hypothesized that Reelin induces the formation of radial glia via activating Notch-1 signaling. We found that Reelin treatment activates Notch-1 signaling and induces BLBP expression (Figure 9) via increasing NICD accumulation (Figure 10). Additionally, we found that Reelin treatment enhanced the interaction between Dab-1, recently identified as a nucleoshuttling protein<sup>50</sup>, and NICD (Figure 23) and increased NICD translocation into the nucleus to induce BLBP expression (Figure 22).

We next questioned how Reelin modulates Notch-1 activation. The first step of the activation of Reelin signaling is the induction of Dab-1 tyrosine phosphorylation after Reelin binds to its receptors<sup>16</sup>. Dab-1 tyrosine phosphorylation then acts as link between Reelin and its downstream kinases. Dab-1 tyrosine phosphorylation forms a binding site for Src family kinases resulting in their activation.

To determine if Dab-1 tyrosine phosphorylation is crucial to mediate Reelin's effect on Notch-1 activation, we used a Dab-1 mutant that cannot be tyrosine phosphorylated in response to Reelin<sup>53</sup>. The use of this mutant completely abolished Reelin's effect on Notch-1 activation and

brought NICD levels back to basal levels (Figure 19). Similarly, inhibiting the activity of Src inhibited Reelin's effect on NICD accumulation (Figure 20).

Finally, Dab-1 overexpression was found to increase the levels of  $\alpha$ -sAPP (Figure 28). It has been recently found that sAPP can enhance neurogenesis by increasing the proliferation of the neuronal progenitors<sup>40</sup>. In addition, we previously found that sAPP can induce the glial differentiation of hNSCs. These data indicate that Dab-1 may also enhance neurogenesis via modulating the processing of APP. However, further investigations of this hypothesis are necessary.

In conclusion, this study show that Reelin signaling, mediated by Dab-1 and Src kinase, activates Notch-1 signaling in hNPCs resulting in the induction of BLBP expression, the formation of radial glia and the generation of neurons. This work is novel because it provides that first evidence that Reelin expression is an important signal for the neuronal differentiation of the hNPCs. It also shows the crosstalk between Reelin and Notch-1 signaling, two major pathways in development and cell fate determination. This study extends our knowledge in understanding the role of Reelin signaling in cell fate determination, differentiation and neurogenesis and provides us with new tools to manipulate the process of neurogenesis for neuroregenerative therapy.

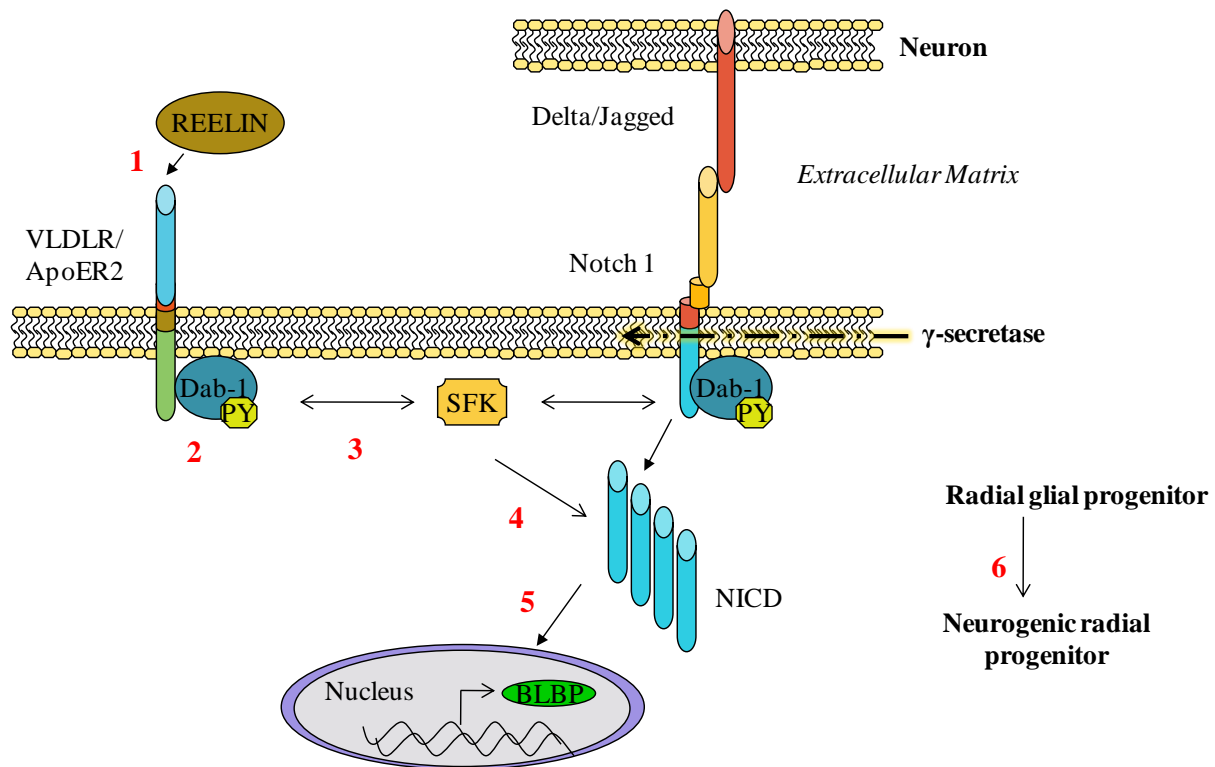


**Figure 33: A schematic diagram that summarizes the role of Reelin signaling in the formation of neurogenic radial glia.**

(1) Reelin binds to its receptors VLDLR and ApoER2 (2) initiating Dab-1 binding to the cytoplasmic domain of VLDLR, ApoER2 and Notch-1 and leading to Dab-1 tyrosine phosphorylation. (3) SFK binds to Dab-1 resulting in SFK activation and the (4) accumulation of NICD. (5) NICD translocates to the nucleus and activates the transcription of BLBP. (6) BLBP expression drives the maturation of the radial glial cell into its neurogenic phase. SFK; *Src* family kinases, NICD; Notch intracellular domain, BLBP; brain lipid binding protein, Dab-1; Disabled-1, VLDLR; very low density lipoprotein, ApoER2; ApoE receptor 2.



## REFERENCES

1. Kennea, N.L., and Mehmet, H. (2002): **Neural stem cells.** *Journal of pathology.* **197**: 536-550
2. Noctor, S.C., Flint, A.C., Weissman, T.A., Wong, W.S., Clinton, B.K., Kriegstein, A.R. (2002): **Dividing precursor cells of the embryonic cortical ventricular zone have morphological and molecular characteristics of radial glia.** *J Neurosci.* **22**: 3161-73
3. Anthony, T.E., Klein, C., Fishell, G., and Heintz, N. (2004): **Radial glia serve as neural progenitors in all regions of the central nervous system.** *Neuron.* **41**: 881-890
4. Kriegstein, A.R., and Gotz, M. (2003): **Radial glia diversity: a matter of cell fate.** *GLIA.* **43**: 37-43
5. Gaiano, N., and Fishell, G. (2002): **The role of Notch in promoting glial neural stem cell fates.** *Annu. Rev. Neurosci.* **25**: 471-90
6. Noctor, S.C, Flint, A.C., Weissman, T.A., Dammerman, R.S., and Kriegstein, A.R. (2001): **Neurons derived from radial glial cells establish radial units in neocortex.** *Nature.* **409**: 714-720
7. Fishell, G., and Kriegstein, A.R. (2003): **Neurons from radial glia: the consequences of asymmetric division.** *Curr opin Neurobiol.* **13**: 34-41
8. Chanas-Sacre, G., Rogister, B., Moonen, G., and Leprince, P. (2000): **Radial glia phenotype: Origin, Regulation and Transdifferentiation.** *J Neurosci Res.* **61**: 357-363
9. Hartfuss, E., Galli, R., Heins, N., and Gotz, M. (2001): **Characterization of CNS precursor subtypes and radial glia.** *Dev Biol.* **229**: 15-30
10. Feng, L., and Heintz, N. (1995): **Differentiating neurons activate transcription of the brain lipid-binding protein gene in radial glia through a novel regulatory element.** *Development.* **121**: 1719-30

11. Hartfuss, E., Forster, E., Bock, H.H., Hack, M.A., Leprince, P., Luque, J.M., Herz, J., Frotscher, M., Götz, M. (2003): **Reelin signaling directly affects radial glia morphology and biochemical maturation.** *Development.* **130**: 4597-609
12. D'Arcangelo, G., Miao, G.G., Chen, S.C., Scares, H.D., Morgan, J.I., Curran, T. (1995): **A protein related to extracellular matrix proteins deleted in the mouse mutant reeler.** *Nature.* **374**: 719-23
13. Dulabon, L., Olson, E.C., Taglienti, M.G., Eisenhuth, S., McGrath, B., Walsh, C.A., Kreidberg, J.A., Anton, E.S. (2000): **Reelin binds alpha3beta1 integrin and inhibits neuronal migration.** *Neuron.* **27**: 33-44
14. Forster, E., Jossin, Y., Zhao, S., Chai, X., Frotscher, M., Goffinet, A.M. (2006): **Recent progress in understanding the role of Reelin in radial neuronal migration, with specific emphasis on the dentate gyrus.** *Eur J Neurosci.* **23**: 901-9
15. Benhayon, D., Magdaleno, S., and Curran, T. (2003): **Binding of purified Reelin to ApoER2 and VLDLR mediates tyrosine phosphorylation of Disabled-1.** *Brain Res Mol Brain Res.* **112**: 33-45
16. Bock, H. H., and Herz, J. (2003): **Reelin Activates Src Family Tyrosine Kinases in Neurons.** *Curr Biol.* **13**: 18-26
17. Ballif, B. A., Arnaud, L., and Cooper, J. A. (2003): **Tyrosine phosphorylation of Disabled-1 is essential for Reelin-stimulated activation of Akt and Src family kinases.** *Brain Res Mol Brain Res.* **117**: 152-9
18. Trommsdorff, M., Gorthardt, M., Hiesberger, T., Shelton, J., Stockinger, W., Nimpf, J., Hammer, R.E. Richardson, J.A. and Herz, J. (1999): **Reeler/Disabled-like disruption of neuronal migration in knockout mice lacking the VLDL receptor and ApoE receptor 2.** *Cell.* **97**: 689-701
19. Forster, E., Tielsch, A., Saum, B., Weiss, K.H., Johanssen, C., Graus-Porta, D., Müller, U., Frotscher, M. (2002): **Reelin, Disabled 1, and beta 1 integrins are required for the formation of the radial glial scaffold in the hippocampus.** *Proc Natl Acad Sci USA.* **99**: 13178-83

20. Luque, J.M., Morante-Oria, J., and Faire'n, A. (2003): **Localization of ApoER2, VLDLR and Dab1 in radial glia: groundwork for a new model of reelin action during cortical development.** *Brain Res Dev Brain Res.* **40**: 195-203
21. Magdaleno, S., Keshvara, L., and Curran, T. (2002): **Rescue of Ataxia and Preplate Splitting by Ectopic Expression of Reelin in reeler Mice.** *Neuron.* **33**: 573-586
22. Zhao, S., Chai, X., and Frotscher, M. (2007): **Balance between Neurogenesis and Gliogenesis in the Adult Hippocampus: Role for Reelin.** *Developmental Neuroscience.* **29**: 84-90
23. Ever, L., and Gaiano, N. (2005): **Radial 'glial' progenitors: neurogenesis and signaling.** *Curr opin Neurobiol.* **15**: 29-33
24. Parks, A.L., Huppert, S.S., and Muskavitch, M.A. (1997): **The dynamics of neurogenic signaling underlying bristle development in *Drosophila melanogaster*.** *Mech Dev.* **63**: 61-74
25. Patten, B.A., Peyrin, J.M., Weinmaster, G., and Corfas, G. (2003): **Sequential signaling through Notch1 and erbB receptors mediates radial glia differentiation.** *J. Neurosci.* **23**: 6132–6140
26. Patten. B.A., Sardi, S.P., Koirala, S., Nakafuku, M., and Corfas, G. (2006): **Notch1 signaling regulates radial glia differentiation through multiple transcriptional mechanisms.** *J. Neurosci.* **26**: 3102-8
27. Baron, M. (2003): **An overview of the Notch signaling pathway.** *Semin Cell Dev Biol.* **14**:113-9
28. Lai, E.C. (2002): **Keeping a good pathway down: transcriptional repression of Notch pathway target genes by CSL proteins.** *EMBO Rep.* **3**: 840–845
29. Anthony, T.E., Mason, H.A., Gridley, T., Fishell, G., and Heintz, N. (2005): **Brain lipid-binding protein is a direct target of Notch signaling in radial glial cells.** *Genes Dev.***19**: 1028-33

30. Weinmaster, G. (1997): **The Ins and Outs of Notch Signaling.** *Mol Cell Neurosci.* **9:** 91-102
31. Gaiano, N., Nye, J.S., Fishell, G. (2000): **Radial glial identity is promoted by Notch1 signaling in the murine forebrain.** *Neuron.* **26:** 395-404
32. Chambers, C.B., Peng, Y., Nguyen, H., Gaiano, N., Fishell, G., Nye, J.S. (2001): **Spatiotemporal selectivity of response to Notch1 signals in mammalian forebrain precursors.** *Development.* **128:** 689-702
33. Maccioni, R.B., Munoz, J.P., and Barbeito, L. (2001): **The molecular bases of Alzheimer's diseases and other neurodegenerative disorders.** *Arch. Med. Res.* **32:** 367-381
34. Vetrivel, K.S., and Thinakaran, G., (2006): **Amyloidogenic processing of  $\beta$ -amyloid precursor protein in intracellular compartments.** *Neurology.* **66:** 69-73
35. Suzuki, T., Araki, Y., Yamamoto, T., and Nakaya, T., (2006): **Trafficking of Alzheimer's disease-related membrane proteins and its participation in disease pathogenesis.** *J. Biochem. (Tokyo).* **139:** 949-955
36. Turner, P.R., O'Connor, K., Tate, W.P., and Abraham, W.C., (2003): **Roles of amyloid precursor protein and its fragments in regulating neural activity, plasticity and memory.** *Prog. Neurobiol.* **70:** 1-32
37. King, G.D., and Turner, R.S., (2004): **Adaptor protein interactions: modulators of amyloid precursor protein metabolism and Alzheimer's disease risk?** *Exp Neurobiol.* **185:** 208-219
38. Trommsdorff, M., Borg, J.P., Margolis, B., and Herz, J., (1998): **Interaction of cytosolic adaptor proteins with neuronal apolipoprotein E receptors and the amyloid precursor protein.** *J Biol Chem.* **273:** 33556-60

39. Kwak YD, Brannen CL, Qu T, Kim HM, Dong X, Soba P, Majumdar A, Kaplan A, Beyreuther K, Sugaya K (2006). **Amyloid precursor protein regulates differentiation of human neural stem cells.** *Stem Cells Dev.* **15**:381-9
40. Caillé I, Allinquant B, Dupont E, Bouillot C, Langer A, Müller U, Prochiantz A (2004). **Soluble form of amyloid precursor protein regulates proliferation of progenitors in the adult subventricular zone.** *Development.* **13**:2173-81
41. Super, H., Uylings, H.B. (2001): **The early differentiation of the neocortex: a hypothesis on neocortical evolution.** *Cereb Cortex.* **11**: 1101- 1109
42. Martin, R., Gutierrez, A., Penafiel, A., Marin-Padilla, M., de la Calle, A. (1999): **Persistence of Cajal-Retzius cells in the adult human cerebral cortex. An immunohistochemical study.** *Histol Histopathol.* **14**: 487-90
43. Beffert, U., Morfini, G., Bock, H.H., Reyna, H., Brady, S.T., Herz, J. (2002): **Reelin-mediated signaling locally regulates PKB/Akt and GSK-3 $\beta$ .** *J Biol Chem.* **277**: 49958-49964
44. D’Arcangelo, G., Nakajima, K., Miyata, T., Ogawa, M., Mikoshiba, K., Curran, T. (1997): **Reelin is a secreted glycoprotein recognized by the CR-50 monoclonal antibody.** *J Neurosci.* **17**: 23-31
45. Feng, L., Heintz, N. (1995): **Differentiating neurons activate transcription of the brain lipid binding protein gene in radial glia through a novel regulatory element.** *Development.* **121**: 1719-1730
46. Rio, C., Rieff, H.I., Qi, P., Khurana, T.S., Corfas, G. (1997): **Neuregulin and erbB receptors play a critical role in neuronal migration.** *Neuron.* **19**: 39–50
47. Liu X, Bolteus AJ, Balkin DM, Henschel O, Bordey A. (2006). **GFAP-expressing cells in the postnatal subventricular zone display a unique glial phenotype intermediate between radial glia and astrocytes.** *GLIA.* **54**: 394-410

48. Gregg, C., Weiss, S. (2003): **Generation of functional radial glial cells by embryonic and adult forebrain neural stem cells.** *J Neurosci.* **23**: 11587- 11601
49. Yoon, K., Nery, S., Rutlin, M.L., Radtke, F., Fishell, G., Gaiano, N. (2004): **Fibroblast growth factor receptor signaling promotes radial glial identity and interacts with Notch signaling in telencephalic progenitors.** *J Neurosci.* **24**: 9497-9506
50. Honda, T., Nakajima, K. (2006): **Mouse Disabled1 (DAB1) is a nucleocytoplasmic shuttling protein.** *J Biol Chem.* **281**: 38951-65
51. Keilani S, Sugaya K (2008): **Reelin induced a radial glial phenotype in human neural progenitor cells by activation of Notch-1.** *BMC Dev Biol*, **8**
52. Morimura, T., Hattori, M., Ogawa, M., and Mikoshiba, K., (2005): **Disabled1 regulates the intracellular trafficking of reelin receptors.** *J Biol Chem.* **280**: 16901-16908
53. Howell, B.W., Herrick, T.M., Hildebrand, J.D., Zhang, Y., and Cooper, J.A. (2000). **Dab1 tyrosine phosphorylation sites relay positional signals during mouse brain development** *Curr. Biol.* **10**: 877–885
54. Hashimoto-Torii K, Torii M, Sarkisian MR, Bartley CM, Shen J, Radtke F, Gridley T, Sestan N, Rakic P (2008): **Interaction between Reelin and Notch signaling regulates neuronal migration in the cerebral cortex.** *Neuron.* **60**: 273-84
55. Vaccari T, Lu H, Kanwar R, Fortini ME, Bilder D (2008): **Endosomal entry regulates Notch receptor activation in Drosophila melanogaster.** *J Cell Biol.* **180**:755-62
56. Fukumori, A., Okochi, M., Tagami, S., Jiang, J., Itoh, N., Nakayama, T., Yanagida, K., Ishizuka-Katsura, Y., Morihara, T., Kamino, K., Tanaka, T., Kudo, T., Tanii, H., Ikuta, A., Haass, C., Takeda, M. (2006): **Presenilin-dependent gamma-secretase on plasma membrane and endosomes is functionally distinct.** *Biochemistry.* **45**: 4907-4914

57. Vetrivel, K.S., Cheng, H., Lin, W., Sakurai, T., Li, T., Nukina, N., Wong, P.C., Xu, H., and Thinakaran, G. (2004): **Association of gamma-secretase with lipid rafts in post-Golgi and endosome membranes.** *J. Biol. Chem.* **279**: 44945–44954
58. Zolkiewska A. (2008). **ADAM proteases: ligand processing and modulation of the Notch pathway.** *Cell Mol Life Sci.* **65**: 2056-68
59. Koo, E.H., and Squazzo, S.L., (1994): **Evidence that production and release of amyloid beta-protein involves the endocytic pathway.** *J. Biol. Chem.* **269**: 17386-9
60. Perez, R.G., Soriano, S., Hayes, J.D., Ostaszewski, B., Xia, W., Selkoe, D.J., Chen, X., Stokin, G.B., and Koo, E.H. (1999): **Mutagenesis identifies new signals for beta-amyloid precursor protein endocytosis, turnover, and the generation of secreted fragments, including Abeta42.** *J Biol. Chem.* **274**: 18851-18856
61. Bu, G., Cam, J., and Zerbinatti, C., (2006): **LRP in amyloid-beta production and metabolism.** *Ann N Y Acad Sci.* **1086**: 35-53
62. Cam, J.A., Zerbinatti, C.V., Li, Y., and Bu, G., (2005): **Rapid endocytosis of the low density lipoprotein receptor-related protein modulates cell surface distribution and processing of the beta-amyloid precursor protein.** *J Biol Chem.* **280**: 15464-70
63. Rogelj, B., Mitchell, J.C., Miller, C.C., and McLoughlin, D.M., (2006): **The X11/Mint family of adaptor proteins.** *Brain Res Rev.* **52**: 305-15
64. King, G.D., Cherian, K., and Turner, R.S., (2004): **X11alpha impairs gamma- but not beta-cleavage of amyloid precursor protein.** *J Neurochem.* **88**: 971-982
65. King, G.D., Perez, R.G., Steinhilb, M.L., Gaut, J.R., and Turner, R.S. (2003): **X11alpha modulates secretory and endocytic trafficking and metabolism of amyloid precursor protein: mutational analysis of the YENPTY sequence.** *Neuroscience.***120**: 143-154

66. Lau, K.F., McLoughlin, D.M., Standen, C., and Miller, C.C., (2000): **X11 alpha and x11 beta interact with presenilin-1 via their PDZ domains.** *Mol Cell Neurosci.* **16:** 557-565
67. Parisiadou, L., and Efthimiopoulos. (2006): **Expression of mDab1 promotes the stability and processing of amyloid precursor protein and this effect is counteracted by X11alpha.** *Neurobiol. Aging.* **28:** 377-88
68. Hoe, H.S., Tran, T.S., Matsuoka, Y., Howell, B.W., and Rebeck, G.W. (2006): **DAB1 and Reelin effects on amyloid precursor protein and ApoE receptor 2 trafficking and processing.** *J. Biol. Chem.* **281:** 35176-35185
69. Herms, J., Anliker, B., Heber, S., Ring, S., Fuhrmann, M., Kretschmar, H., Sisodia, S., and Muller, U., (2004): **Cortical dysplasia resembling human type 2 lissencephaly in mice lacking all three APP family members.** *EMBO J.* **23:** 4106-15
70. Pfaffl, M.W., (2001): **A new mathematical model for relative quantification in real-time RT-PCR.** *Nucleic Acids Res.* **29:** 2002-2007
71. Edbauer, D., Willem, M., Lammich, S., Steiner, H., and Hass, C. (2002): **Insulin-degrading enzyme rapidly removes the beta-amyloid precursor protein intracellular domain (AICD).** *J Biol Chem.* **277:** 13389-93
72. Pinnix, I., Musunuru, U., Tun, H., Sridharan, A., Golde, T., Eckman, C., Ziani-Cherif, C., Onstead, L., Sambamurti, K. (2001): **A novel  $\gamma$ -secretase assay based on detection of the putative C-terminal fragment-gamma of amyloid beta protein precursor.** *J Biol Chem.* **276:** 481-7
73. McGill, M.A., and McGlade, C.J., (2003): **Mammalian numb proteins promote Notch1 receptor ubiquitination and degradation of the Notch1 intracellular domain.** *J Biol Chem.* **278:** 23196-203
74. Park, T.J., Hamanaka, H., Ohshima, T., Watanabe, N., Mikoshiba, K., and Nukina, N. (2003): **Inhibition of ubiquitin ligase Siah-1A by disabled-1.** *Biochem Biophys Res Commun.* **302:** 671-8



75. Bock, H., H., Jossin, Y., May, P., Bergner, O., and Herz, J. (2004): **Apolipoprotein E receptors are required for reelin-induced proteasomal degradation of the neuronal adaptor protein Disabled-1.** *J Biol Chem.* **279**: 33471-9
76. Gotthardt, M., Trommsdorff, M., Nevitt, M.F., Shelton, J., Richardson, J.A., Stockinger, W., Nimpf, J., and Herz, J. (2000): **Interactions of the low density lipoprotein receptor gene family with cytosolic adaptor and scaffold proteins suggest diverse biological functions in cellular communication and signal transduction.** *J Biol Chem.* **275**: 25616-25624
77. Stolt, P.C., and Bock, H.H., (2006): **Modulation of lipoprotein receptor functions by intracellular adaptor proteins.** *Cell Signal.* **18**: 1560-71
78. Howell, B.W., Lanier, L.M., Frank, R., Gertler, F.B., and Cooper, J.A. (1999): **The disabled 1 phosphotyrosine-binding domain binds to the internalization signals of transmembrane glycoproteins and to phospholipids.** *Mol Cell Biol.* **19**: 5179-88